

IMEXON AND GEMCITABINE: MECHANISMS OF SYNERGY
AGAINST HUMAN PANCREATIC CANCER

by

NICHOLAS ORDUÑO ROMÁN

A Dissertation Submitted to the Faculty of the
COMMITTEE ON PHARMACOLOGY AND TOXICOLOGY (GRADUATE)

In Partial Fulfillment of the Requirements
For the Degree of

DOCTOR OF PHILOSOPHY

In the Graduate College

THE UNIVERSITY OF ARIZONA

2 0 0 5

THE UNIVERSITY OF ARIZONA
GRADUATE COLLEGE

As members of the Dissertation Committee, we certify that we have read the dissertation

prepared by Nicholas Orduño Román

entitled Imexon and Gemcitabine: Mechanisms of Synergy against Human Pancreatic Cancer

and recommend that it be accepted as fulfilling the dissertation requirement for the

Degree of Doctor of Philosophy

Robert T. Dorr, Ph.D. Date: 4/12/05

Terrence J. Monks, Ph.D. Date: 4/12/05

Nathan J. Cherrington, Ph.D. Date: 4/12/05

Garth Powis, D. Phil. Date: 4/12/05

Terry H. Landowski, Ph.D. Date: 4/12/05

Final approval and acceptance of this dissertation is contingent upon the candidate's submission of the final copies of the dissertation to the Graduate College.

I hereby certify that I have read this dissertation prepared under my direction and recommend that it be accepted as fulfilling the dissertation requirement.

Dissertation Director: Robert T. Dorr Date 4/12/05

STATEMENT BY AUTHOR

This dissertation has been submitted in the partial fulfillment of requirements for the advance degree at The University of Arizona and is deposited in the University Library to be made available to borrowers under rules of the Library.

Brief quotations from this dissertation are allowable without special permission, provided that accurate acknowledgement of the source is made. Request for permission for extended quotation from or reproduction of this manuscript in whole or in part may be granted by the head of the major department or the Dean of the Graduate College when in his or her judgment the proposed use of the material is in the interests of scholarship. In all other instances, however, permission must be obtained from the author.

SIGNED: _____Nicholas O. Roman_____

ACKNOWLEDGEMENTS

I am thankful to all the people who helped me complete my research project. Foremost, I would like to express my gratitude and appreciation to my research advisor Dr. Robert T. Dorr. His guidance and instruction were invaluable. I thank Dr. Terry Landowski for her knowledge and expertise; her advice was thought provoking and stimulating. I would like to thank the members of the Dorr laboratory, Dr. Steven Stratton, Mary Ann Raymond, Betty Samulitus, Ross Meyers, and Alan Pourpak, for their support and contributions to this project. I would also like to thank my dissertation committee members Dr. Terrence Monks, Dr. Nathan Cherrington, and Dr. Garth Powis for their valuable time and advice in completing this project. Finally, I would like to thank Dr. Russell Scara and Pastors Steve and Teresa Hall and Bill and Margie Cooper, for their continual effort, support and inspiration toward fulfilling my hopes and calling.

DEDICATION

I would like to dedicate this dissertation to my family, to my wife Lisa Marie, who gave me encouragement, support and unceasing laughter throughout my endeavor, to my son Nicholas James, who was born during this project and whose life has brought me immeasurable joy, and above all, to the Lord Jesus Christ, for His infinite wisdom, creativity and sacrifice for me.

TABLE OF CONTENTS

LIST OF FIGURES.....	9
LIST OF TABLES.....	12
ABBREVIATIONS.....	13
ABSTRACT.....	15
1. CHAPTER : INTRODUCTION AND OVERVIEW.....	18
1.1. Pancreatic cancer.....	18
1.2. Current treatment.....	22
1.3. Imexon.....	30
1.4. Gemcitabine.....	39
1.5. Gemcitabine metabolism.....	44
1.6. Summary.....	57
2. CHAPTER : MATERIALS AND METHODS.....	60
2.1. Chemicals.....	60
2.2. Cell cultures.....	61
2.3. Cytotoxicity assays.....	61
2.4. Median effect analysis.....	63
2.5. In vivo SCID mice study.....	65
2.6. [¹⁴ C]-imexon uptake.....	67
2.7. [³ H]-gemcitabine uptake.....	67
2.8. Deoxycytidine kinase assay.....	68
2.9. Deoxycytidine deaminase assay.....	69

TABLE OF CONTENT- Continued

2.10. Phosphorylase assay.....	71
2.11. Ribonucleotide reductase assay.....	72
2.12. Western Blot.....	73
2.13. RT-PCR.....	74
2.14. Cell cycle analysis.....	75
2.15. Gemcitabine DNA incorporation.....	75
2.16. ⁶⁰ Co irradiation.....	76
2.17. Statistical analysis.....	77
3. CHAPTER : RESULTS.....	78
3.1. Cytotoxicity analysis.....	78
3.1.1. Schedule dependence.....	78
3.1.2. MTT IC50 values.....	78
3.1.3. Median effect analysis.....	79
3.2. Analysis of <i>in vivo</i> anti-tumor activity.....	92
3.2.1. Tumor growth inhibition model.....	92
3.2.2. Tumor regression model.....	93
3.3. Transport assays.....	98
3.3.1. [¹⁴ C]-imexon uptake.....	98
3.3.2. [³ H]-gemcitabine uptake.....	98
3.4. Enzyme assays.....	102
3.4.1. Deoxycytidine kinase assay.....	102
3.4.2. Deoxycytidine deaminase assay.....	102

TABLE OF CONTENTS- *Continued*

3.4.3. Phosphorylase assay.....	103
3.4.4. Ribonucleotide reductase assay.....	104
3.5. RNR protein and mRNA expression.....	111
3.6. Cell Cycle Analysis.....	115
3.6.1. Propidium iodide staining.....	115
3.6.2. Gemcitabine DNA incorporation.....	115
3.7. p38 MAP kinase.....	120
3.8. ⁶⁰ Co irradiation.....	122
4. DISCUSSION.....	128
4.1. Mechanisms of Synergy.....	128
4.2. Summary.....	139
4.3. Future Studies.....	141
REFERENCE LIST.....	146

LIST OF FIGURES

Figure 1: Chemotherapeutic strategies for the treatment of pancreatic cancer	29
Figure 2: Synthesis and structure of imexon.....	36
Figure 3: Chemical basis for biologic activity of imexon	37
Figure 4: Imexon: mechanistic schema.....	38
Figure 5: Structure of gemcitabine.....	43
Figure 6: Gemcitabine activation pathway.....	44
Figure 7: Gemcitabine inactivation pathway.....	45
Figure 8: Deoxycytidine deaminase active site.....	54
Figure 9: Ribonucleotide reductase.....	55
Figure 10: Ribonucleotide reductase catalytic site.....	56
Figure 11: Imexon: schedule-dependence.....	82
Figure 12: IC ₅₀ values of imexon in PANC-1, MIA PaCa-2, MutJ and BxPC-3 cells.....	84
Figure 13: IC ₅₀ values of gemcitabine in PANC-1, MIA PaCa-2, MutJ and BxPC-3 cells.....	85
Figure 14: Median effect analysis of 1:1, 1:2 and 2:1 ratios of imexon (μMol): gemcitabine (nMol) in PANC-1 cells.....	86
Figure 15: Median effect analysis of 1:1 ratio of imexon (μMol): gemcitabine (nMol) in PANC-1, MIA PaCa-2, MutJ and BxPC-3 cells.....	87
Figure 16: Median effect analysis of 1:1 ratio of imexon (μMol): gemcitabine (nMol) with sequential imexon or gemcitabine treatment in PANC-1 cells.....	88

LIST OF FIGURES- Continued

Figure 17: Median effect analysis of 1:1 ratio of imexon (μ Mol): gemcitabine (nMol) with sequential imexon or gemcitabine treatment in MIA PaCa-2 cells.....	89
Figure 18: Median effect analysis of 1:1 ratio of imexon (μ Mol): gemcitabine (nMol) with sequential imexon or gemcitabine treatment in MutJ cells.....	90
Figure 19: Median effect analysis of 1:1 ratio of imexon (μ Mol): gemcitabine (nMol) with sequential imexon or gemcitabine treatment in BxPC-3 cells.....	91
Figure 20: Tumor growth of PANC-1 cells inoculated in SCID mice treated 24 hr post-injection with imexon and/or gemcitabine.....	94
Figure 21: Tumor growth of PANC-1 cells inoculated in SCID mice treated 40 d post-injection with imexon, gemcitabine, or combination.....	96
Figure 22: Percent control tumor growth of PANC-1 cells inoculated in SCID mice treated 40 d post-injection with imexon, gemcitabine, or combination.....	97
Figure 23: Imexon uptake.....	100
Figure 24: Gemcitabine uptake.....	101
Figure 25: Deoxycytidine kinase activity.....	106
Figure 26: HPLC chromatograph of deoxycytidine deaminase activity.....	107
Figure 27: Deoxycytidine deaminase activity.....	108
Figure 28: Phosphorylase activity.....	109
Figure 29: Ribonucleotide reductase activity.....	110
Figure 30: Protein expression of ribonucleotide reductase M ₁ and M ₂ subunits.....	113

LIST OF FIGURES- Continued

Figure 31: mRNA of ribonucleotide reductase M ₁ and M ₂ subunits.....	114
Figure 32: Cell cycle analysis of PANC-1 cells.....	118
Figure 33: DNA incorporation of gemcitabine.....	119
Figure 34: p38 activation.....	121
Figure 35: ⁶⁰ Co irradiation of PANC-1 cells.....	124
Figure 36: ⁶⁰ Co irradiation of MIA PaCa-2 cells.....	125
Figure 37: ⁶⁰ Co irradiation of MutJ cells.....	126
Figure 38: ⁶⁰ Co irradiation of BxPC-3 cells.....	127
Figure 39: Mechanisms of action of imexon and gemcitabine.....	144
Figure 40: Proposed mechanisms of synergy of imexon and gemcitabine.....	145

LIST OF TABLES

Table 1: PanIN classification of human pancreatic cancer cells.....	21
Table 2: Schedule dependence of imexon in PANC-1 human pancreatic cancer cells.....	81
Table 3: IC ₅₀ concentrations of imexon and gemcitabine in PANC-1, MIA PaCa-2, MutJ and BxPC-3 human pancreatic cancer cell.....	83
Table 4: SCID mice analysis: NCI criteria.....	95
Table 5: Cell cycle analysis of PANC-1 human pancreatic cancer cells.....	117

ABBREVIATIONS

5'-NU	5'-Nucleotidase
AMP	Adenosine-5'-monophosphate
ADP	Adenosine-5'-diphosphate
ATP	Adenosine-5'-triphosphate
AUC	Area under the curve
CMB	<i>p</i> -chloromercuribenzoate
d	Days
dA	Deoxyadenonsine
dC	Deoxycytidine
dCD	Deoxycytidine deaminase
dCMP	Deoxycytidine-5'-monophosphate
dCDP	Dexoycytidine-5'-diphosphate
dCK	Deoxycytidine kinase
dG	Deoxyguanosine
dNTPs	Deoxynucleotide triphosphates
dUMP	Deoxyuridine-5'-monophosphate
dUDP	Deoxyuridine-5'-diphosphate
dUTP	Deoxyuridine-5'-triphosphate
GEM-TP	Gemcitabine triphosphate
GSH	Glutathione
GSSG	Glutathione disulfide
Gy	Gray
hr	Hour
HO	Heme Oxygenase
HPLC	High performance liquid chromatography
IP	Intraperitoneal
kDa	Kilodalton
kg	Kilogram
μMol	Micromolar
min	Minute
mMol	millimolar
MTT	3-(4,5-dimethylthiazol-2-yl)-2,5-diphenyl-2H-tetrazolium
NAC	N-acetylcysteine
NaCl	Sodium Chloride
NADPH	β-nicotinamide adenine dinucleotide phosphate reduced)
nm	Nanometer
nMol	Nanomolar
NSCLC	Non-small cell lung cancer
PBS	Phosphate buffered saline
RT PCR	Real-time polymerase chain reaction

ABBREVIATIONS- *Continued*

PI	Propidium iodide
pMol	Picomolar
PyNase	Pyrimidine nucleoside phosphorylase
ROS	Reactive oxygen species
RNR	Ribonucleotide reductase
s	Seconds
SCID	Severe combined immune deficient
TPase	Thymidine phosphorylase
Trx	Thioredoxin
UPase	Uridine phosphorylase

ABSTRACT

Imexon is an iminopyrrolidone aziridine which previously has shown activity against a variety of human cancer types, including multiple myeloma and pancreatic adenocarcinoma. Recently, mechanistic studies in the MIA PaCa-2 human pancreatic cancer cell line have demonstrated binding to sulfhydryls, build-up of reactive oxygen species (ROS), perturbations in mitochondrial membrane potential (MMP), and activation of caspases 3, 8 and 9. Because imexon binds sulfhydryls and generates ROS, it was hypothesized that imexon would have considerable activity against pancreatic cancer by promoting oxidative stress in cells which are already oxidatively challenged and in combination with gemcitabine by interacting with key sulfhydryl-dependent enzymes involved with gemcitabine metabolism. *In vitro* anti-tumor activity of imexon and gemcitabine was evaluated in PANC-1, MIA PaCa-2, MutJ, and BxPC-3 human pancreatic cancer cell lines. Interactions between imexon and gemcitabine were assessed with simultaneous drug exposure at a fixed (imexon: gemcitabine) ratio using median effect analysis. The PANC-1, MutJ, and BxPC-3 cells demonstrated synergy with combination

treatment. Severe combined immune deficient (SCID) mice bearing PANC-1 cells treated with imexon and gemcitabine demonstrated tumor growth inhibition and regression. Imexon inhibited ribonucleotide reductase (RNR) at drug concentrations ≥ 100 μMol . This is similar to the selective RNR inhibitor hydroxyurea, suggesting that imexon may enhance gemcitabine-mediated inhibition of RNR as a mechanism of synergy. An S phase accumulation of PANC-1 cells occurred at ≥ 300 μMol imexon at 24 hr. This was associated with a ≥ 2 -fold increase of radiolabeled gemcitabine incorporation into PANC-1 DNA at ≥ 100 μMol imexon. Therefore the mechanisms of synergy between imexon and gemcitabine appear to include: (1) cell cycle arrest in S-phase, and (2) inhibition of RNR. Both actions would increase the uptake of the active metabolite, gemcitabine-triphosphate, (GEM-TP), into DNA. Arresting cells in S-phase would increase the time of cellular incorporation of deoxynucleotides, including GEM-TP, into DNA. Similarly, RNR inhibition reduces the availability of normal deoxynucleotides which compete with GEM-TP for incorporation. Overall, these data demonstrate that imexon is uniquely synergistic with gemcitabine *in vitro* and *in vivo* and support the

rationale for combining the agents in clinical trials for the treatment of pancreatic cancer.

1. CHAPTER

INTRODUCTION AND OVERVIEW

1.1. Pancreatic cancer

Pancreatic cancer remains the fourth leading cause of cancer deaths in males and females, accounting for approximately 5% of all cancer related deaths in the United States. In 2003, an estimated 30,700 new cases of pancreatic cancer were diagnosed in the United States and an approximately equivalent number of patients died from the disease in the same year (Willett and Clark, 2003). The reason for this trend is that pancreatic cancer produces few or no symptoms until locally advanced or metastatic disease occurs. In fact, at the time of diagnosis, <15% of all patients have resectable tumors, the only curable form of the disease. Adenocarcinoma of the pancreas has a 5 year mean-survival-rate of 8 months, 7 months and 3-6 months for patients with localized disease, locally advanced disease and metastatic disease, respectively. Unfortunately, an overall 5-year-survival-rate is less than 5%. Risk factors include smoking, alcohol, obesity, diabetes mellitus, pancreatitis, and a family history of the disease (Royal, 2004; Beger et al., 2003).

Despite recent advances in understanding the underlying molecular events leading to pancreatic cancer, the disease remains largely incurable. In the past 15 years, researchers have formulated a step-wise progression model based upon histopathology, clinical, and genetic evidence. This model led to a standard nomenclature of the histologic characteristics of pancreatic intraepithelial neoplasms (PanIN) was adopted (Hruban et al., 2001). The classification system characterizes the transition of early pancreatic columnar epithelial changes with progressive dysplasia as sequential PanIN lesions (Table 1). Clinical studies have correlated pancreatic duct lesions as precursors to pancreatic adenocarcinoma and molecular examinations have identified key genetic events involved in the progression toward neoplasia (Royal, 2004). For example, point mutations of proteins such as *K-ras* and *Her2/neu*, an epidermal growth factor receptor (EGFR) are associated with abnormal cell growth regulation. Mutations resulting in the inactivation of the tumor suppressor gene *p16* are associated with abnormal cell cycle arrest. These mutations are considered PanIN-1 and PanIN-2 lesions and appear to be key events occurring early in the progression toward pancreatic cancer. In contrast, mutations of other

tumor suppressor genes involved with cell cycle arrest and DNA repair such as p53, DPC4 and BRCA2, are associated with PanIN-3 lesions and occur later in the development of pancreatic cancer (Weyrer et al., 1996).

Table 1: Histologic characteristics of the pancreatic intraepithelial neoplasm (PanIN) lesions.

	Histopathological characteristics	Common genetic mutations
PanIN 1A	Columnar transition Retention of apical nuclei Intracellular mucin near the lumen aspect	<i>K-ras</i> Her2/neu
PanIN 1B	Micropapillary or papillary Transition	
PanIN 2	Nuclear atypia/crowding/enlargement Loss of nuclear polarity	p16
PanIN 3	Apical mitosis Prominent nucleoli Dystrophic goblet cells Cribriform architecture Luminal necrosis	p53 DPC4 BRCA-2

Table 1: Histologic characteristics of the pancreatic intraepithelial neoplasm (PanIN) lesion and predominate genetic mutations.

1.2. Current treatment options for pancreatic cancer

At the time of diagnosis, approximately 10-15% of patients present with localized disease, or resectable cancer, and 85-90% of patients present with locally advanced or metastatic tumors (Royal, 2004). Localized disease is pancreatic cancer confined to the pancreatic tail or body, which can be resected with preservation of the pancreatic head or cancer found in the head of the pancreas requiring pancreaticoduodenectomy. Currently, surgical resection of localized disease offers the only potential form of cure for patients. Still, patients that undergo surgical resection have a median survival of 11-20 months and 5-year-survival-rate of 7-25% (Alexakis et al., 2004). Locally advanced disease characterizes pancreatic cancer that has invaded major vascular structures such as the celiac or superior mesenteric artery and metastatic disease is cancer that has spread to other sites within the body (Royal, 2004). Locally advanced and metastatic disease are not amenable to potentially curable resection and are treated with gemcitabine, palliative therapy for pain, radiation therapy, and/or investigational chemotherapeutic agents (Goldstein et al., 2004).

Current FDA approved chemotherapeutic agents include 5-FU, mitomycin C, and gemcitabine. Gemcitabine gained FDA approval in 1997 for the treatment of locally advanced and metastatic pancreatic cancer due to a minor increase in median-survival-rate over the 5-FU control arm (4.41 months vs. 5.65 months for gemcitabine, $p=0.0025$). In addition gemcitabine induced alleviation of disease related symptoms such pain, low performance status, and weight loss (Burris, III et al., 1997b). Subsequent clinical trials combining gemcitabine with other anti-tumor agents have, so far, confirmed the clinical superiority of gemcitabine as a single-agent. Regimens of gemcitabine plus cisplatin, oxaliplatin, or irinotecan, did not significantly increase median-survival-rates among patients compared to gemcitabine alone, and in some cases resulted in overall increased toxicities (Heinemann V. et al., 2003; Louvet C. et al., 2003; Bramhall et al., 2001). Combinations of 5-FU with other agents, such as the FOLFIRINOX combination (5-FU/leucovorin, irinotecan and oxaliplatin), have been promising with a preliminary median-survival-rate of 9.5 months (Korc et al., 1986a). The more recent combination of gemcitabine plus 5-FU, irinotecan, leucovorin and oxaliplatin (G-FLIP regimen) has produced a preliminary

median-survival-rate of 10.3 months, but long-term results in these studies are not yet available.

With a better understanding of the molecular pathogenesis of pancreatic cancer, several novel agents designed to target pancreatic cancer cell abnormalities have been developed. These agents target proteins or mRNA's over-expressed in growth and differentiation pathways such as epidermal growth factor receptors (EGFR) known to be upregulated in pancreatic cancer (Figure 1) (Murphy et al., 2001; Korc et al., 1986b). However, in recent clinical trials, these newer agents have shown no significant improvements over gemcitabine. This includes the farnesyl transferase inhibitors (FTIs) R115777 (Cohen et al., 2003), the matrix metalloproteinase (MMP) inhibitor BAY 12-9566 (Moore et al., 2003), and the proteasome inhibitor bortezomib (Fahy et al., 2003). In contrast, combinations of gemcitabine plus the VEGF inhibitor bevacizumab, celecoxib (COX-2 inhibitor), and the EGFR inhibitor erlotinib (OSI-774) have provided encouraging results (Pino et al., 2004), as well as other combination studies of gemcitabine plus ISIS-2503, a phosphorothioate oligonucleotide antisense inhibitor of the human *H-ras* mRNA expression (Alberts et al., 2004). However, long-term

follow-up of these clinical studies are still pending, and, so far, none have demonstrated a significant impact on median-survival-rates over current therapy. Hence, new treatment strategies for this devastating disease must be found. One new strategy involves taking advantage of the pro-oxidant state, i.e. increased concentrations of active oxygen and organic peroxides and radicals, in which pancreatic cancer cells thrive, thereby encouraging preferential "oxidative" cell death to this cancer cell population.

Reactive oxygen species (ROS) such as H_2O_2 , superoxide ($O_2^{\cdot-}$), and the hydroxyl radical ($OH\cdot$) are generated *in vivo* by leakage of electrons from the mitochondrial electron transport chain or NADPH cytochrome P450 reductase in the endoplasmic reticulum (Kamata and Hirata, 1999). Production of ROS at low levels is necessary for certain metabolic functions, regulation of signal transduction pathways, and transcription factors. Under normal circumstances, cells are protected from increased ROS, or oxidative stress, by antioxidant enzymes. Antioxidant enzymes such as superoxide dismutase (SOD) convert superoxide radicals to hydrogen peroxide, which is then converted to water by catalase. Other antioxidants such as glutathione (GSH), and

thioredoxin (TRX), reduce oxidized sulfhydryl groups (GSSG) on cysteine residues of proteins (Meister, 1994; Cullen et al., 2003b). In contrast, high levels of ROS result in DNA and membrane damage and alterations of cellular redox status. Increased cellular oxidation leads to excessive oxidation of sulfhydryl groups (RSH) and activation of stress signaling or redox sensitive pathways (Adler et al., 1999b). Further, activation of stress pathways have been linked to activation of stress-responsive kinase pathways and mitochondrial initiation of stress-induced apoptosis by cytochrome c release (Matsuzawa and Ichijo, 2005a; Ueda et al., 2002b).

Research has shown that human pancreatic cells respond to reduction/oxidation, (redox)-active, stress acutely by increasing expression of oxidative stress proteins such as heme oxygenase (HO), thioredoxin, glutaredoxin and NADPH:quinine oxidoreductase (NQO₁) in order to generate reducing agents (NAD⁺, NADP⁺) necessary to reduce oxidized sulfhydryl groups and cysteine residues formed by increased ROS (Nakamura et al., 2000; Sato et al., 1997). However, in chronic inflammatory disease states and in pancreatic adenocarcinoma, antioxidant enzymes such as manganese superoxide dismutase (MnSOD), catalase, and glutathione

peroxidase, are significantly decreased compared to normal pancreatic tissue. Currently, the molecular reasons for these changes remain unclear (Cullen et al., 2003a).

Research has shown that ROS and antioxidants affect human cancer cell growth. For example, forced expression of MnSOD in human pancreatic cancer cells reduced cell growth by decreasing doubling time *in vitro*, and increased median-survival when injected into nude mice (Weydert et al., 2003; Cullen et al., 2003c). Further, superoxide levels were found to be increased in H-vRas12 transformed fibroblasts, and adenoviral transfer of MnSOD in v-Ha-ras transformed human keratinocytes attenuated superoxide generation. These results suggested that a phagocytic-like NADPH oxidase within keratinocytes could be activated by the dominant v-Ha-ras mutation, and could produce excessive superoxide (Irani et al., 1997; Yang et al., 1999). These findings are relevant, since human pancreatic cancers have >90% *K-ras* mutations.

Thus, pancreatic cancer cells thrive in a pro-oxidative state with loss of net anti-oxidant capacity. This led to the hypothesis that this oxidatively challenged environment would render pancreatic cancer cells susceptible to pro-oxidant -apoptotic agents. This especially includes agents

that bind antioxidant molecules such as glutathione, since glutathione depletion has been shown to induce apoptosis in pancreatic cancer (Schnelldorfer et al., 2000).

Pancreatic Cancer: Novel Therapeutic Targets

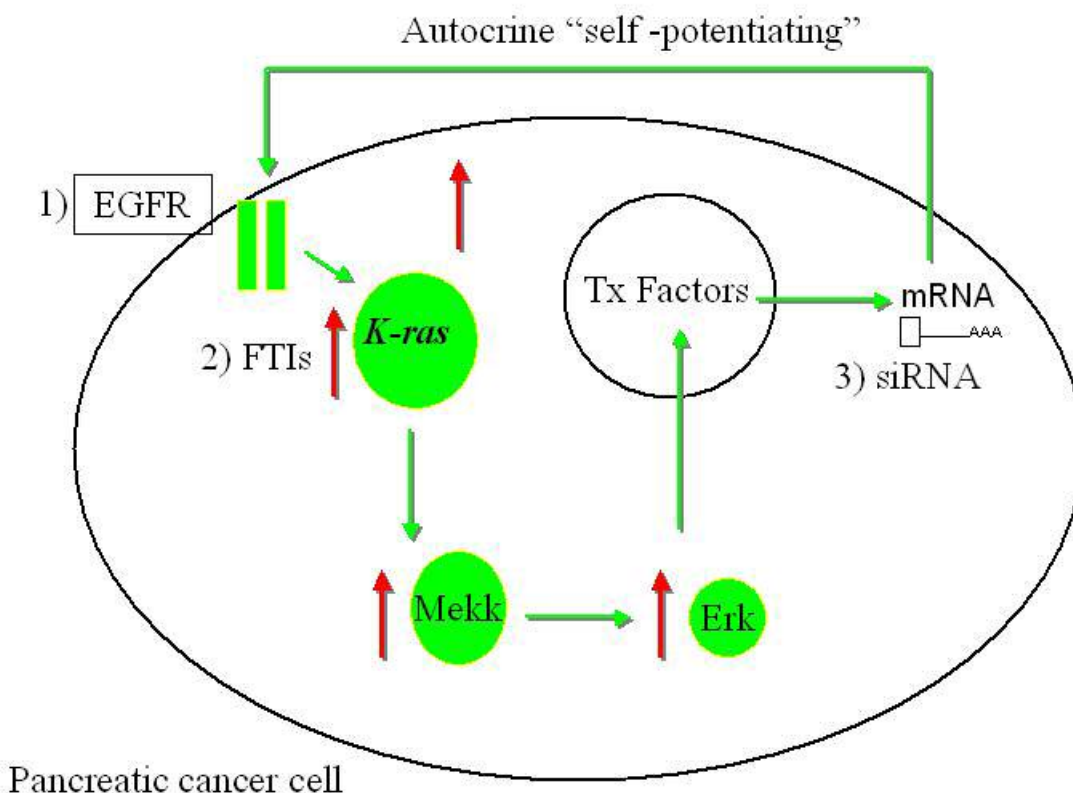


Figure 1 Novel therapeutic targets for the treatment of pancreatic cancer. The illustration shows novel agents that target proteins over-expressed in “self-potentiating” pathways such as the (1) epidermal growth factor receptor (EGFR, VEGF), a commonly over-expressed tyrosine kinase (TKs) receptor and (2) farnesyl transferase inhibitors (FTIs), which block farnesylation and activation of *ras*. Other targets include inhibition of mRNA used for the translation of over-expressed proteins by (3) small inhibitory RNA (siRNA).

1.3. Imexon

Numerous aziridine-containing compounds were originally synthesized and screened in the 1960's due to their potential activity as immunomodulatory and anticancer agents (Goodridge et al., 1963). It was later determined that the effective anti-cancer aziridines contained two aziridine rings and alkylated nucleophilic atoms on guanine residues in DNA (Reynolds, 1995; Dorr and Von Hoff, 1994). By 1975, one aziridine, 2-cyanoaziridine-1-carboxamide, was found to be carcinostatic against PIE 2-3 sarcoma in Wistar rats (Bicker and Fuhse, 1975). Interestingly, the molecule lacked DNA alkylating activity and increased the total number of leukocytes in rats (Bicker, 1975). Eventually, 2-cyanoaziridine-1-carboxamide was modified by cyclization with KOH and methanol. The compound was named imexon (Figure 2) (Bicker et al., 1978).

Imexon (4-imino-1,3-diazabicyclo-[3.1.0] hexan-one) is an iminopyrrolidone aziridine compound that demonstrates immunomodulatory and anticancer activity. For example, imexon has been shown to stimulate humoral and cell mediated immune responses in the Rauscher murine leukemia retrovirus system. The Rauscher leukemia retrovirus model provides an *in vivo* model of the human acquired immune deficiency

syndrome for testing the ability of antiviral agents and biological response modifiers to suppress viremia and retroviral disease (Chirigos et al., 1990; Chirigos et al., 1991). Imexon also enhanced delayed type hypersensitivity reactions and lymphocyte mitogen response *in vivo* and activated macrophages, natural killer cells and cytotoxic T-lymphocytes *in vitro* (Micksche et al., 1977). In an early anti-tumor evaluation, imexon demonstrated cell growth inhibition against ten fresh human cancer cell lines in a colony-forming assay, including multiple myeloma, lymphoma, lung, sarcoma, and pancreatic cancer. Human myeloma cells were the most sensitive to imexon mediated cell growth inhibition compared to the other nine cell lines, with an IC_{50} value of 0.2 $\mu\text{g}/\text{mL}$. Compared to more resistant fresh human tumors, pancreatic cancer cells were also sensitive to imexon with an IC_{50} value of only 3.6 $\mu\text{g}/\text{mL}$. For example, sarcoma and lymphoma tumor specimens had IC_{50} values of 39.0 and 20.1 $\mu\text{g}/\text{mL}$, respectively (Salmon and Hersh, 1994). Subsequent studies showed that imexon demonstrated *in vivo* tumor growth inhibition against large cell lymphoma cells inoculated in the right rear flank of severe combined immune deficient SCID mice (Hersh et al., 1993).

In preliminary human studies of fixed low-doses, imexon was found to be effective and well-tolerated. Thirteen patients received long-term imexon treatment for 3-39 months. Six patients were considered to be of high risk for relapse and seven of these patients were considered to be refractory to standard therapies (Sagaster et al., 1995). Disease progression was stabilized in an additional four of six patients with breast cancer, in one patient with NSCLC and in one patient with liver cancer, who received a total dose of 11,000 mg given during a 24-months period. One of four patients with non-small cell lung cancer (NSCLC) achieved complete remission (>14 years without evidence of disease). Treatment was not associated with myelosuppression, renal dysfunction, or elevated hepatic enzymes. With several doses of 100 mg given i.v., toxicities were mild, including nausea and vomiting in the absence of antiemetics (Micksche et al., 1978). Currently, imexon is in phase I/II clinical trials and at the clinically tolerated dose of 750 mg/m², peak plasma levels of 45 mg/mL, (405 µMol), exceed the preliminary IC₅₀ values in human tumor cell lines *in vitro*.

Previous studies have demonstrated the chemical mechanism by which imexon binds cellular thiols as classical

aziridine ring opening (glutathione) or a more complex nucleophilic attack of sulfur at the cyclic amidine moiety (cysteine) (Figure 3) (Iyengar et al., 2004a). Biological studies in RPMI 8226 multiple myeloma cells have shown that imexon is schedule-dependent; greater than 3-fold concentrations were required to achieve 50% growth inhibition for imexon exposures ≤ 24 hr as determined by MTT analysis. The data showed that 1683 ± 379 μMol imexon was needed to inhibit 50% cell growth at 6 hr compared to 41 ± 2 μMol at 48 hr. Treatment of RPMI 8226 cells with 500 μMol imexon (IC_{65}) for 24 hr also significantly depleted cellular thiols such as glutathione (GSH), glutathione disulfide (GSSG) and cysteine. These actions were prevented with 24 hr pretreatment of 10 mMol N-acetylcysteine (NAC). Myeloma cells treated with 45 μMol imexon for 24 hr led to degeneration of the mitochondrial ultrastructure; mitochondria were swollen and contained lipid droplets compared to control cell. Concentrations ≥ 45 μMol imexon at 48 hr also induced cytosolic oxidative stress that was detected by measuring oxidized nucleotides using an antibody for 8-hydroxydeoxyguanosine (Dvorakova et al., 2000). Studies revealed that 180 μMol imexon exposure led to a loss of the mitochondrial membrane potential (MMP) and cytochrome

C release in NCI-H929 myeloma cells and in NB-4 acute promyelocytic leukemia cells as early as 4 hr in a time-dependent manner (Dvorakova et al., 2001). Subsequent studies demonstrated that 180 μ Mol imexon caused poly(ADP-ribose) polymerase (PARP) cleavage and activated caspases 3 and 9 in a time-dependent manner, consistent with observations of apoptotic cell death at ≥ 45 μ Mol imexon determined by Annexin V staining and flow cytometry analysis (Dvorakova et al., 2002). Concentrations of ≥ 80 μ Mol imexon were also found to induce apoptosis by a caspase-8 dependent mechanism in dexamethasone -sensitive (C2E3) and dex-resistant (1-414) multiple myeloma cell lines in a dose-dependent manner (Evens et al., 2004). These observations led to the generation of a proposed mechanistic schema of imexon activity in multiple myeloma cells (Figure 4).

Recent mechanistic studies in human MIA PaCa-2 pancreatic cancer cells have demonstrated that imexon is schedule-dependent and results in imexon-induced G_2/M arrest, activation of caspases 3, 8 and 9 and induction apoptosis (Shoji F. et al., 2004). Because imexon binds cellular thiols and generates ROS, it was hypothesized that imexon would have considerable activity against human pancreatic cancer as a single-agent by promoting increased

oxidative stress in already oxidatively-challenged cells. These observations also led to the hypothesis that imexon would augment the cytotoxic effects of gemcitabine in pancreatic cancer cells by interacting with key sulfhydryl-dependent enzymes involved with gemcitabine metabolism, namely deoxycytidine deaminase (dCD) and ribonucleotide reductase (RNR).

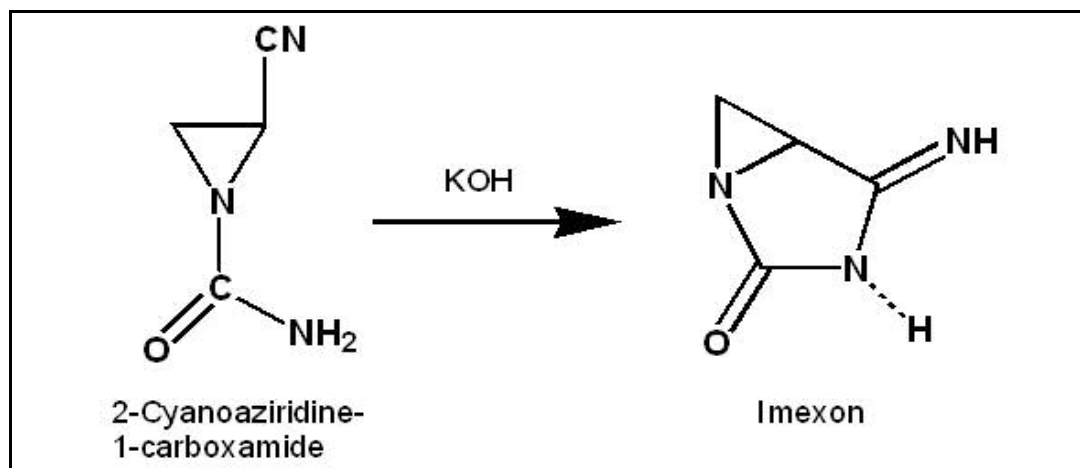


Figure 2 Formation of imexon (4-imino-1,3-diazabicyclo-[3.1.0] hexan-2-one), (M.W. 111.1), from it's precursor, 2-cyano aziridine, 1-carboxamide.

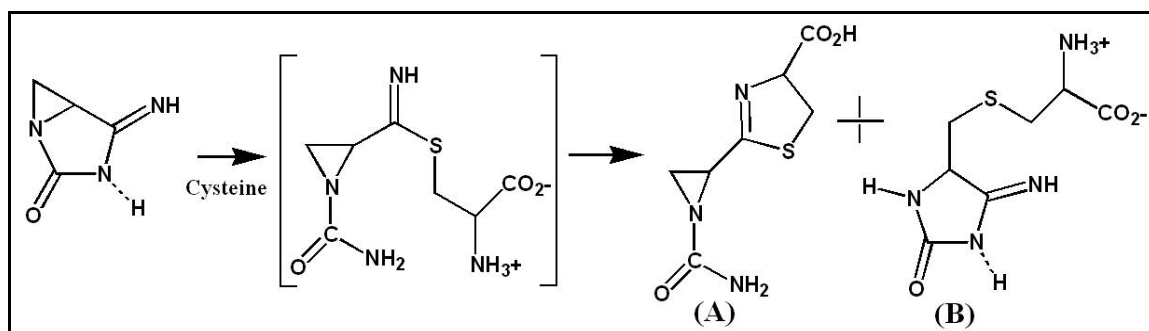


Figure 3 Chemical basis for imexon biological activity with cysteine. At room temperature, imexon readily reacts with cysteine resulting in the thiazolidine ring-based product A, and at higher temperatures (>50°C), the aziridine ring opened product B.

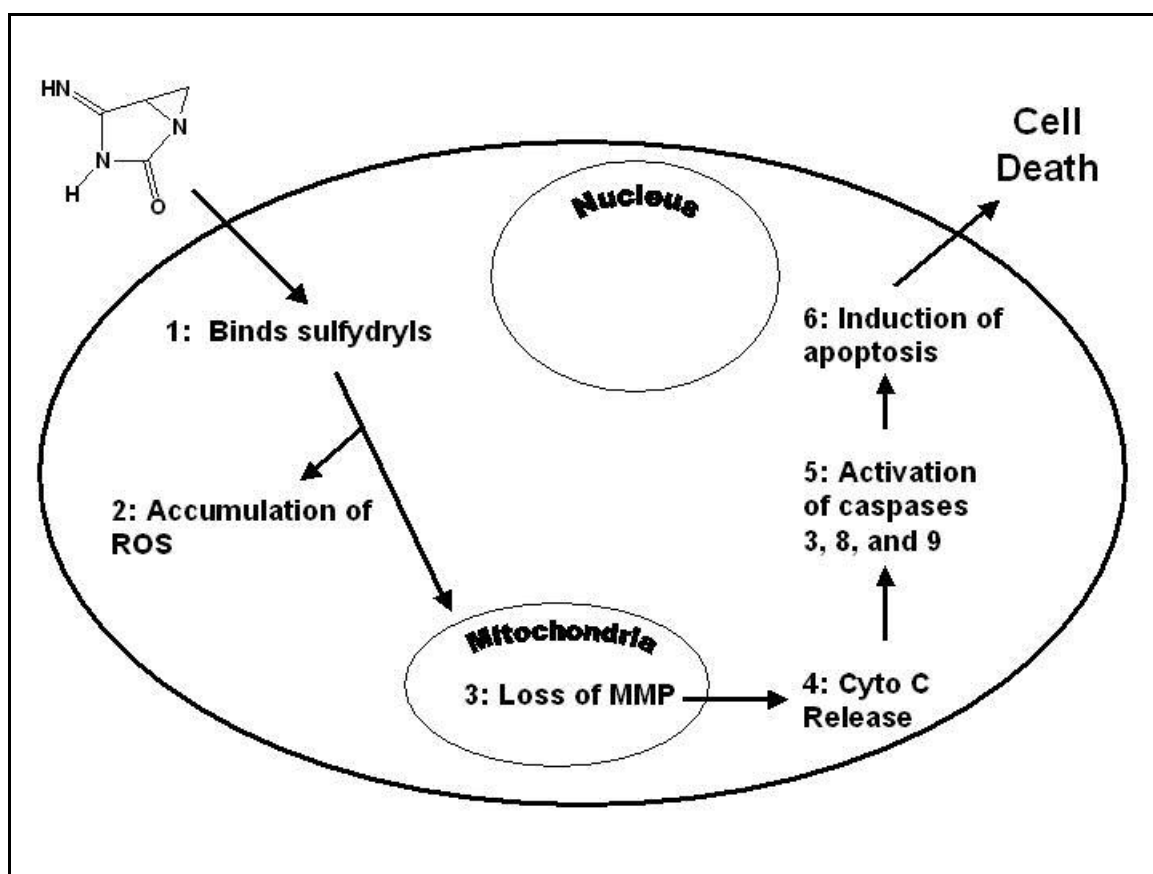


Figure 4 Imexon: mechanistic schema in multiple myeloma cells. Imexon diffuses into a tumor cell and binds sulfhydryl containing molecules (GSH, GSSH and cysteine) resulting in an accumulation of reactive oxygen species (ROS), leading to a loss of mitochondrial membrane potential (MMP), with subsequent cytochrome C release, caspase activation leading to apoptotic cell death.

1.4. Gemcitabine

Gemcitabine (dFdC, 2',2'-difluorodeoxycytidine, Gemzar® (Figure 5) is a deoxycytidine analog that was originally synthesized in the 1980's by Eli Lilly Research Laboratories (Indianapolis, IN) (Hertel et al., 1987). Preliminary evaluation of gemcitabine demonstrated that it was a potent antiviral compound, inhibiting replication of both DNA and RNA viruses (DeLong et al., 1986). However, the drug was found to have a poor, (narrow), therapeutic index *in vivo*. Gemcitabine was then discarded as a potential antiviral but was further evaluated as an anticancer agent (Hertel et al., 1990a).

Preliminary mechanistic studies demonstrated that once gemcitabine becomes incorporated into DNA, only one more deoxynucleotide is incorporated into the growing DNA strand. Thereafter, the DNA polymerase enzyme is unable to continue incorporating deoxynucleotides, resulting in "masked" DNA chain termination (Figure 6) (Ruiz, V et al., 1993b). Incorporation of gemcitabine into DNA also resulted in the formation of large size double-stranded DNA fragments and nucleosomal-sized DNA fragments that were found to be critical to gemcitabine-induced apoptosis. When human T lymphoblastoid CCRF-CEM cells were treated with gemcitabine

for 48 hr, apoptotic bodies and DNA fragmentation by pulsed-field gel electrophoresis were observed, while cells simultaneously treated with the DNA synthesis inhibitor aphidicolin did not demonstrate these results (Huang and Plunkett, 1995). Gemcitabine mediated apoptosis was later correlated with activation of the p38 mitogen-activation protein kinase (MAPK) pathway, a stress-activated protein kinase (SAPK) pathway associated with stress response and programmed cell death (Ding and Adrian, 2001). Gemcitabine activated p38 MAPK in Pk-1 and PCI-43 human pancreatic cancer cells in a dose- and time-dependent manner, while the p38 MAPK inhibitor, SB203580, significantly reduced gemcitabine mediated apoptosis in both cell lines (Habiro et al., 2004). Gemcitabine inhibited other important enzymes such as ribonucleotide reductase, which mediates the rate-limiting step in deoxygenated nucleotide synthesis. Gemcitabine also inhibited cytidine triphosphate (CTP) synthase resulting in a "self-potentiating" mechanism of action (Heinemann et al., 1995; Plunkett et al., 1996d). CTP synthase is required for the formation of deoxycytidine triphosphate (dCTP) for DNA synthesis and repair and decreased dCTP levels result in less competition for incorporation of gemcitabine into DNA (Plunkett et al.,

1995b). Major inactivation of the drug occurred by enzymatic deamination to uridylate, mediated by deoxycytidine deaminase, and minor inactivation results from 5'-nucleosidase and phosphorylase enzymatic activities (Figure 7) (Galmarini et al., 2001b).

The initial anti-tumor evaluation of gemcitabine revealed that it was effective against leukemia cells and rodent fibroblasts (Plunkett et al., 1989). Gemcitabine was also a potent radiosensitizer in human pancreatic cancer cells. PANC-1 and BxPC-3 human pancreatic cancer cell lines treated with noncytotoxic levels of gemcitabine for 24 hr demonstrated enhanced cell death (Ratios of 1.7-1.8, where ratios >1 indicate radiosensitization) with ⁶⁰Co irradiation (Lawrence et al., 1996). Other studies showed that gemcitabine was active against a wide spectrum of murine solid tumors and xenografts derived from human head and neck tumors (Hertel et al., 1990b; Boven et al., 1991). In phase II clinical trials gemcitabine produced clinical responses against a variety of solid tumors (Lund et al., 1993; Kaye, 1994) and demonstrated efficacy as a single-agent against non-small cell lung cancer (NSCLC) (Burkes and Shepherd, 1995; Hansen and Sorensen, 1997). A phase II trial in 1994 determined that gemcitabine had marginal activity against

pancreatic adenocarcinoma without producing excessive toxicity (Casper et al., 1994). In 1996 a phase II clinical trial showed that patients with advanced pancreatic cancer responded modestly to gemcitabine therapy, with limited positive improvement on several patient benefit parameters (Carmichael et al., 1996). Finally, a randomized study in 1997 revealed that gemcitabine was superior to a "standard" treatment of pancreatic cancer using 5-fluorouracil (5-FU) (Burris, III et al., 1997a). This study showed improvements in clinical benefit response (23.8% and 4.8% for gemcitabine and 5-FU-treated patients, respectively ($p = .0022$)), and an increase in the median duration of survival of 1.2 months ($p = .0025$). The survival rate at 12 months was 18% and 2% for gemcitabine and 5-FU-treated patients, respectively. Gemcitabine became approved by the FDA in 1997 and is currently approved in the treatment of pancreatic, lung and bladder cancers (Culine, 2002; Spigel and Greco, 2003).

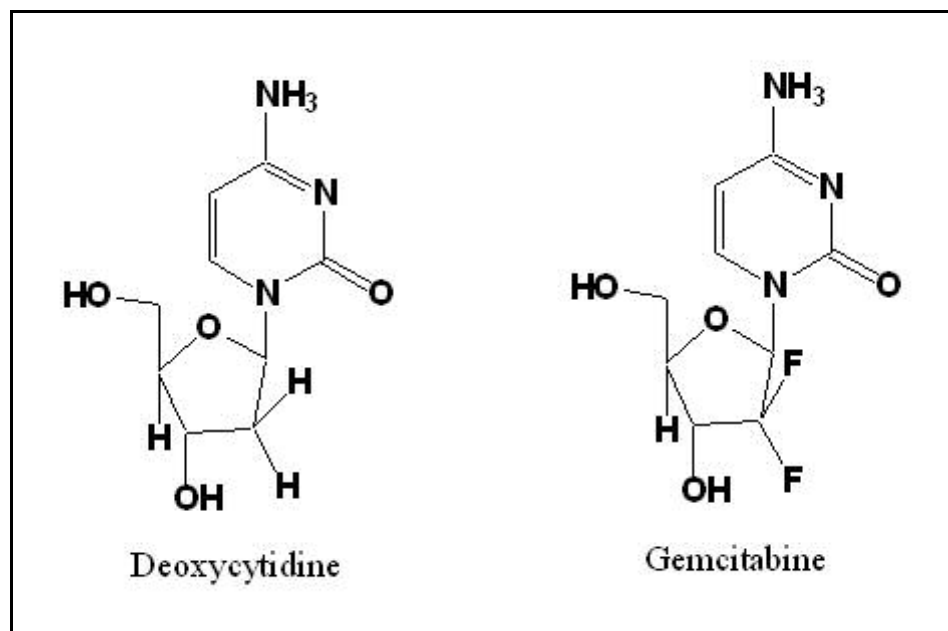


Figure 5 Structure of Gemcitabine (dFdC, 2', 2'-difluorodeoxycytidine, Gemzar®), M.W. 263.2.

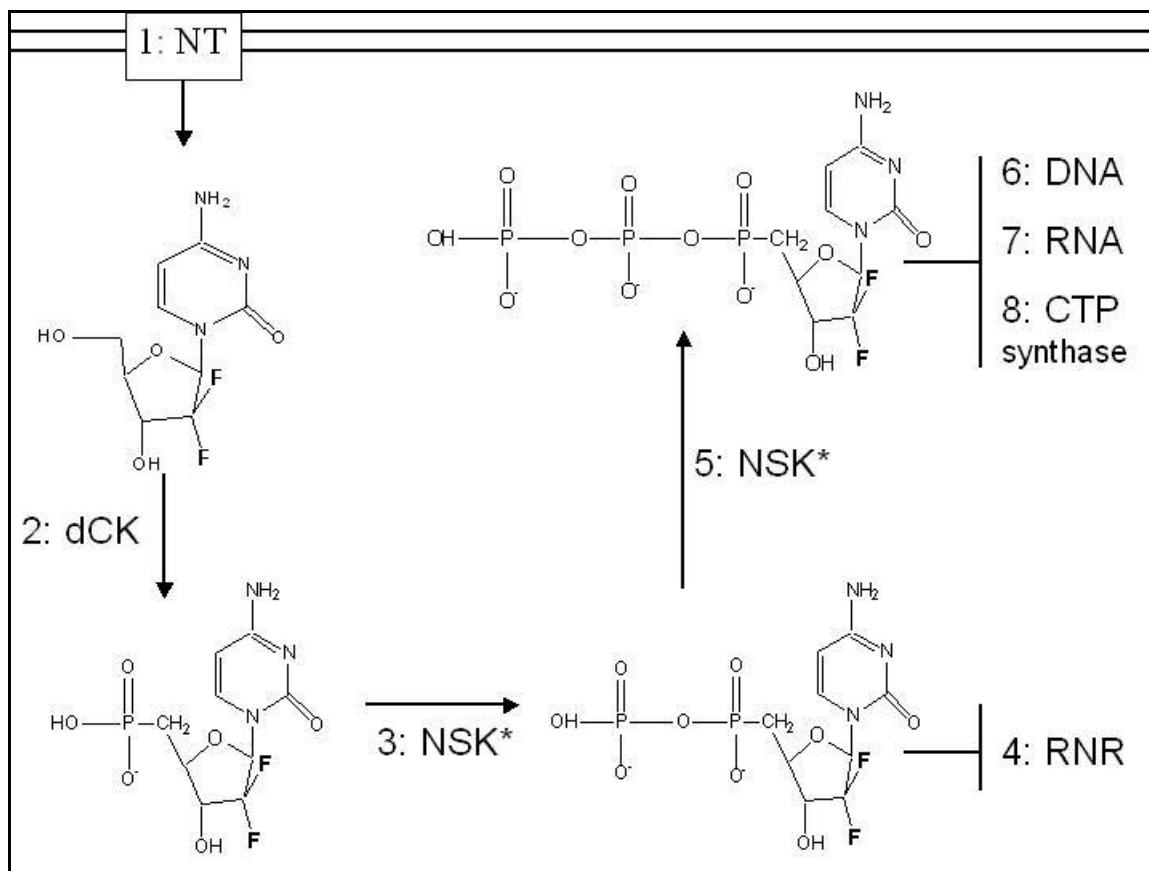


Figure 6 Activation pathway of gemcitabine. 1) Gemcitabine is transported into a cell via nucleotide transporters, 2) phosphorylated by deoxycytidine kinase (dCK) and 3) non specific kinases (NSK*). In the diphosphorylated form gemcitabine inhibits, 4) ribonucleotide reductase (RNR). With subsequent 5) phosphorylation gemcitabine becomes incorporated into 6) DNA and causes "masked" DNA chain termination, 7) inhibits RNA synthesis, and 8) CTP synthase.

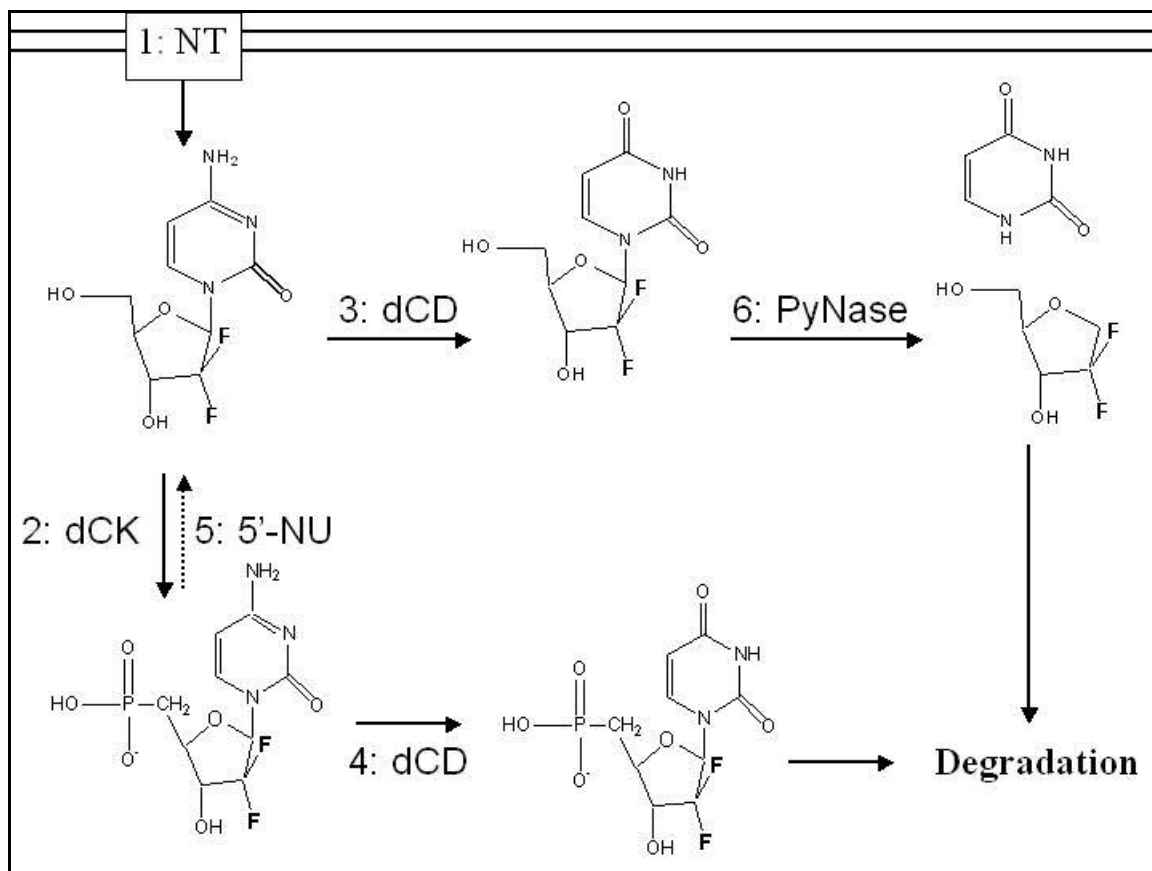


Figure 7 Inactivation pathways of gemcitabine; Gemcitabine is 1) transported across cellular membranes (NT); 2) phosphorylated and activated by deoxycytidine kinase (dCK) 3,4); deaminated by deoxycytidine deaminase (dCD); 5,6) degraded by phosphorylase (PyNase) and/or 5'-nucleotidases.

1.5. Gemcitabine Metabolism

Due to the hydrophilicity of nucleosides like gemcitabine, their physiological uptake is mediated through nucleoside transport (NT) systems. Mammalian NTs are divided into two classes, human equilibrative transporters (hENTs) and concentrative nucleoside transporters (hCNTs) (Griffith and Jarvis, 1996). Transporters in both systems are important in mediating gemcitabine uptake, and thereby play a role in drug sensitivity and resistance in cancer.

Equilibrative transporters are low-affinity pumps, driven by concentration gradients of nucleoside permeants and can be subclassified as equilibrative sensitive, (*es*), or equilibrative insensitive, (*ei*), as determined by transporter inhibition by nitrobenzylthioinosine. Currently, hENT1, hENT2, hENT3 and hENT4 are classified as members of the SLC29 gene family (Baldwin et al., 2004). Anticancer nucleoside drugs such as cytarabine and gemcitabine are handled predominantly by the hENT1 and hENT2 transporters (Clarke et al., 2002) and a correlation between decreased hENT1 expression in tumors from patients with gemcitabine-treated pancreatic adenocarcinoma has been correlated with reduced survival (Spratlin et al., 2004).

Concentrative transporters are high-affinity pumps and are driven by transmembrane sodium (Na^+) gradients. Human CNTs are members of the SLC28 gene family and subtyped into three classes: hCNT1, hCNT2, and hCNT3 (Gray et al., 2004). Specifically, the hCNT1 and hCNT3 have been shown to mediate gemcitabine uptake (Ritzel et al., 2001; Mackey et al., 1999). The overexpression of the hCNT1 transporter has been shown to confer sensitivity to gemcitabine (Garcia-Manteiga et al., 2003). Transporters highly expressed in pancreatic tissue include hCNT2 and hCNT3 and are responsible for the cytosolic accumulation of gemcitabine in pancreatic cancer (Damaraju et al., 2003). To determine if imexon augments the cellular accumulation of gemcitabine, gemcitabine uptake in the presence of imexon was assessed.

Deoxycytidine kinase (dCK) is a 60 kDa, constitutively expressed protein that phosphorylates the pyrimidine and purine deoxyribonucleosides including deoxycytidine (dC), deoxyadenosine (dA) and deoxyguanosine (dG). Deoxycytidine kinase is not expressed in brain, muscle, or liver and is highly expressed in lymphoid and some neoplastic tissues. The enzyme contains an allosteric regulating site that binds deoxycytidine triphosphate (dCTP) which inhibits enzymatic activity (Eriksson et al., 2002). Phosphorylation of

gemcitabine by dCK is the rate-limiting step in the activation of the drug and is necessary for cytotoxicity (Heinemann V. et al., 1988). Research has shown that dCK protein levels are strongly correlated with gemcitabine sensitivity of human tumor cell lines derived from the pancreas, lung, and colon in nude mice (Kroep et al., 2002b) and gene transfer of the dCK gene in HT-29 colon carcinoma cells resulted in an increased retention of gemcitabine in the tumor compared to wild-type controls (Blackstock et al., 2001b). Further, decreased dCK expression correlated with acquired resistance to gemcitabine in non-small cell lung cancer (NSCLC) (Achiwa et al., 2004). An A6000 ovarian cancer cell line lacking measurable dCK activity was found to be resistant to gemcitabine, as well as to other dCK requiring drugs such as 5-aza-2'deoxyctidine and 2-chlorodeoxyadenosine (Ruiz van Haperen V.W., 1994). Interestingly, studies of purified dCK protein have demonstrated the need for reducing agents such as dithiothreitol, 2-mercaptoethanol, and thioredoxin for full enzymatic function (Bohman and Eriksson, 1990). Recent research has shown that reducing agents can be activators of dCK, suggesting that the enzyme may be regulated by cellular redox potential (Liou et al., 2002c). Because dCK activity

has been correlated to regulation by cellular redox potential, dCK activity in the presence of imexon was measured in order to determine if imexon enhanced gemcitabine activation.

Deoxycytidine deaminase (dCD) catalyzes the hydrolytic deamination of cytidine and deoxycytidine (dC), to their corresponding uridine derivatives. These are available either for scavenging of pyrimidine nucleotide precursors or for generation of carbon and nitrogen sources (Somasekaram et al., 1999b). Major inactivation of cytosine nucleoside-based agents, including gemcitabine, occurs by dCD (Plunkett et al., 1996a), and dCD levels have been shown to correlate with drug sensitivity *in vitro* and *in vivo* (Momparler and Laliberte, 1990; Neff and Blau, 1996c). Interestingly, dCD is a 15 KDa homotetrameric enzyme composed of four identical subunits containing an essential zinc atom in the active site that is coordinated by three necessary cysteine residues, at positions C65, C99, and C102 (Figure 8) (Vincenzetti et al., 2003a). Deoxycytidine deaminase is sulfhydryl-dependent, and pro-oxidants such as CMB inhibit enzymatic activity (Camiener, 1967d). Research has shown that increased dCD activity correlated with decreased sensitivity to gemcitabine *in vivo* (Momparler and Laliberte,

1990). And, forced expression of dCD conferred cellular resistance to gemcitabine *in vitro* (Neff and Blau, 1996b). Because dCD is a sulfhydryl-dependent enzyme, imexon mediated inhibition of dCD was measured to determine if imexon treatment results in a greater half-life of gemcitabine.

Normal salvage of pyrimidine nucleosides occurs by the pyrimidine nucleoside phosphorylases (PyNase). Specifically, uridine phosphorylase, (UPase), and thymidine phosphorylase, (TPase), catalyze the reversible phosphorolysis of uridine to uracil, and thymidine to thymine, respectively (Johansson, 2003b). Uridine phosphorylase has been shown to activate fluoropyrimidine-based anti-tumor agents such as 5-fluorouracil, 5-azacytidine, and 1-(3-*C*-ethynyl- β -D-ribo-pentofuranosyl)-cytosine/-uracil, although the impact of UPase mediated inactivation of gemcitabine is not completely understood (Van Rompay et al., 2001b). Further, PyNase levels in tumor cells have been associated with sensitivity to fluoropyrimidines. Overexpression of PyNase increases the sensitivity of murine adenocarcinoma CT26 cells to 5'-deoxy-5-fluorouridine *in vitro* and *in vivo*, and inhibition of UPase with 2,2'-anhydro-5-ethyluridine, (ANEUR), decreases

the anti-tumor activity of 5-fluoro-2'-deoxyuridine (Nagata et al., 2002; Iigo et al., 1990). For the reason that PyNase activity results in the inactivation of gemcitabine, imexon mediated inhibition of PyNase activity was investigated to determine if imexon treatment results in a greater half-life of gemcitabine.

In the diphosphorylated state, gemcitabine is a suicide inhibitor of ribonucleotide reductase (RNR), the rate-limiting enzyme in the formation of deoxynucleotides for DNA synthesis and repair (Pereira et al., 2004c). Ribonucleotide reductase consists of two subunits, M_1 and M_2 . The M_1 subunit is a 170,000 kDa homodimer containing two effector binding sites and two substrate binding sites. The M_2 catalytic subunit is an 88,000 kDa homodimer containing four nonheme iron molecules in the diiron-oxo sites that are required for the formation of a tyrosyl radical (Figure 9). The tyrosyl radical is then transferred to the M_1 subunit for deoxygenation of the ribose ring (Sintchak et al., 2002).

Ribonucleotide reductase is a thiol-dependent enzyme, requiring at least five reduced cysteine residues for enzymatic activity. The M_1 subunit contains critical cysteines at positions C225 and C462 that form an

intermediate disulfide. This is reduced by two other cysteines at positions C754 and C759 located on M₁, and ultimately by thioredoxin or glutaredoxin. The active site also contains an active cysteine at C439 that is converted into a thiyl radical that is responsible for abstraction of the hydrogen atom from the ribose ring of the substrate (Figure 10) (Kolberg et al., 2004b).

Research has shown that gemcitabine inhibits RNR activity by suicide inhibition. Once diphosphorylated, gemcitabine becomes incorporated into the substrate-binding site, and due to the presence of the fluorine atom on β -face on the 2'-position of the ribose ring, resulting in radical loss from the M₂ subunit on cysteine 439 (Pereira et al., 2004b). Resistance to gemcitabine in pancreatic cancer has been associated with M₂ overexpression, and gemcitabine mediated cytotoxicity is enhanced with simultaneous M₂ subunit inhibition (Duxbury et al., 2004c). Conversely, overexpression of the mRNA for the M₁ protein has been negatively associated with survival in gemcitabine-treated patients with non-small cell lung cancer (NSCLC); two gemcitabine-resistant NSCLC cell lines, H358-G200 and H460-G400, demonstrated increased M₁ subunit expression compared

to control H460 cells in response to chronic gemcitabine treatment. M_1 subunit upregulation was considered to be a result of overcoming gemcitabine mediated inactivation of M_1 subunit activity (Davidson et al., 2004b).

RNR inhibition would result in decreased deoxycytidine triphosphate (dCTP) for DNA synthesis and repair, and facilitate gemcitabine incorporation into DNA. Because RNR activity is dependent upon cysteine residues, imexon mediated inhibition of RNR activity was measured to determine if imexon RNR inhibition augments gemcitabine cytotoxicity as a mechanism of enhancing gemcitabine cytotoxicity.

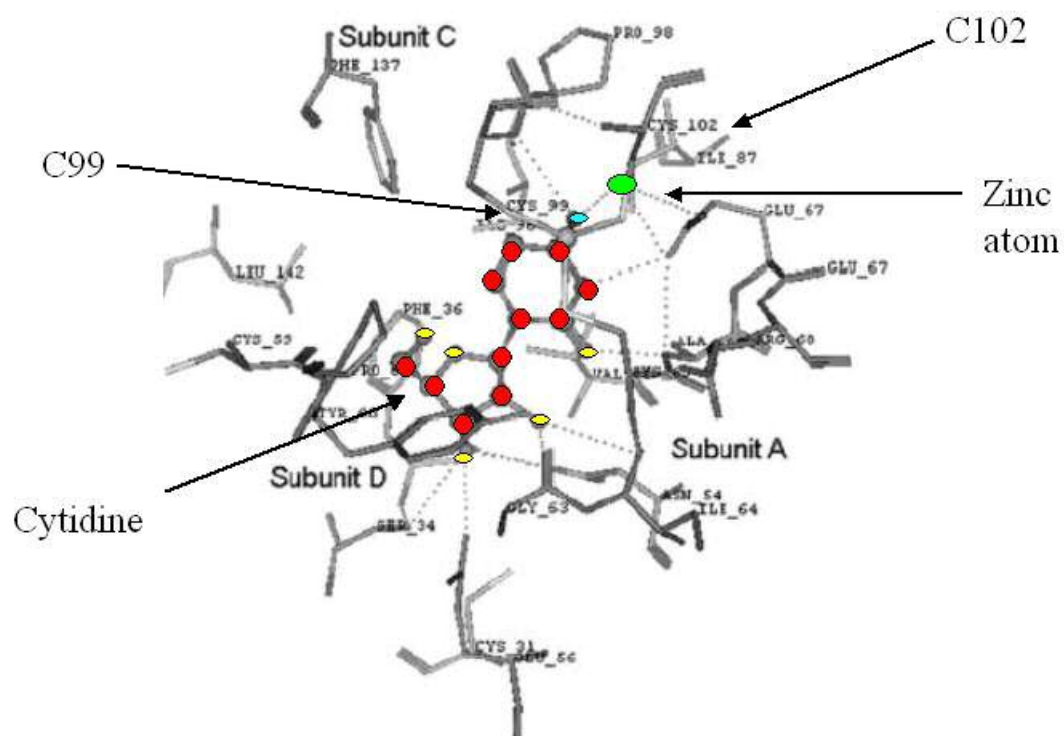


Figure 8 Active site of human deoxycytidine deaminase (dCD). The dCD active site is occupied by the nucleoside cytidine. Cysteine residues located at position C65 (not shown), C99, and C102 coordinate the Zinc atom in the active site necessary for enzymatic deamination. Illustration adapted from Carlow et al. (Carlow et al., 1999).

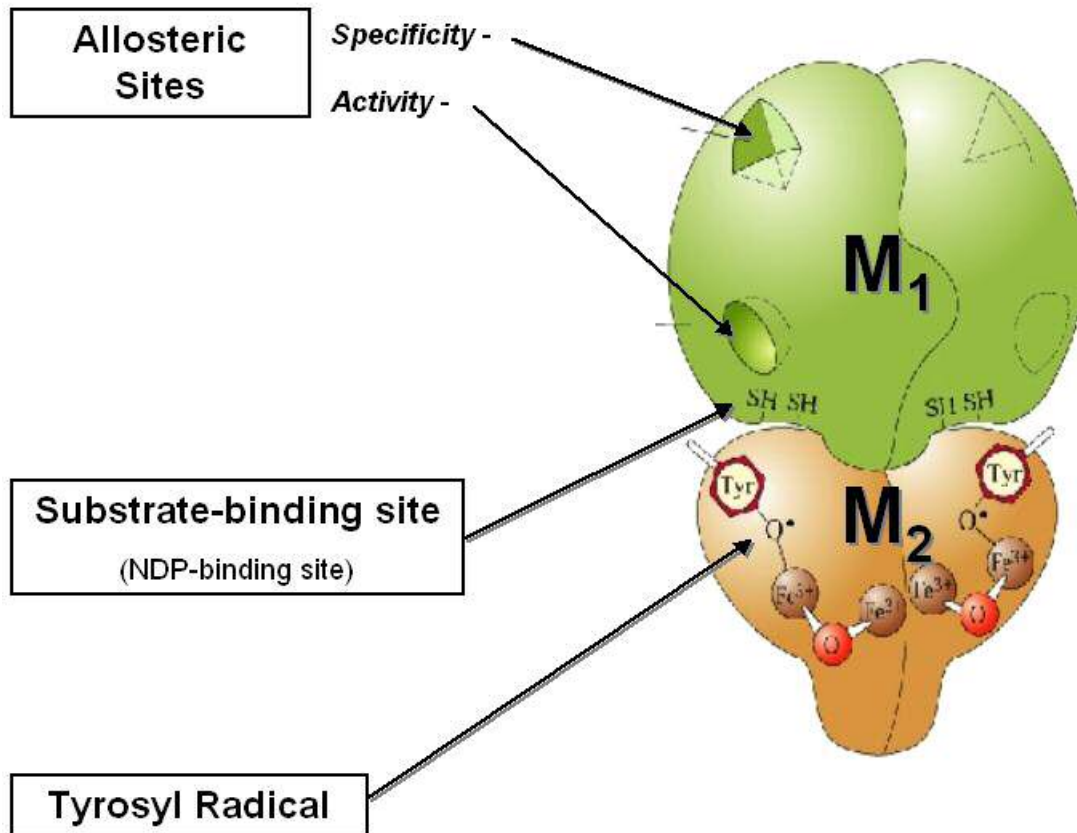


Figure 9 Ribonucleotide Reductase (RNR) enzyme. RNR contains M_1 and M_2 subunits. The M_1 subunit contains an allosteric site that contains specificity and active sites. The specificity site determines what nucleotide diphosphate (NDP) will be reduced in the substrate binding site. The active site binds deoxyadenosine triphosphate (dATP) or adenosine triphosphate (ATP) and is required for enzymatic activity. Illustration adapted from *Molecular Biology of the Cell*, 4th ed. (Alberts et al., 2002).

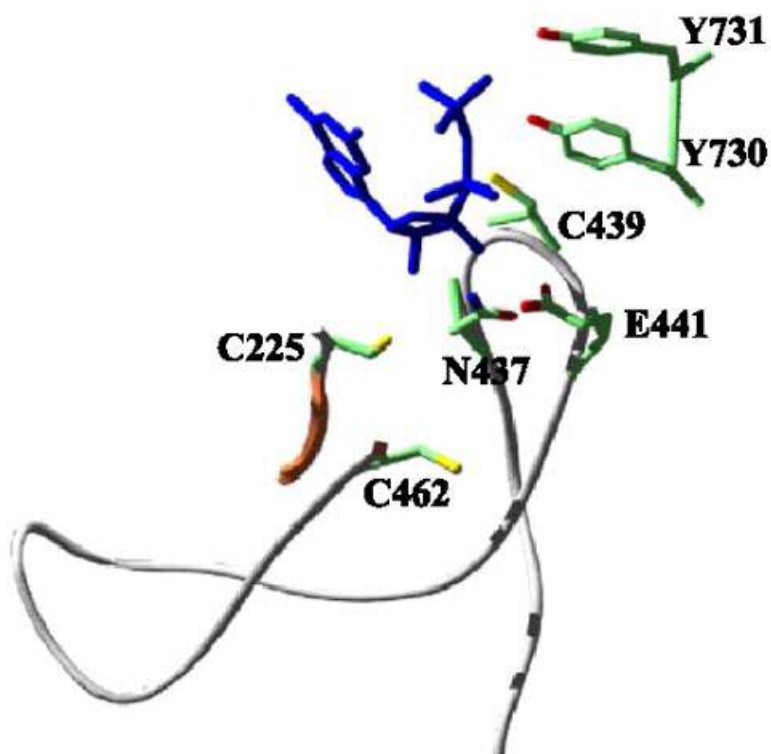


Figure 10 Conserved active site of ribonucleotide reductase class Ia from *E. coli* in reduced form. The M_1 subunit also includes the substrate-binding site containing cysteine pairs located at positions C225 and C462 in the active site are required for deoxygenation of the bound NDP. The generation of the tyrosyl radical occurs in the M_2 subunit and long-range radical transfer reaches the active site by tyrosines located at positions Y730 and Y731. The tyrosyl radical is then transferred to a conserved cysteine at position C439 that is necessary for abstraction of the hydrogen atom from the ribose ring of the substrate. Illustration borrowed from Kolberg, et al. (Kolberg et al., 2004a).

1.6. Summary

The overall goal of this study is to characterize the potential mechanisms of synergy between imexon and gemcitabine in human pancreatic cancer cell lines. It has been established that disease of the pancreas is associated with a shift toward a net-oxidative state and decreased antioxidant capacity. Studies have shown that imexon binds biologically important cellular thiols with iminopyrrolidone and aziridine ring-opening. This leads to cellular stress, generation of ROS and the induction of apoptosis (Iyengar et al., 2004b). Therefore, pancreatic cancer cells should be susceptible to the cellular stress promoted by imexon. The activation of gemcitabine requires the redox-sensitive enzyme dCK, and major inactivation of the drug occurs by the sulfhydryl-dependent enzyme dCD (Galmarini et al., 2001d). Gemcitabine also inhibits the thiol-dependent enzyme RNR, which catalyzes the rate-limiting step of producing deoxynucleotides (dNTPs) for DNA synthesis and repair (Galmarini et al., 2002). Based on the observation that imexon binds cellular thiols leading to oxidative stress, and that gemcitabine activity is influenced by thiol-containing enzymes, **a new hypothesis was developed: synergy**

is due to a biochemical interaction between gemcitabine and imexon. Specific aims to test are: (1) determine if the interaction of imexon and gemcitabine enhances drug uptake, (2) determine if imexon enhances activation of gemcitabine by dCK, (3), determine if imexon inhibits the inactivation of gemcitabine by dCD, (4), determine if imexon augments RNR inhibition, and (5), determine if imexon enhances incorporation of gemcitabine into DNA by a cell cycle direct effect. The cytotoxicity of imexon and gemcitabine was characterized by MTT analysis in PANC-1, MIA PaCa-2, MutJ and BxPC-3 human pancreatic cancer cells and applied in median effect analysis to determine if the combined drug effect *in vitro* was antagonistic, additive or synergistic. The combined drug effect of imexon and gemcitabine was investigated in SCID mice bearing PANC-1 epithelioid carcinoma cells. Because the cytosolic accumulation of gemcitabine is dependent upon nucleoside transport, the effect of imexon on gemcitabine uptake was investigated. The interaction between imexon and the redox-sensitive enzyme dCK and sulfhydryl-dependent enzyme dCD in the gemcitabine resistant PANC-1 cell line was investigated. To determine if imexon inhibited thiol-dependent RNR activity, deoxygenation of cytidine-diphosphate (CDP) was assessed in

PANC-1 cells. In addition, RNR M₁ and M₂ protein subunits and mRNA levels were measured to determine if RNR components were altered in response to imexon treatment. Cell cycle analysis was done to determine if imexon-induced an S phase accumulation of PANC-1 cells leading to enhanced gemcitabine DNA incorporation as a mechanism of synergy. To determine if imexon activated p38, p38 phosphorylation in PANC-1 cells was investigated. Finally, imexon and ⁶⁰Co irradiation were evaluated in combination to evaluate imexon sensitization of pancreatic cancer cells to ionizing radiation.

2. CHAPTER

MATERIALS AND METHODS

2.1. Chemicals

Imexon (4-imino-1,3-diazabicyclo[3.1.0.]-hexan-one) was obtained from the Pharmaceutical Resources Branch of the National Cancer Institute, Bethesda, MD under a Rapid Access to Intervention in Development (RAID) grant to R. Dorr. The drug is supplied as a 99.6% pure lyophilized white powder (M.W. 111.1), which has water solubility of approximately 5-10 mg/mL. A stock solution (40 μ Mol) was prepared in ddH₂O, sterile filtered and stored at -80°C. Gemcitabine was obtained from Eli Lilly and Company (Indianapolis, IN). Radiolabeled [¹⁴C]-imexon (5.5 mCi/mMol; labeled at the carbonyl position in the iminopyrrolidone ring) was obtained from Gene Mash, Ph.D., director of the Synthetic Chemistry Core Service of the Arizona Cancer Center, Tucson, AZ (Jagadis et al., 2005). Radiolabeled [³H]-gemcitabine (11 Ci/mMol) and [¹⁴C]-cytidine diphosphate (405 mCi/mMol) were obtained from Moravek Biochemicals (Mercury Lane Brea, CA). Radiolabeled [³H]-deoxycytidine (22 Ci/mMol) was obtained from Amersham biosciences, Buckinghamshire, UK. Filter paper, P81, was purchased from Whatmann (Florham Park, NJ).

All other chemicals were the highest purity available and were obtained from Sigma unless otherwise noted.

2.2. Cell cultures

Three human pancreatic cancer cell lines were obtained from seed stocks at the American Type Culture Collection, (ATCC Number), Rockville, MD. These cell lines included the poorly-differentiated adenocarcinoma BxPC-3, (CRL-1687) (Loor et al., 1982), largely undifferentiated epithelial carcinoma MIA PaCa-2, (CRL-1420) (Yunis et al., 1977), and ductal epithelioid carcinoma PANC-1 (CRL-1469) (Lieber et al., 1975). The poorly differentiated MutJ cell line, (UACC-462), (Korc et al., 1986c) was obtained from the Cell Culture Shared Service of the Arizona Cancer Center. All adherent cell lines were cultured at 37°C in a humidified atmosphere of 5% CO₂ and 95% air in RPMI 1640 media (GIBCO-BRL Products, Grand Island, NY) supplemented with 10% (v/v) heat inactivated bovine calf serum (Hyclone Laboratories, Logan, UT), 2 mMol L-glutamine, penicillin (100U/mL) and streptomycin (100 µg/mL).

2.3. Cytotoxicity assays

Cellular dehydrogenase activity reflects mitochondrial activity of living cells to metabolize 3-(4,5-

dimethylthiazol-2-yl)-2,5-diphenyl tetrazolium bromide, (MTT) (Sigma Chemical Co., St. Louis, MO) to a blue formazan crystal based upon a method developed by Mosmann (Mosmann, 1983). Adherent pancreatic cell lines in RPMI media 1640 were dispensed in 100 μ L aliquots into 96-well plates with a final number of 2,000-5,000 cells per well. After 24 hr, 100 μ l of drug solution was added to each well in order to achieve the final desired single or combined drug concentration in 200 μ L per well. Plates were incubated at 37°C for an indicated time, followed by the addition of 50 μ L of MTT solution (1mg/mL) to each well for 4 hours at 37°C. The 96-well plates were then centrifuged for 5 min at 2000 rpm, the medium aspirated, and 100 μ L of DMSO (Baxter Healthcare Co., Muskegon, MI) was added to each well. Plates were shaken for 5 minutes and O.D. was read at 540 nm on a microplate reader (Biomek 1000, Beckman Instruments, Palo Alto, CA). The data are expressed as the percent of cells surviving compared to control cells, calculated from absorbance corrected for background absorbance.

$$\% \text{Cell Surviving} = \frac{(\text{Sample}_{\text{O.D.}} - \text{Background}_{\text{O.D.}})}{(\text{Control}_{\text{O.D.}} - \text{Background}_{\text{O.D.}})} \times 100$$

The surviving fraction of cells was determined by dividing the mean absorbance values of the drug-treated sample or by

vehicle-treated cells. The IC_{50} for each drug is defined as the drug concentration that inhibits growth to 50% of untreated control and calculated from sigmoidal analysis of the dose-response curve.

Imexon in buffered saline was added to cells undergoing non-confluent growth for a variety of time periods to assess the schedule-dependence of drug-induced growth inhibition. These time periods ranged from 8 hours to 120 hours at 37°C. The integrated IC_{50} x exposure time (mMol x hours) was used as an assessment of the schedule-dependency of imexon (AUC). Exposures with the lowest AUC represent the most effective scheduling. Differences greater than 20% in AUC are considered to be schedule-dependent.

2.4. Median Effect Analysis

Drug interaction between imexon (μ Mol) and gemcitabine (nMol) was assessed at a fixed ratio using median effect analysis (Chou and Talalay, 1984). The median effect principle allows for the analysis of multiple drugs in cellular systems based upon the pharmacologic median doses, or required drug concentrations for 50% growth inhibition (IC_{50} values). The procedure determines the combined drug effect, regardless of whether the effects of the drug are

completely independent or not, or the dose-effect curves are hyperbolic (first-order) or sigmoidal (higher order). Median effect analysis results in a fixed ratio, or combination index (CI), where $CI < 1$, $CI = 1$ and $CI > 1$ indicate synergistic, additive, and antagonistic effects, respectively. Analysis for mutually exclusive drug effects was determined by the following formula:

$$CI = (D)_1 / (D_x)_1 + (D)_2 / (D_x)_2$$

$(D_x)_1$ and $(D_x)_2$ are the concentrations of imexon and gemcitabine, respectively, and $(D)_1$ and $(D)_2$ are the drug concentrations required to inhibit cell growth by 50%.

To determine if sequential treatment with imexon or gemcitabine affected the combination index (CI) compared to simultaneous drug administration, pancreatic cells were treated with imexon or gemcitabine 24 hr. Cells were exposed to continuous imexon or gemcitabine for 24 hr, with subsequent addition of the other drug. Combination indices were obtained after 120 hr of continuous exposure to both drugs. Data analysis was performed as described above using Microcal Origin software (Originlab Corporation, Northampton, MA).

2.5. In vivo SCID mice study

Female SCID mice were purchased from a breeding colony maintained by University of Arizona Animal Care facility (Tucson, AZ). Mice were housed according to the guidelines of the American Association for Laboratory Animal Care under protocols approved by the University of Arizona Institutional Animal Care and Use Committee. Mice were housed in standard microisolator caging on wood chip bedding and provided with Isoblox (Harlan/Teklad, Madison, WI). Mice received standard sterilized rodent chow (Harlan/Teklad, Madison, WI) and sterile water *ad libitum*. Mice were maintained on a 12 hour/12 hour light/dark schedule. All protocols were approved by the Institutional Animal Care and Use Committee for the University of Arizona. At the termination of the experiment, mice were euthanized according to procedures outlined by the American Veterinary Medical Association.

Immune deficient SCID mice were injected with 10×10^6 PANC-1 cells in the right rear flank. After 24 hr or 40 d, for the tumor growth inhibition assay, or for the tumor regression model, imexon treated mice were injected IP with 100 mg/kg imexon, repeated every 24 hr for nine consecutive days. Gemcitabine treated mice were injected IP with 180

mg/kg gemcitabine on days 1, 5 and 9. Mice receiving combined therapy were injected IP with 100 mg/kg imexon every 24 hr for nine consecutive days and 180 mg/kg gemcitabine days 1, 5 and 9. Tumor length and width was measured twice every ten days post PANC-1 cell injection and tumor volume was calculated using the formula tumor volume (TV) = (length x width²)/2.

The end points for assessing solid tumor response in the SCID mice involved four calculations. These calculations were based upon NCI criteria (Bissery and Chabot, 1991). First, the Tumor Growth Inhibition value (T/C) at a median tumor weight of 750 to 1500 mm³:

$$T/C (\%) = \frac{\text{Median Tumor weight of the treated mouse}}{\text{Median tumor weight of the control mouse}} \times 100$$

Compounds are considered active if the T/C value is less than 42%, and highly active if the T/C is $\leq 10\%$. The Tumor Growth Delay value (T-C) is the difference in the median time for the tumors in each group to reach 750 to 1,500 mm³, and the tumor doubling time, (Td) is determined from a log linear growth plot in the control cells over the range of tumor cell volumes from 100 to 1,000 mm³. This then allows for the calculation of the Tumor Cell Kill:

$$\text{Log}_{10} \text{ cell kill} = \frac{\text{T-C value in days}}{3.32 \times \text{Td}}$$

2.6. Imexon uptake

PANC-1 cells were simultaneously exposed to radiolabeled imexon ($[^{14}\text{C}]$ -imexon, 55.04 mCi/mMol) and 10 nMol gemcitabine for 5, 15, 30, 60, 120, and 240 min. Briefly, 0.5×10^6 PANC-1 cells were seeded in 6-well plates and exposed to 500 μMol $[^{14}\text{C}]$ -imexon. After exposure, the cells were washed three times with ice-cold PBS and lysed with 1.0 mL of a lysis buffer containing 30 mMol Hepes, 7.5, 10 mMol NaCl, 5 mMol MgCl_2 , 25 mMol NaF, 1 mMol EGTA, 1% Triton-X-100 and 10% glycerol. The solution was aspirated and spun at 13,000 rpm for 5 min and 200 μl of supernatant containing free $[^{14}\text{C}]$ -imexon was counted in 2.0 mL of Ecolite scintillation cocktail. Experiments were performed three times in triplicate and data were expressed as the average number of disintegrations per minute (DPM) \pm S.E. per time point.

2.7 Gemcitabine uptake

PANC-1 cells were simultaneously exposed to radiolabeled gemcitabine ($[^3\text{H}]$ -gemcitabine, 11.0 Ci/mMol) and 100 or 300 μMol imexon for 15, 30, 60 and 120 min. Briefly, 0.25×10^6 PANC-1 cells were seeded in 24-well plates and

treated with 100 nMol [³H]-gemcitabine and 100 or 300 μMol imexon. As a control, cells were treated with 100 nMol [³H]-gemcitabine and 1.0 μMol unlabeled gemcitabine. After treatment, the cells were washed three times with ice-cold PBS and lysed with 500 μL 0.1% NaOH and 0.1% SDS solution. The wells were rinsed with 2.0 mL PBS. The free solution containing [³H]-gemcitabine was counted in 5.0 mL of Ecolite scintillation cocktail. Experiments were performed three times in triplicate and data were expressed as the average number of disintegrations per minute (DPM)±S.E. per time point.

2.8. Deoxycytidine kinase assay

Deoxycytidine kinase activity was measured according to the method of Bouffard *et al.* (Bouffard *et al.*, 1993). Briefly, 2-3 x 10⁷ PANC-1 cells were washed in 10 mL of 0.9% NaCl. Cells were then centrifuged at 200 *g* for 5 min and resuspended in 1 mL of 0.9% NaCl and transferred to a 1.5 mL Eppendorf centrifuge tube. The cells were centrifuged at 12,000 *g* for 5 s and resuspended in 200 μL of 5 mMol Tris-Cl, pH 7.4. Next, the cells were freeze-thawed three times and centrifuged at 12,000 *g* for 15 min. Supernatant was removed and adjusted to 50 mMol Tris-Cl, pH 7.4 and stored

at -80°C until enzyme assay. Protein concentrations were determined utilizing the bicinchonic acid reagent (Pierce Chemical Co.) and bovine serum albumin as the standard. The incubation mixture consisted of 100 mMol Tris-Cl at pH 8.0, 10 mMol ATP, 5 mMol MgCl_2 , 100 pMol [^3H]-deoxycytidine (22 Ci/mMol), 5 μL of enzyme plus imexon and incubated at 37°C for 30 min. The experiment was stopped by diluting the drug reaction mixture with 3 mL of cold 0.0001 N HCl. The mixture was then placed on Whatmann P81 phosphocellulose disc (Whatmann, Clifton, NJ). P81 disc were washed once with H_2O , 1 mL of NHCl and 3 mL of H_2O twice before use. The incubation mixture flowed through the disc by gravity. It was allowed to dry and was placed in 2.0 mL Ecolite scintillation fluid and assayed using a Beckman LS5000TD spectrometer. Experiments were performed three times in triplicate and data were expressed as the average number of disintegrations per minute (DPM) \pm S.E. per time point.

2.9. Deoxycytidine deaminase assay

The dCD mediated conversion of deoxycytidine monophosphate (dCMP) to deoxyuridine monophosphate (dUMP) was monitored by an HPLC analysis capable of efficiently separating both nucleotides (Camiener, 1967c). Briefly, 2-3

$\times 10^7$ PANC-1 cells were washed in 10 mL of 0.9% NaCl. Cells were then centrifuged at 200 g for 5 min and resuspended in 1 mL of 0.9% NaCl and transferred to a 1.5 mL Eppendorf centrifuge tube. The cells were centrifuged at 12,000 g for 5 s and resuspended in 200 μ L of 5 mMol Tris-Cl, pH 7.4. Next, the cells were freeze-thawed three times and centrifuged at 12,000 g for 15 min. Supernatant was removed and adjusted to 50 mMol Tris-Cl, pH 7.4 and stored at -80°C until enzyme assay. Protein concentrations were determined utilizing the bicinchonic acid reagent (Pierce Chemical Co., Rockford IL) and bovine serum albumin was used as the standard.

The incubation medium consisted of 100 mMol Tris-HCl (pH 8.0), 10 mMol ATP, 65 mMol MgCl_2 , 100 mMol dCMP and appropriate amount of enzyme in a total volume of 200 μ L. The reaction mixture was incubated at 37° for 30 min. The reaction was stopped by deproteinization at 96°C for 5 min. After centrifugation, 20 μ L of the supernatant was measured by HPLC analysis using an Adsorbosphere® C18 nucleoside/nucleotide, column 7 μ M, 250 x 4.6 mm (Alltech Associates Inc., Waukegan Rd. Deerfield, IL). The gradient consisted of buffer A: 60 mMol $\text{NH}_4\text{H}_2\text{PO}_4$ & 5 mMol

tetrabutylammonium phosphate, pH 5.0 and buffer B: methanol & 5 mMol tetrabutylammonium phosphate; 10 to 20% B over 10 min with a flow rate of 1.5 mL/min. UV detection was set at 254 nm. Deoxycytidine deaminase activity was determined from the percentage of dUMP appearing.

2.10. PyNase assay

Initially, $2-3 \times 10^7$ PANC-1 cells were washed in 10 mL of 0.9% NaCl. Cells were centrifuged at 200 g for 5 min and suspended in 1 mL of 0.9% NaCl and transferred to a 1.5 mL Eppendorf centrifuge tube. The cells were centrifuged at 12,000 g for 5 s and resuspended in 200 μ l of 5 mMol Tris-Cl, pH 7.4. Next, the cells were freeze-thawed three times and centrifuged at 12,000 g for 15 min. The supernatant was removed and adjusted to 50 mMol Tris-Cl, pH 7.4 and stored at -80°C until enzyme assay. Protein concentrations were determined utilizing the bicinchonic acid reagent (Pierce Chemical Co.) and bovine serum albumin as the standard. The 160 μ L incubation mixture contained 25 mMol Tris-Cl, pH 7.4, 136.0 pMol [^3H]-deoxycytidine (22 Ci/mMol), 40 μ g of enzyme with or without imexon. The mixture was incubated for 30 min at 37°C and the experiment was stopped by boiling the samples at 95°C for 5 min. The mixture was then placed on

Whatmann P81 phosphocellulose disc. The P81 discs were washed once with H₂O, 1 mL of NHCl and then twice with 3 mL of H₂O before use. The incubation mixture flowed through the disc by gravity. The disc was allowed to dry and was placed in Ecolite scintillation fluid and assayed using a Beckman LS5000TD spectrometer.

2.11. Ribonucleotide reductase assay

The ribonucleotide reductase assay was followed according to the method of Zhou, *et al.* with slight modifications (Zhou *et al.*, 2002a). Briefly, PANC-1 cells were plated at 1×10^6 cells per well in triplicate in 60-mm² plates. The cells were treated with drug for 2 hr, rinsed two times with solution A (150 mMol sucrose, 80 mMol KCl, 35 mMol HEPES, pH 7.4, 5 mMol KPO₄, pH 7.4, 5 mMol MgCl₂, and 0.5 mMol CaCl₂) and permeabilized with 0.025 mg/mL lysolecithin in Solution A. Plates were rinsed one time with 37°C PBS, and then incubated with [¹⁴C]-CDP (6 µL/sample) in Solution B (50 mMol HEPES, pH 7.4, 10 mMol MgCl₂, 8 mMol DTT, 0.06 mMol FeCl₃, 7.5 mMol KPO₄, pH 7.4, 0.75 mMol CaCl₂, 10 mMol phosphoenolpyruvate, 0.2 mMol dGDP, dADP and dTDP) for 1 hr at 37°C. Following incubation the cells were rinsed three times with ice-cold PBS, two times with 5% TCA and incubated at 80°C for 30 min in 1 mL 5% TCA.

Next, 0.1% SDS, 0.1 N NaOH was added to each well, rinsed with 1 mL PBS and counted in 8 mL Ecolite scintillation fluid.

2.12. Western blot analysis

Pancreatic cancer cells treated with imexon were washed with PBS and lysed using a buffer consisting of 30 mMol HEPES, pH 7.5, 10 mMol NaCl, 5 mMol MgCl₂, 25 mMol NaF, 1 mMol EGTA, 1% Triton-X-100, 10% glycerol supplemented with phenylmethylsulfonyl fluoride (PMSF, 2 mMol), soybean trypsin inhibitor (STI, 25 µg/mL), aprotinin (10 µg/mL), leupeptin (25 µg/mL), and dithiothreitol (100 mMol, all Sigma) on ice. The resulting lysate was spun for 20 minutes at 4°C. The protein content of lysate was determined using bicinchoninic acid reagent (Pierce Chemical Co.). Next, 6X sample buffer (Laemmli et al., 1970) was added to the samples and they were boiled for 10 min and placed on ice. Protein aliquots were then loaded (50 µg/lane) on 8-10 % SDS-polyacrylamide gel for size fractionation by electrophoresis. Proteins were then transferred overnight onto Immobilon-P PVDF[®] transfer membrane (Millipore, Bedford, MA) at 65 mV overnight. Membranes were then blocked with 5% milk protein in Tris buffered saline/0.05% Tween (TBST).

Membranes were then immunostained with either (ribonucleotide reductase subunit 1) goat anti-M₁ polyclonal antibody (1:100, Santa Cruz Biotechnology, Santa Cruz, CA), 2) goat anti-M₂ (ribonucleotide reductase subunit polyclonal antibody (1:100, Santa Cruz Biotechnology, Santa Cruz, CA), 3) rabbit polyclonal anti -p38 or -phospho-p38 (1:1000, Cell Signaling, Beverly, MA), 4) or monoclonal anti- β -actin (1:10000, Sigma, St. Louis, MO). Membranes were washed and incubated with mouse anti-goat IgG antisera conjugated to horseradish peroxidase (1:10000 Jackson ImmunoResearch Laboratories, Inc., West Grove, PA) or anti-mouse IgG antisera (1:10000 Jackson ImmunoResearch Laboratories, Inc., West Grove, PA). Antibody complexes were detected using the ECL chemiluminescence detection system (Amersham, Pharmacia Biotech, Piscotaway, NJ). Protein band densities were analyzed utilizing Image Quant Software, version 5.0 (Molecular Dynamics, Sunnyvale, CA).

2.13. Quantitative real-time PCR

Ribonucleotide reductase (RNR) mRNA levels were measured by reverse transcriptase (RT) PCR using the Applied Biosystems Kit (Foster City, CA) Taqman®. Probe and primer sets for RNR subunits M₁ (Genbank sequence NM 001033) and M₂

(Genbank sequence NM 001034) were obtained from the Assays-on-Demand™. The conserved ribosomal subunit L-30 housekeeping gene was amplified concurrently, as an internal standard for equivalent mRNA amount. All primers were designed to amplify across an intron/exon boundary, to ensure genomic DNA would not be amplified.

2.14. Cell cycle analysis: propidium iodide

PANC-1 cells (0.5×10^6) were seeded in 100 mm² plates. After exposure to drug, the cells were trypsinized, placed in a 15 mL centrifuge tube filled with ice-cold PBS and centrifuge at 1200 RPM for 5 min. The supernatant was aspirated and the pellet was resuspended in 1 mL of ice-cold PBS. Three mL of 70% cold ethanol was added to the cells and they were stored overnight at 4°C. The cells were centrifuged at 1500 RPM for 10 min and resuspended in 0.5 mL cold PBS. Next, 25 μ L of RNase A and 1/40 volume of 1.6 mg/mL propidium iodide were added. The cells were then incubated at 37°C for 30 minutes and analyzed on the FACScan at the Flow Cytometry Shared Services (FCSS) (San Jose, CA) and analyzed using Cell Quest software (BD, San Jose, CA).

2.15. Gemcitabine DNA incorporation assay

Radiolabeled gemcitabine incorporation into DNA was assessed according to the method of Mayr with minor

modifications (Mayr et al., 1997a). Briefly, 100 mm² plates were seeded with 0.5 x 10⁶ PANC-1 cells. Cells were simultaneously exposed to 100 nMol [³H]-gemcitabine and 300 or 500 μMol imexon for 4, 8 and 24 hr. After exposure, the cells were rinsed 3 times with ice-cold PBS, three times with 500 μL of ice-cold 5% TCA, and 1 time with 500 μL ice-cold PBS. Following the final PBS wash, 500 μL of ice-cold 5% TCA was added and the plates were incubated at 80°C for 30 min. Plates were allowed to cool and 1 mL of 0.1% NaOH and 0.1% SDS were added to each well. The wells were rinsed and total contents analyzed for radioactivity in 5 mL of Ecolite scintillation fluid and counted using a Beckman LS5000TD spectrometer.

2.16. ⁶⁰Co irradiation of human pancreatic cancer cells

Human pancreatic cancer cells in cell culture were trypsinized, centrifuged at 2000 x g for 10 min, and resuspended in media at a concentration of 1 x 10⁶ cells per mL. Cell suspensions were used to seed 96-well plates at 2000 cells per well. After 24 hr various concentrations of imexon was added to each column of wells for a period of 24 hr prior to ⁶⁰Co irradiation. The dose in Gy of ⁶⁰Co irradiation was determined by the following formula, where t = time, DR_c = calibrated dose rate for the day, PSF = Peak

scatter factor, FCC = fractonal depth dose, S = Jaws of scatter factor, SSD = source to surface distance, d = depth of prescription, and Δt = time error:

$$t = \frac{\text{Dose}}{[(DR_c)(PSF)(FDD)(S)[(80 + d)/(SSD + d)]^2(0.99)] \pm \Delta t}$$

Following ^{60}Co irradiation, plates were incubated for 96 hr @ 37°C and cell death was analyzed using MTT assay.

2.17. Statistical Analyses:

Paired sample T-test comparisons were used to analyze differences in the enzyme assays and flow cytometry studies.

3. CHAPTER RESULTS

3.1. Cytotoxicity analysis

3.1.1. Schedule dependence of imexon in PANC-1, MIA PaCa-2, MutJ and BxPC-3 human pancreatic cancer cell lines

In vitro anti-tumor activity of imexon and gemcitabine was evaluated in PANC-1, MIA PaCa-2, MutJ and BxPC-3 human pancreatic cancer cells by MTT analysis. The data suggests that the effect of imexon is highly dependent upon the period of drug exposure (Figure 11). As indicated by the integral concentration x time, ($c \times t$), calculations for 50% inhibition, a >4-fold exposure is required for drug exposures ≤ 24 hours than for longer exposures in the PANC-1 cell line (Table 2). Notably, the $c \times t$ value for drug exposure times ≥ 48 hours were nearly constant at approximately 7542.0 $\mu\text{M}\cdot\text{hr}$ for the PANC-1 cell line.

3.1.2. MTT IC_{50} values of imexon and gemcitabine in PANC-1, MIA PaCa-2, MutJ and BxPC-3 human pancreatic cancer cell lines

Figures 12 and 13 display the results from three different MTT experiments in the PANC-1, MIA PaCa-2, MutJ and BxPC-3 human pancreatic cancer cell lines treated for

120 hours with various concentrations of imexon and gemcitabine. Imexon and gemcitabine mean(S.D.) IC₅₀ values were 55.8±9.3 µMol and 9.2±5.6 nMol, respectively in the four human pancreatic cancer cells. The PANC-1 human pancreatic cancer cell line was more resistant to the cytotoxic effects of gemcitabine, requiring >2-fold gemcitabine than the MIA PaCa-2 cell line, with an IC₅₀ value of 17.1±2.6. The inhibitory concentrations at 120 hr for both imexon and gemcitabine are summarized in Table 3. The data suggest that human pancreatic cancer cells are not equally sensitive to the cytotoxic effects mediated by gemcitabine.

3.1.3. Median effect analysis of imexon and gemcitabine in combination against PANC-1, MIA PaCa-2, MutJ and BxPC-3 human pancreatic cancer cell lines

Drug interaction between imexon and gemcitabine was assessed at fixed ratios of (imexon: gemcitabine) 1:1, 1:2 and 2:1 and analyzed using median effect analysis by Chou and Talalay (Chou and Talalay, 1984). The PANC-1 human pancreatic cancer cell line demonstrated the greatest synergy at a fixed ratio of 1:1 imexon (µMol): gemcitabine (nMol) compared to fixed ratios of 1:2 or 2:1 (Figure 14).

At a fixed ratio of 1:1, the PANC-1, MutJ and BxPC-3 cells demonstrated synergy with ≥ 50 μMol imexon, whereas the MIA PaCa-2 cells showed synergy at ≥ 250 μMol imexon (Figure 15). To determine if sequential treatment with imexon or gemcitabine would alter the cytotoxic effect of the other agent, pancreatic cancer cell lines were exposed to imexon or gemcitabine first for 24 hr, and then combined with the other agent for a total of 120 hr. The data show that synergy was not enhanced with a 24 hr sequential drug treatment of either agent alone (Figures 16-19).

Table 2 Schedule-dependence of imexon in PANC-1 cells.

Time (hr)	PANC-1 IC ₅₀ (μMol)	Concentration x time for IC ₅₀ (μMol.hr)
8	1,701.4 ± 214.0	13,611.2
24	470.8 ± 96.5	11,299.2
48	252.0 ± 17.1	12,096.0
72	96.5 ± 6.2	6,948.0
120	62.1 ± 4.0	7,452.0

Table 2 IC₅₀ values of imexon for PANC-1 human pancreatic cancer cells determined by MTT assay. The results show that imexon is schedule dependent, requiring >4 times the drug concentration for exposures ≤48 hr. The results represent mean±S.E. of three experiments.

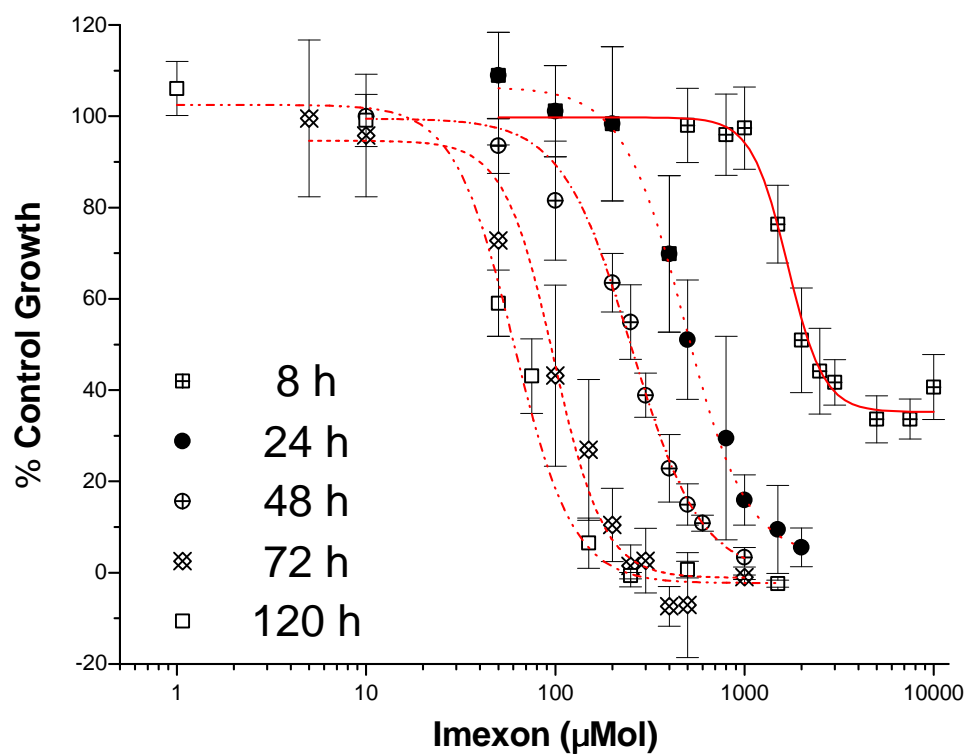


Figure 11 Cytotoxicity of imexon in PANC-1 human pancreatic cancer cells. Data shows schedule dependence of imexon in PANC-1 cells obtained by MTT analysis after 8, 24, 48, 72 and 120 hours treatment. The data represents mean \pm S.E. of three experiments.

Table 3 Imexon and gemcitabine cytotoxicity against PANC-1, MIA PaCa-2, MutJ and BxPC-3 human pancreatic cancer cells.

Cell Line	Gemcitabine IC ₅₀ (nMol)	Imexon IC ₅₀ (μMol)	Time (hr)
PANC-1	17.1 ± 2.6	62.1 ± 4.0	120
MIA PaCa-2	7.1 ± 0.2	53.0 ± 0.4	120
MutJ	8.6 ± 0.2	45.9 ± 3.4	120
BxPC-3	4.0 ± 0.3	55.8 ± 5.9	120

Table 3 IC₅₀ values for imexon and gemcitabine at 120 hr by MTT analysis. IC₅₀ values of imexon for human pancreatic cancer cells, with mean 55.8±9.3 μMol. IC₅₀ concentrations of gemcitabine for human pancreatic cancer cells, with mean(S.D.) 9.2±5.6 nMol. The data represents mean±S.E. of three experiments.

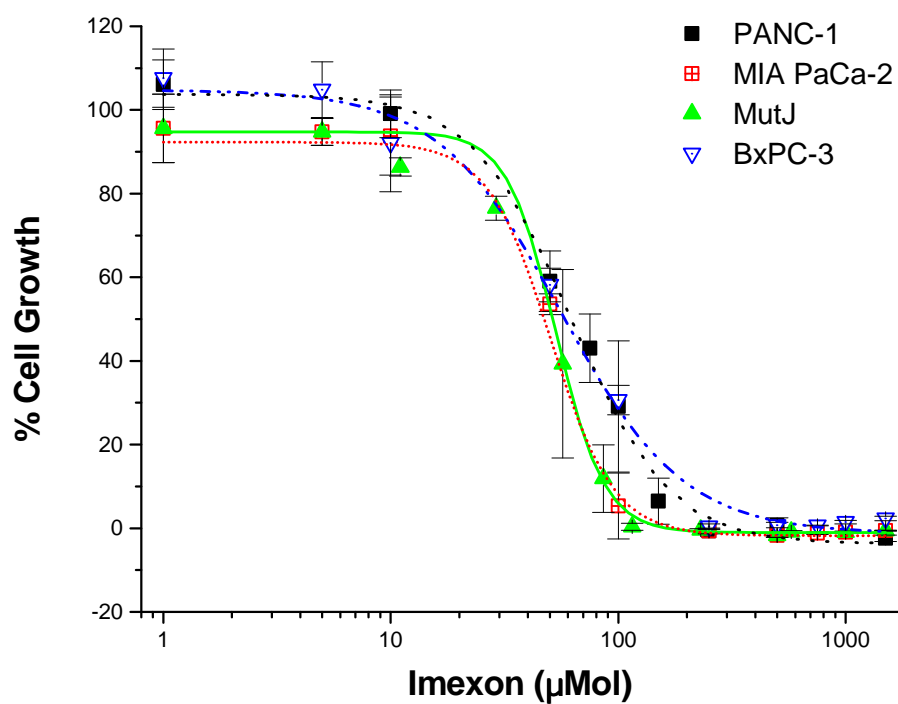


Figure 12 Cytotoxicity of imexon in PANC-1, MIA PaCa-2, MutJ and BxPC-3 human pancreatic cancer cells. The data shows IC₅₀ values obtained by MTT analysis after 120 hours continuous imexon exposure with mean 55.8 ± 9.3 µMol. The data represents mean \pm S.E. of three experiments.

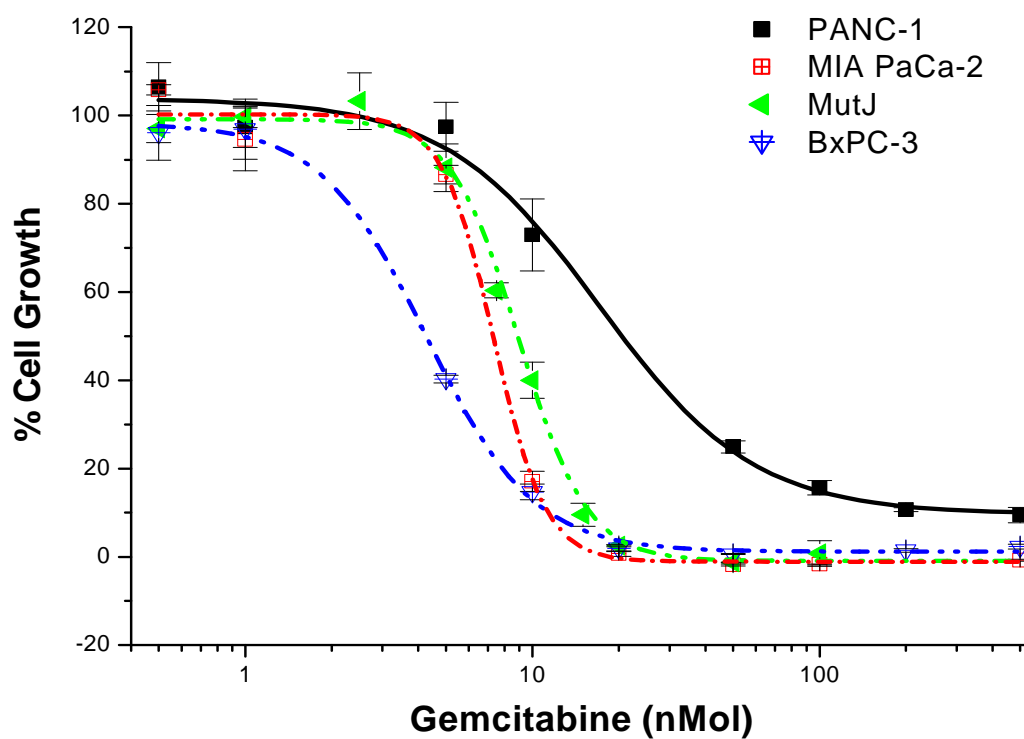


Figure 13 Cytotoxicity of gemcitabine in PANC-1, MIA PaCa-2, MutJ and BxPC-3 human pancreatic cancer cells. The data shows IC₅₀ values obtained by MTT analysis after 120 hours continuous gemcitabine treatment with mean (S.D.) 9.2±5.6 nMol. The data represents mean±S.E. of three experiments.

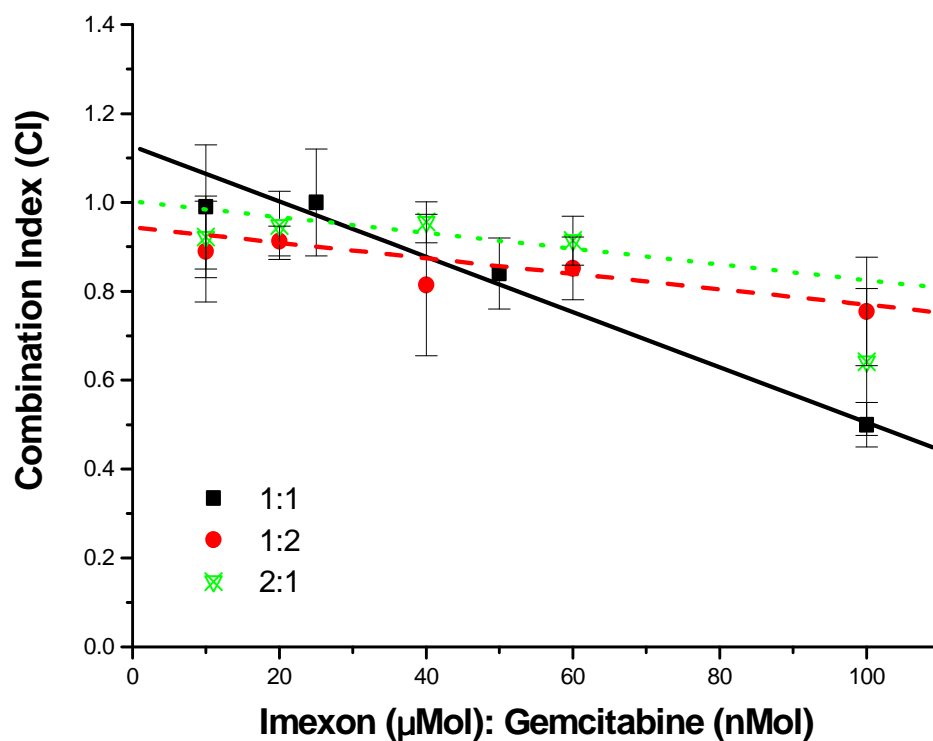


Figure 14 Median effect analyses in PANC-1 human pancreatic cancer cells. The data shows combination indices measured by MTT assay imexon and gemcitabine. Median effect analysis results in a combination index (CI), where $CI < 1$, $CI = 1$ and $CI > 1$ indicate synergistic, additive, and antagonistic effects, respectively. The data represents mean \pm S.E. of three experiments and a fixed ratio of 1:1, 1:2 or 2:1.

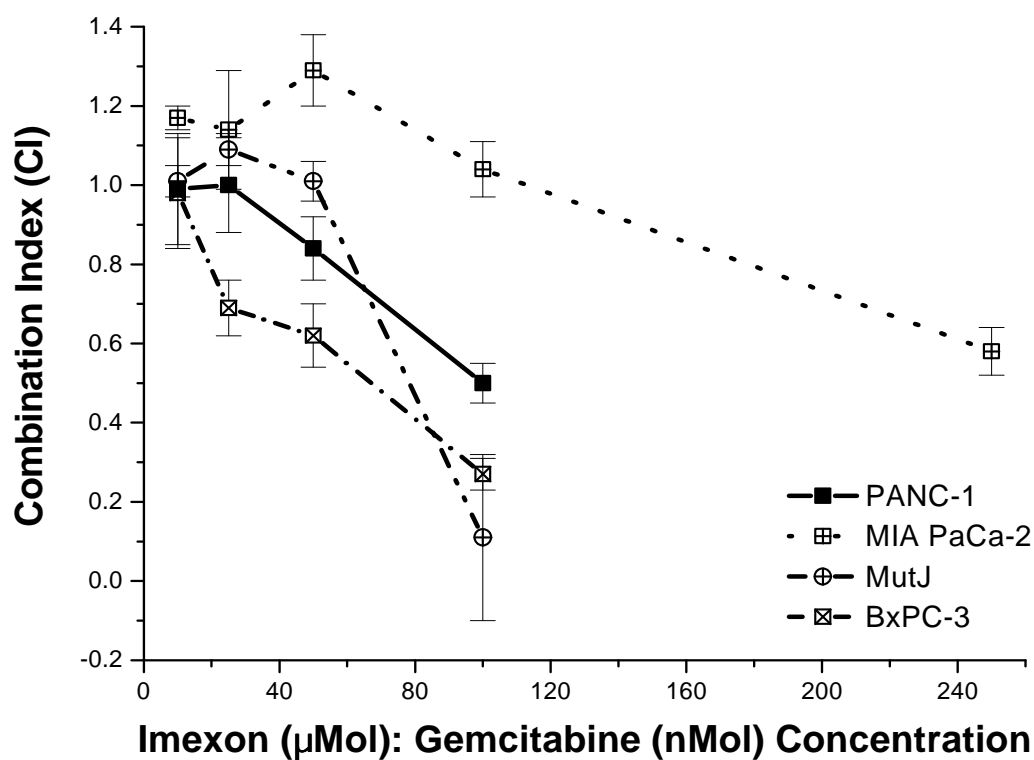


Figure 15 Median effect analysis in PANC-1, MIA PaCa-2, MutJ and BxPC-3 human pancreatic cancer cells. The data shows combination indices obtained by MTT analysis of imexon and gemcitabine combinations. Median effect analysis results in a combination index (CI), where $CI < 1$, $CI = 1$ and $CI > 1$ indicate synergistic, additive, and antagonistic effects, respectively. The data represents mean \pm S.E. of three experiments and a fixed ratio of 1:1.

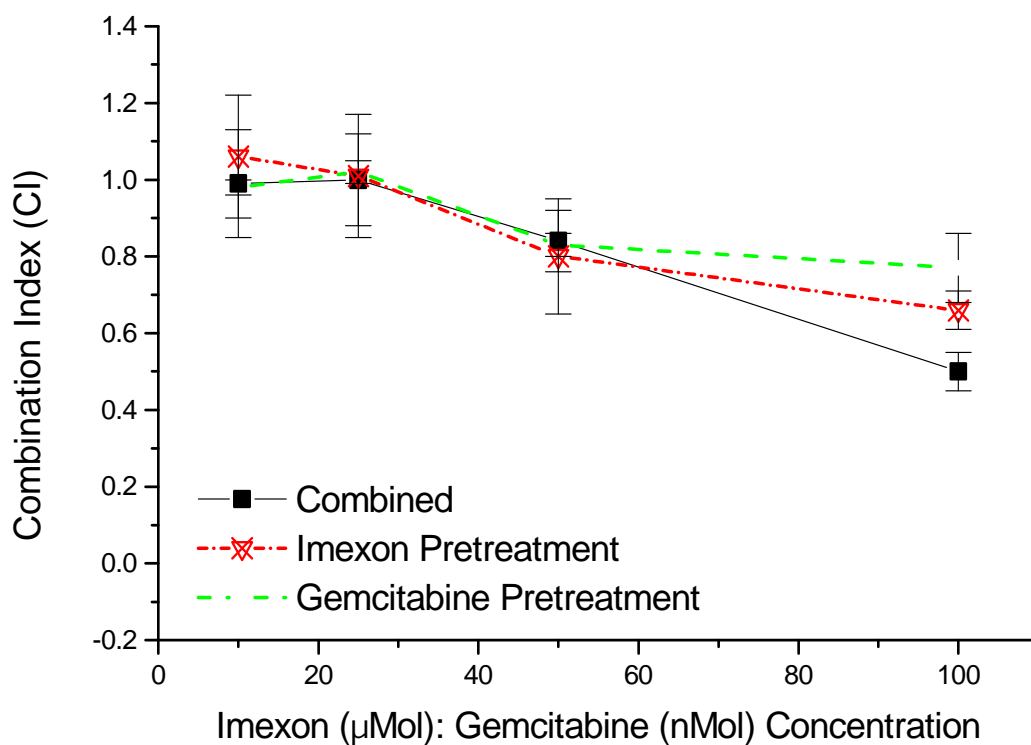


Figure 16 Median effect analyses in PANC-1 human pancreatic cancer cells with 24 hr sequential treatment with imexon or gemcitabine. The data shows combination indices obtained by MTT analysis of imexon and gemcitabine combinations. Median effect analysis results in a combination index (CI), where $CI < 1$, $CI = 1$ and $CI > 1$ indicate synergistic, additive, and antagonistic effects, respectively. The data represents mean \pm S.E. of three experiments and a fixed ratio of 1:1.

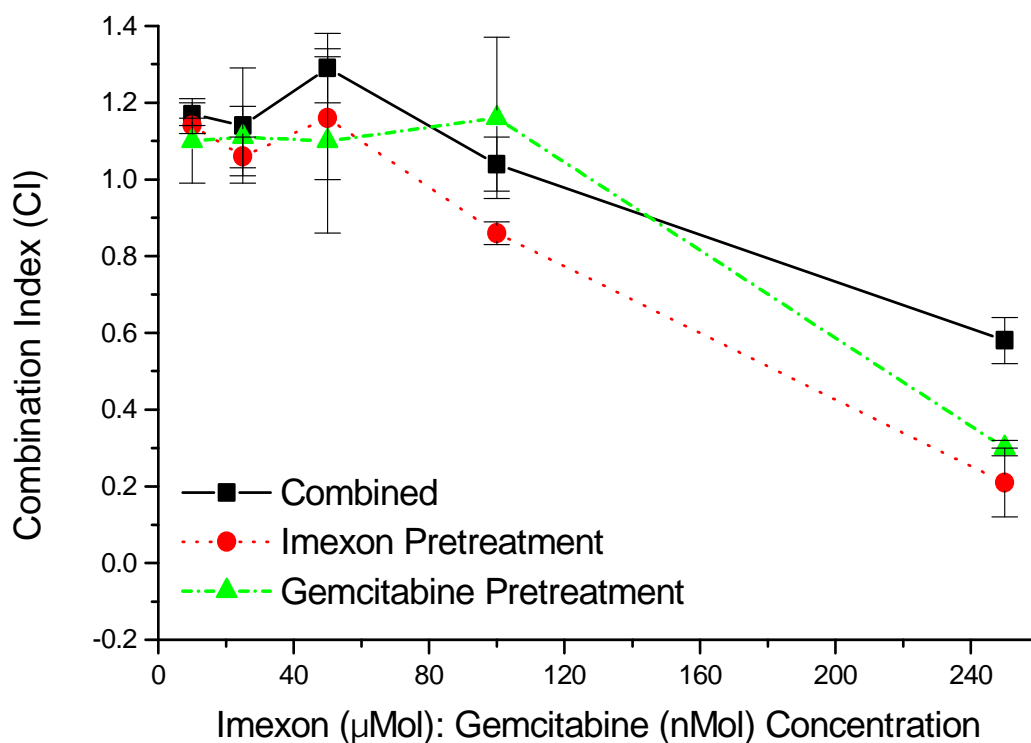


Figure 17 Median effect analyses in MIA PaCa-2 human pancreatic cancer cells with 24 hr sequential treatment with imexon or gemcitabine. The data shows combination indices obtained by MTT analysis of imexon and gemcitabine combinations. Median effect analysis results in a combination index (CI), where $CI < 1$, $CI = 1$ and $CI > 1$ indicate synergistic, additive, and antagonistic effects, respectively. The data represents mean \pm S.E. of three experiments and a fixed ratio of 1:1.

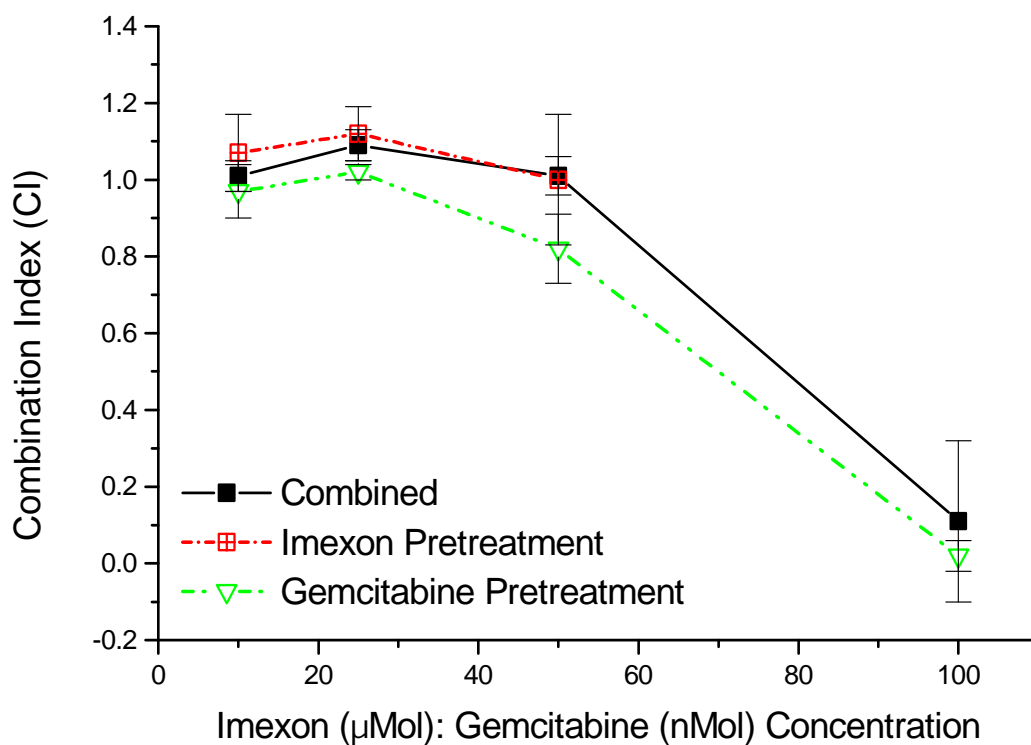


Figure 18 Median effect analyses in MutJ human pancreatic cancer cells with 24 hr sequential treatment with imexon or gemcitabine. The data shows combination indices obtained by MTT analysis of imexon and gemcitabine combinations. Median effect analysis results in a combination index (CI), where $CI < 1$, $CI = 1$ and $CI > 1$ indicate synergistic, additive, and antagonistic effects, respectively. The data represents $\text{mean} \pm \text{S.E.}$ of three experiments and a fixed ratio of 1:1.

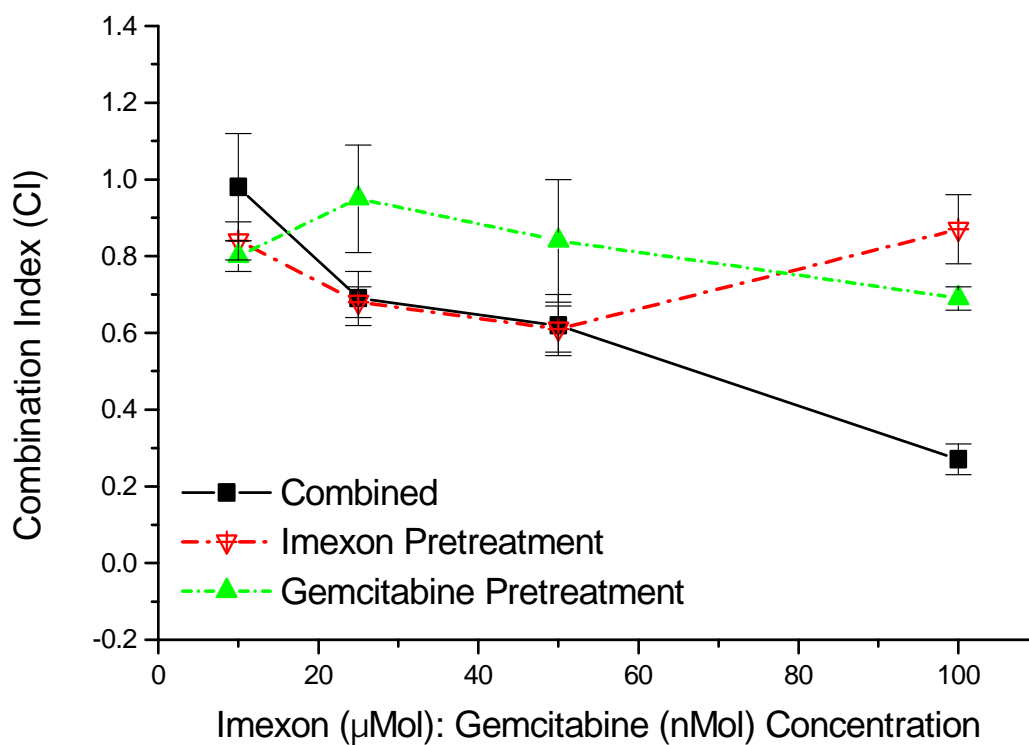


Figure 19 Median effect analyses in BxPC-3 human pancreatic cancer cells with 24 hr sequential treatment with imexon or gemcitabine. The data shows combination indices obtained by MTT analysis of imexon and gemcitabine combinations. Median effect analysis results in a combination index (CI), where $CI < 1$, $CI = 1$ and $CI > 1$ indicate synergistic, additive, and antagonistic effects, respectively. The data represents mean \pm S.E. of three experiments and a fixed ratio of 1:1.

3.2. Analysis of *in vivo* anti-tumor activity

3.2.1. Tumor growth inhibition model

To determine if imexon and gemcitabine possessed anti-tumor activity *in vivo*, severe combined immune deficient (SCID) mice were inoculated with PANC-1 human pancreatic cancer cells. The SCID mice were treated with imexon, gemcitabine, or a combination starting 24 hr post-tumor inoculation (Figure 20). Mice receiving imexon or gemcitabine alone demonstrated no significant delay in tumor growth volume (T-C) compared to control mice, with median tumor volume reaching 500 mm³ by days 89.1, 85.3 and 84.1, for control, imexon, and gemcitabine treated mice, respectively. Mice receiving the combination treatment had a calculated (T-C) of 112.4 d, demonstrating a difference >20 days to reach a median tumor volume of 500 mm³ compared to control mice. At day 100, Tumor Growth Inhibition values (T/C) were 104.1%, 81.1%, and 24.4% for imexon, gemcitabine and combination treated mice, respectively. Importantly, only mice treated with the combination had a (T/C) value less than 42%. This is considered an "active" combination by National Cancer Institute (NCI) standards. The tumor-doubling-time (Td) was 9.8, 13.7, 18.0 and 13.7 days for control mice, imexon, gemcitabine and the combination,

respectively (Table 4). The Tumor Cell Kill value (TCK) for control, imexon, gemcitabine, and combination treated mice were 2.8, 2.6, 2.6 and 3.5, respectively. The data suggests that significant tumor growth inhibition of PANC-1 cells *in vivo* only occurs with combination treatment, and tumor growth inhibition with single-agent treatment results in similar PANC-1 cell growth *in vivo* as mice receiving no treatment.

3.2.2. Tumor regression model

In vivo evaluation of treating established subcutaneous PANC-1 tumors in SCID mice was also performed (Figure 21). The SCID mice were treated with imexon, gemcitabine, or a combination 40 d post-tumor inoculation. At this time, the mean tumor size was approximately $25.8 \pm 12.6 \text{ mm}^3$. Mice receiving imexon or gemcitabine had modest degrees of tumor growth inhibition, (T-C) values of 40.6 d and 56.8 d. In contrast, mice receiving the combination treatment had a (T-C) value of 74.3 d, and tumors regressed approximately 75% following combination therapy (Figure 22). The Tumor Growth Inhibition values (T/C) for combination treated mice was 25.4% and is considered an active drug combination by NCI standards.

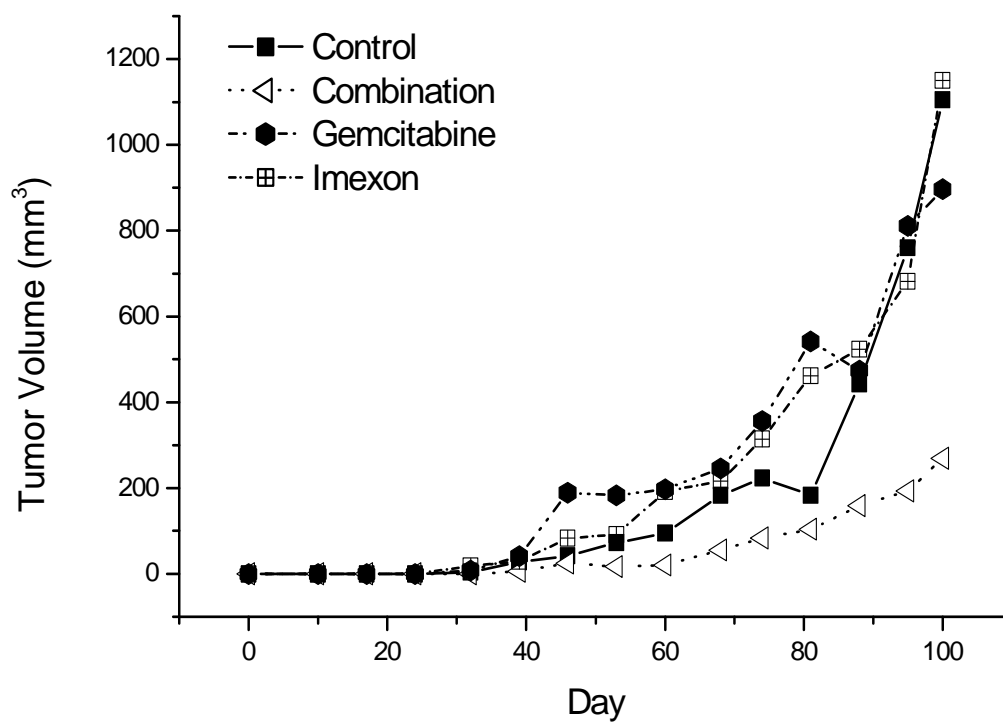


Figure 20 Tumor volume (mm³) of SCID mice inoculated with PANC-1 human pancreatic cancer cells. The data shows tumor volume of SCID mice treated 24 hr after tumor cell injection. Data represents an n=4 for each group.

Table 4 SCID mice analysis: NCI criteria.

	(T-C) (days)	(T/C) (%)	(Td) (days)	(TCK)
Control	89.1	100.0	9.8	2.8
Imexon	85.3	104.1	13.7	2.6
Gemcitabine	84.1	81.1	18.0	2.6
Combination	112.4	24.4	13.7	3.5

Table 4 Analysis of PANC-1 tumor growth in SCID mice by NCI criteria. SCID mice were inoculated with PANC-1 cells and treated 24 hr post-tumor inoculation. The table shows the Tumor Growth Volume (T-C), Tumor Growth Inhibition (T/C), Tumor Doubling Time (Td) and Tumor Cell Kill (TCK) values determined by exponential growth curve analysis.

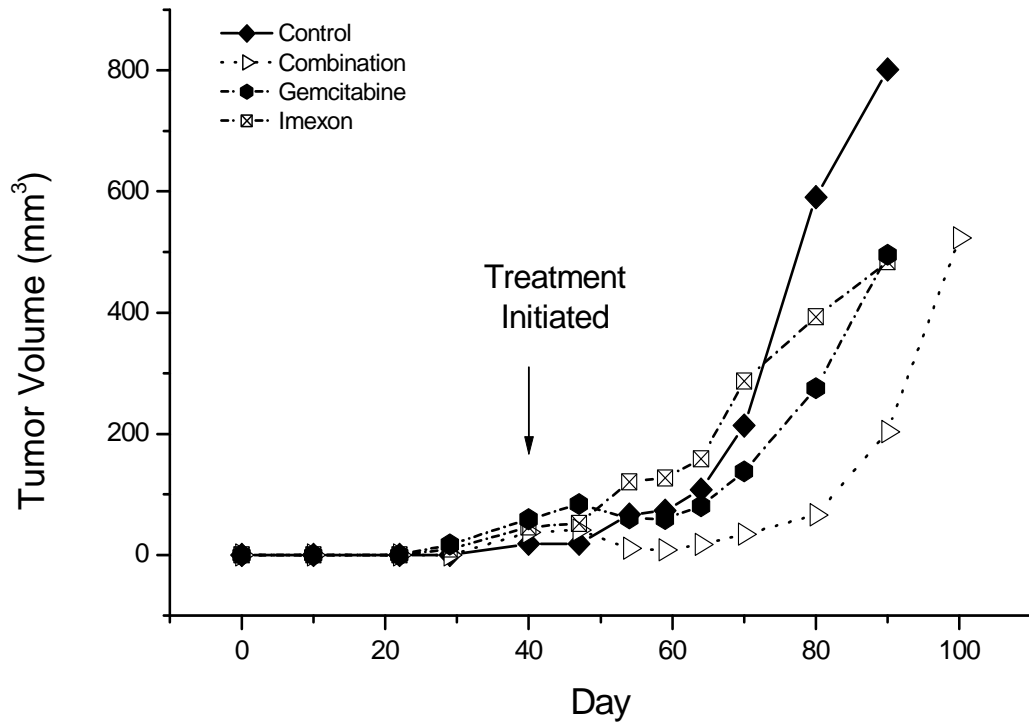


Figure 21 Tumor volume (mm³) of SCID mice inoculated with PANC-1 human pancreatic cancer cells. The data shows tumor volume of SCID mice treated 40 d after tumor cell injection. Data represents an n=4 for each group.

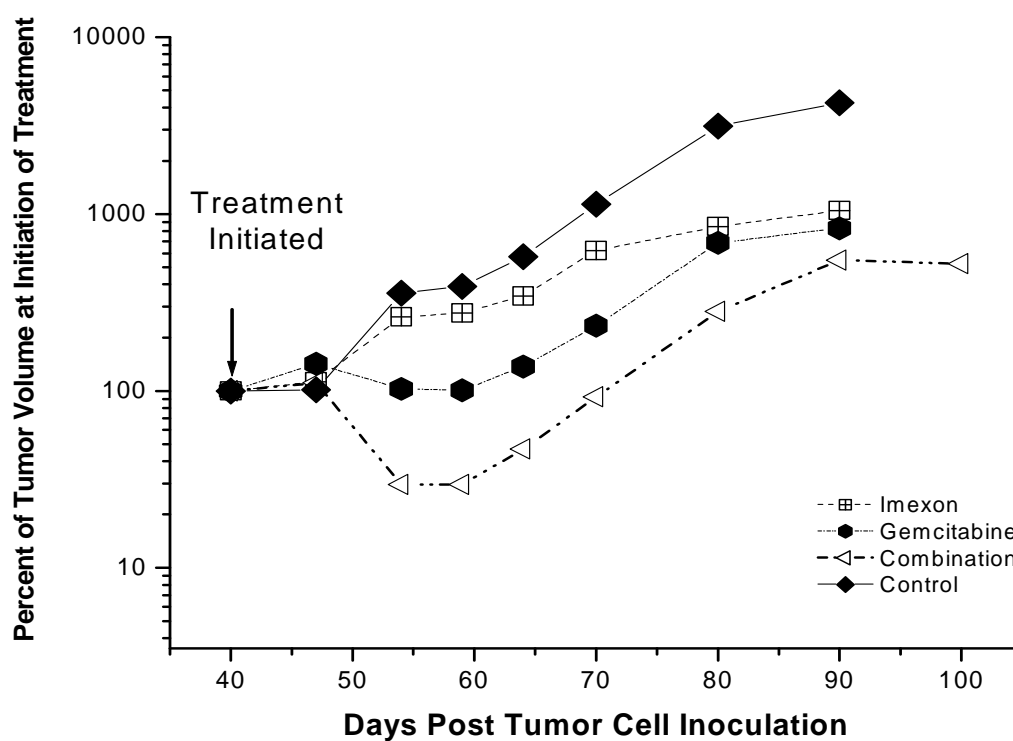


Figure 22 Percent tumor volume (mm^3) of SCID mice inoculated with PANC-1 human pancreatic cancer cells. The data represents percent tumor volume of SCID mice treated 40 d after tumor cell injection. Data represents the mean volume of $n=4$ animals in each group.

3.3. Analysis of [¹⁴C]-imexon and [³H]-gemcitabine uptake in pancreatic cancer cells

3.3.1. [¹⁴C]-imexon uptake

To assess the uptake of imexon in the presence of gemcitabine, PANC-1 cells were exposed to 500 μ Mol [¹⁴C]-imexon and 10 nMol gemcitabine. Because imexon is a small molecule and does not require specific transport processes to enter cells, these studies are based on the hypothesis that gemcitabine would not alter the diffusion of imexon into the cytosolic compartment. At time points ranging from 5 min to 4 hr, imexon diffusion was not significantly affected by the presence of 10 nMol gemcitabine (Figure 23).

3.3.2. [³H]-gemcitabine uptake

Cellular uptake of gemcitabine is mediated by several nucleoside transporters (Clarke et al., 2002). To determine if the observed synergy was related to enhanced gemcitabine uptake, PANC-1 cells were exposed to 100 nMol [³H]-gemcitabine in the presence of 100 or 300 μ Mol imexon. At time points ranging from 15 min to 4 hr, gemcitabine transport was not significantly affected by the presence of 100 or 300 μ Mol imexon (Figure 24). In contrast, 1.0 μ Mol unlabeled gemcitabine competitively inhibited radiolabeled gemcitabine uptake. These data suggest that imexon does not

enhance nucleoside transporter mediated uptake of
gemcitabine.

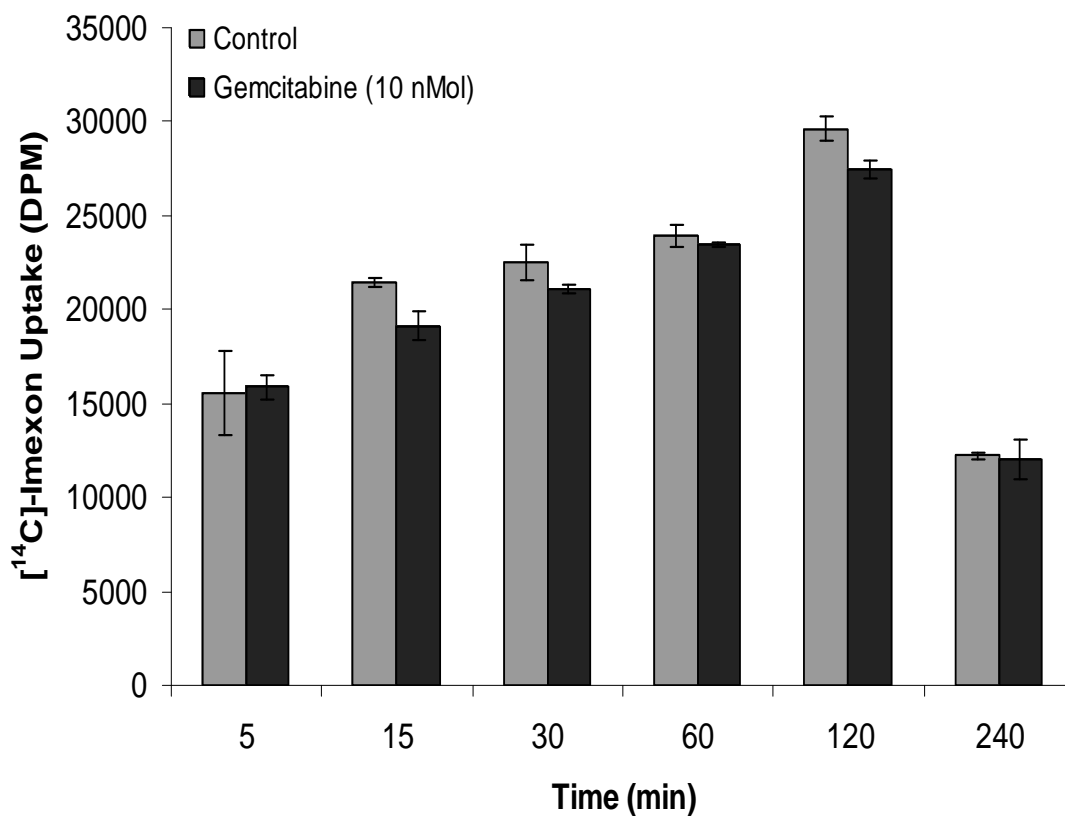


Figure 23 Uptake of [^{14}C]-imexon in PANC-1 cells. Data shows that in the presence of 10 nMol gemcitabine, diffusion of radiolabeled imexon into the PANC-1 cytosolic compartment was unaffected. The data represents mean \pm S.E. of three experiments.

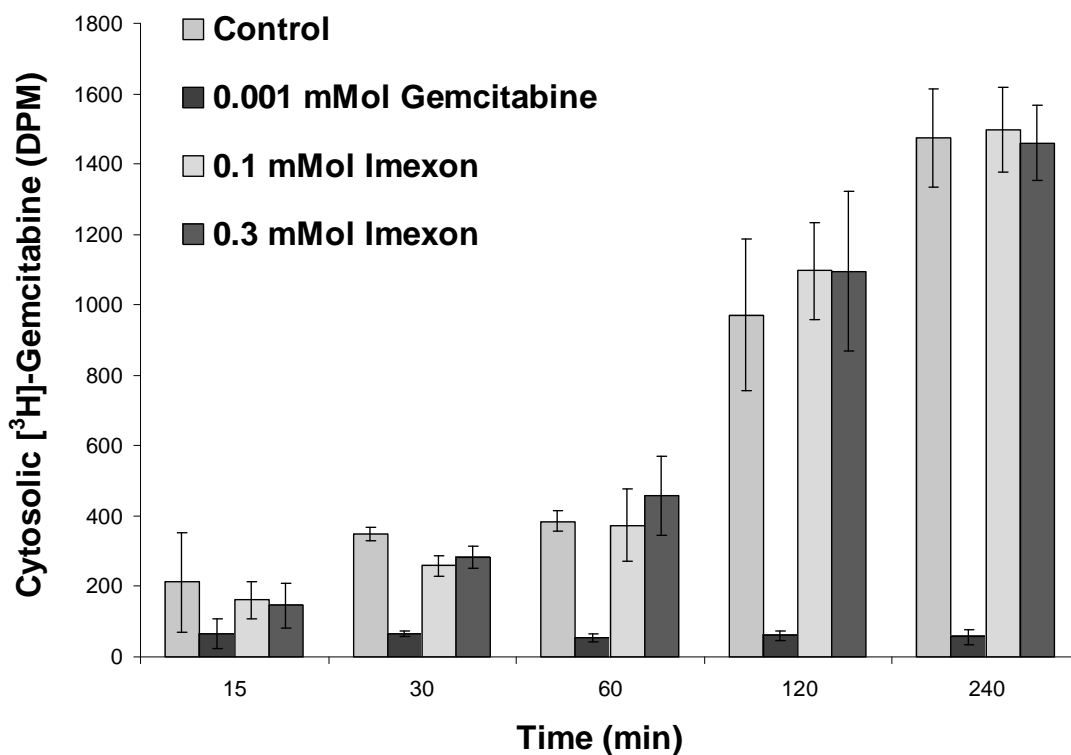


Figure 24 Uptake of [³H]-gemcitabine in PANC-1 cells. The data shows that in the presence of 100 and 300 μ Mol unlabeled imexon, cytosolic accumulation of gemcitabine was unaffected, whereas 1.0 μ Mol unlabeled gemcitabine competitively inhibited cytosolic accumulation of [³H]-gemcitabine. The data represents mean \pm S.E. of three experiments.

3.4. Enzymatic assays

3.4.1. Analysis of deoxycytidine kinase (dCK) activity

In order to be incorporated into DNA, gemcitabine must be phosphorylated by deoxycytidine kinase (dCK) (Van Rompay et al., 2000b). Studies have shown that dCK requires reducing agents such as dithiothreitol, mercaptoethanol, or thioredoxin for enzymatic function (Bohman and Eriksson, 1990) and that reductants can be activators of dCK (Liou et al., 2002b). Because dCK activity has been correlated to regulation by cellular redox potential, dCK activity in the presence of imexon was measured in order to determine if imexon enhanced gemcitabine activation. Protein obtained from PANC-1 cell lysates containing dCK was used to measure the enzymatic phosphorylation of deoxycytidine (dC) to deoxycytidine monophosphate (dCMP). In the presence of ≥ 1.0 mMol imexon, dCK mediated phosphorylation of dC was unaffected (Figure 25). Thus, these data suggest that imexon does not enhance activation of gemcitabine.

3.4.2. Analysis of deoxycytidine deaminase (dCD) activity

The primary route of gemcitabine inactivation involves deamination of the cytidine base by deoxycytidine deaminase (dCD). Prior research has shown that dCD contains a sulfhydryl-rich active site and requires reduced sulfhydryls

to recycle enzymatic function (Camienner, 1967a; Costanzi et al., 2003). These observations led to the hypothesis that imexon would inhibit dCD activity, resulting in an extended half-life of gemcitabine as a mechanism of synergy. Cell lysates containing dCD were obtained from PANC-1 cells and were incubated with 100 mMol deoxycytidine monophosphate (dCMP) in the presence of imexon or *p*-chloromercuribenzoate (CMB), a known dCD inhibitor. Figure 26 shows a sample containing dCMP (5.1 min) that has been deaminated by dCD resulting in the formation of dUMP (3.2 min). These peaks are consistent with retention times of peaks obtained with purified nucleotides. Panel A and B show dUMP formation with increasing protein concentration and time (min) (Figure 27). Panel C shows that imexon concentrations up to 1.0 mMol have no effect on dCD activity, whereas the thiol oxidant, CMB, significantly inhibited dCD activity in a dose-dependent manner at all concentrations ≥ 1.0 μ Mol. Therefore, imexon does not inhibit the major inactivation route of gemcitabine.

3.4.3. Analysis of phosphorylase (PyNase) activity

A minor pathway for inactivation of gemcitabine involves 5'-nucleosidase and phosphorylase activity (Galmarini et al., 2001a). The phosphorylase enzymes,

specifically uridine phosphorylase (UPase), have been shown to metabolize fluoropyrimidines by phosphorylytic cleavage of uridine, deoxyuridine, and thymidine to corresponding free bases, plus ribose-1-phosphate (Johansson, 2003a). These experiments are based on the hypothesis that imexon may inhibit phosphorylase activity, resulting in a longer half-life of gemcitabine. To determine if phosphorylase activity was affected by imexon, protein obtained from PANC-1 cells containing UPase was used to study the phosphorolysis of radiolabeled deoxycytidine (dC) in the presence of imexon. Panel A and B show UPase activity with increasing concentrations of protein and time (min) (Figure 28). Panel C shows that in the presence of ≥ 10 mMol imexon, phosphorylase activity was unaffected. In contrast, the positive control, unlabeled dC, competitively inhibited enzymatic cleavage of the radiolabeled substrate. Thus, imexon does not inhibit phosphorylytic inactivation of gemcitabine.

3.4.4. Analysis of ribonucleotide reductase (RNR) activity

Ribonucleotide reductase (RNR) catalyzes the rate-limiting step in deoxynucleotide formation for DNA synthesis and repair (Eklund et al., 2001b). Both the M_1 and M_2 subunits contain sulfhydryl groups which are necessary for

enzymatic deoxygenation of nucleotide diphosphates and regeneration of enzymatic activity (Kolberg et al., 2004c). These experiments are based on the hypothesis that imexon mediated inhibition of RNR would result in decreased deoxynucleotide pools. This would facilitate greater gemcitabine DNA incorporation as another possible mechanism of synergy. PANC-1 cells were treated with 100, 300 and 500 μ Mol imexon or 0.1 or 2.5 mMol hydroxyurea. The data show that ≥ 100 μ Mol imexon concentrations significantly inhibited RNR mediated deoxygenation of radiolabeled cytidine diphosphate ($p < 0.005$). Of note these results are superior to those obtained with 1 and 2.5 mMol hydroxyurea, the only commercially-available inhibitor of RNR with anti-tumor activity (Figure 29).

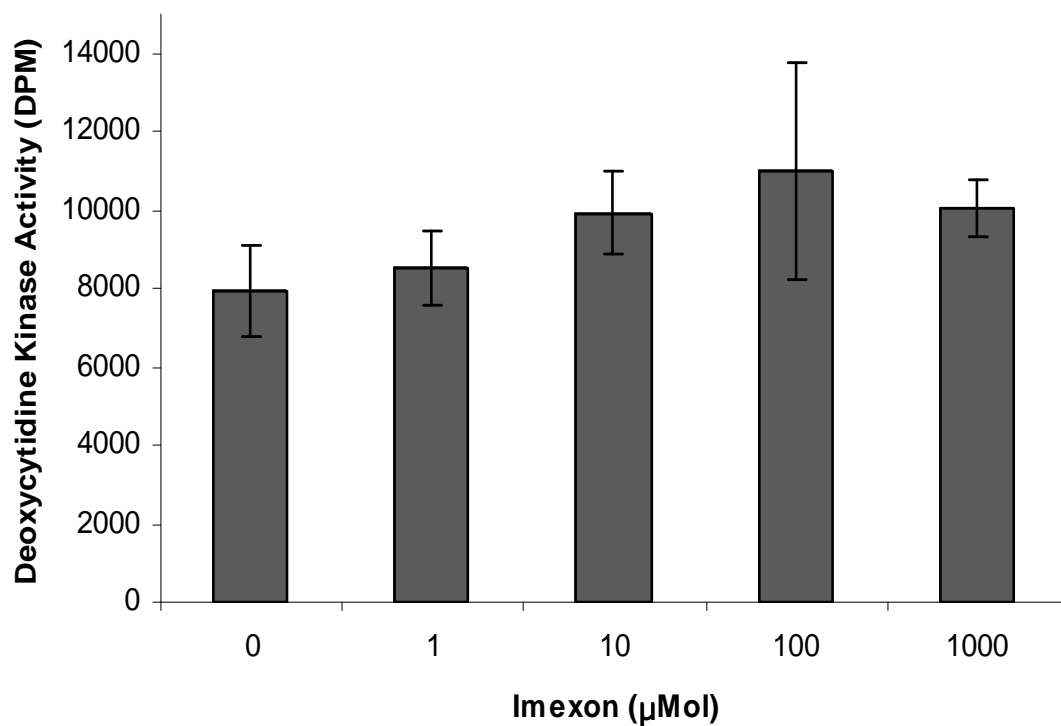


Figure 25 Deoxycytidine kinase (dCK) activity in PANC-1 cell lysates. Data shows that in the presence of imexon ≥ 1.0 μMol , dCK activity was unaffected and phosphorylated equivalent amounts of deoxycytidine as control samples. The data represents mean \pm S.E. of three experiments.

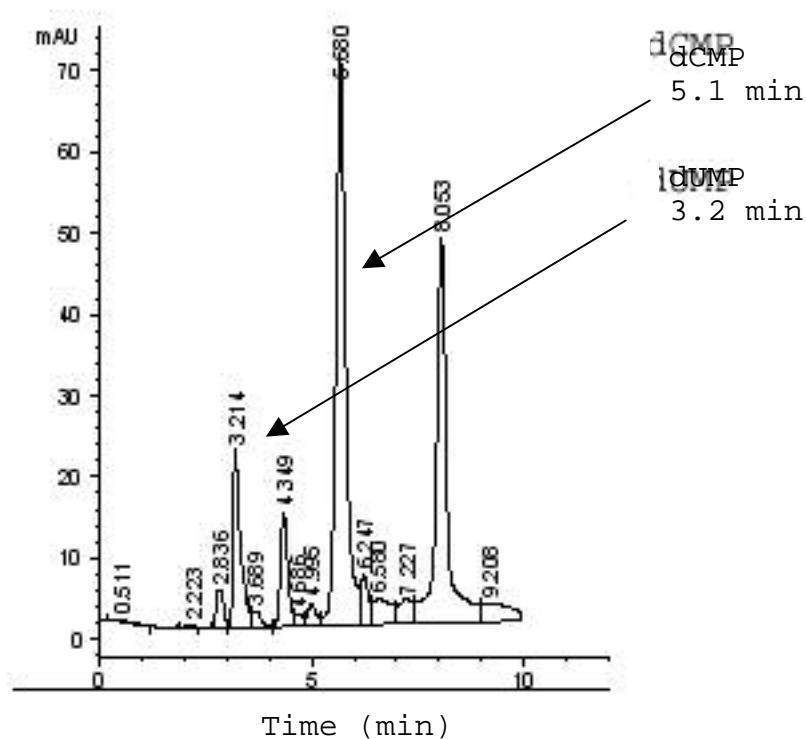


Figure 26 HPLC profile of deoxycytidine monophosphate (dCMP) and deoxyuridine monophosphate (dUMP). The chromatograph shows a sample containing dCMP (5.1 min) that has been deaminated by dCD resulting in the formation of dUMP (3.2 min). These peaks are consistent with retention times of peaks obtained with purified nucleotides.

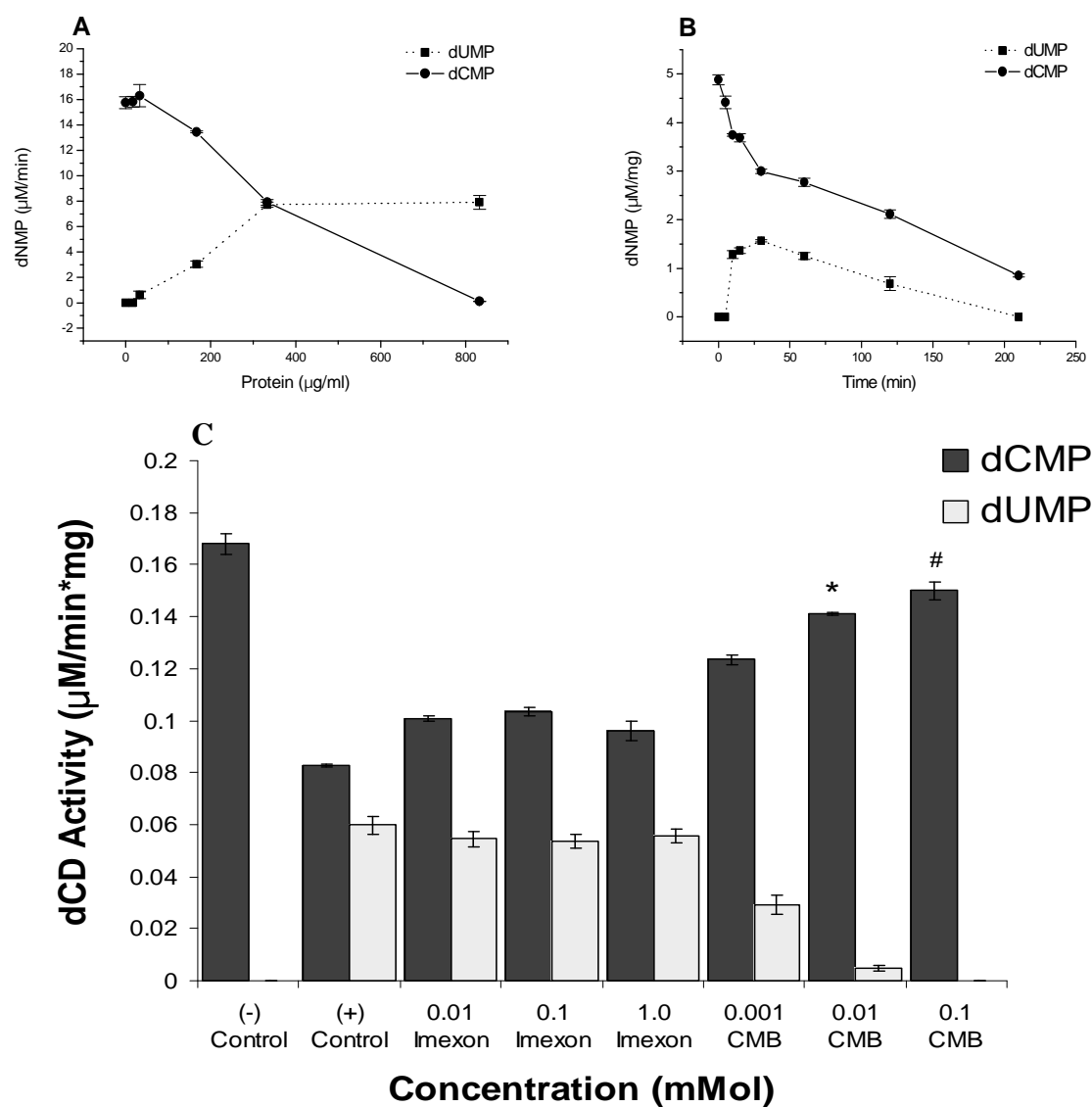


Figure 27 Deoxycytidine deaminase (dCD) activity in PANC-1 cell lysates. The data represents enzymatic deamination by deoxycytidine deaminase. Panel A represents dUMP formation with increasing enzyme; panel B represents dUMP formation with increasing time (min). Panel C shows dUMP formation in the presence of imexon or *p*-chloromercuribenzoate (CMB); no enzymatic inhibition of dCD occurs in the presence of ≥ 1.0 μMol imexon, whereas CMB inhibited dCD activity in a dose-dependent manner. Inhibition of dCD by CMB was significant at 0.01 and 0.1 mMol (* $p < 0.05$, # $p < 0.01$). The data represents mean \pm S.E. of three experiments.

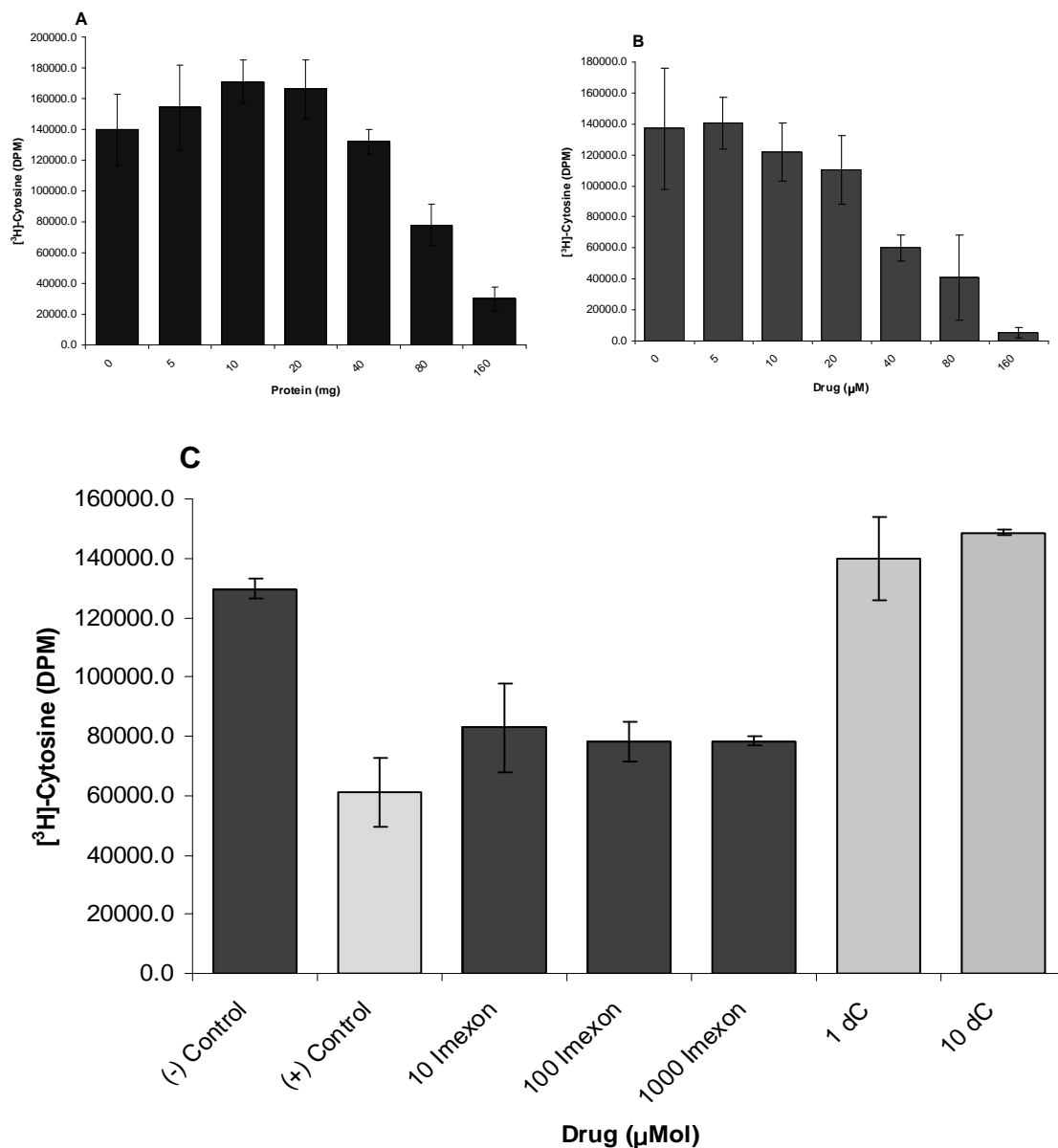


Figure 28 Phosphorylase (PyNase) activity in PANC-1 cell lysates. Panel A shows PyNase activity with increasing concentrations of protein, and panel B shows PyNase activity with increasing time (min). In the presence of $\geq 10 \mu\text{Mol}$ imexon PyNase activity was unaffected, whereas the allosteric inhibitor, deoxycytidine (dC), competitively inhibited PyNase activity (Panel C). The data represents mean \pm S.E. of three experiments.

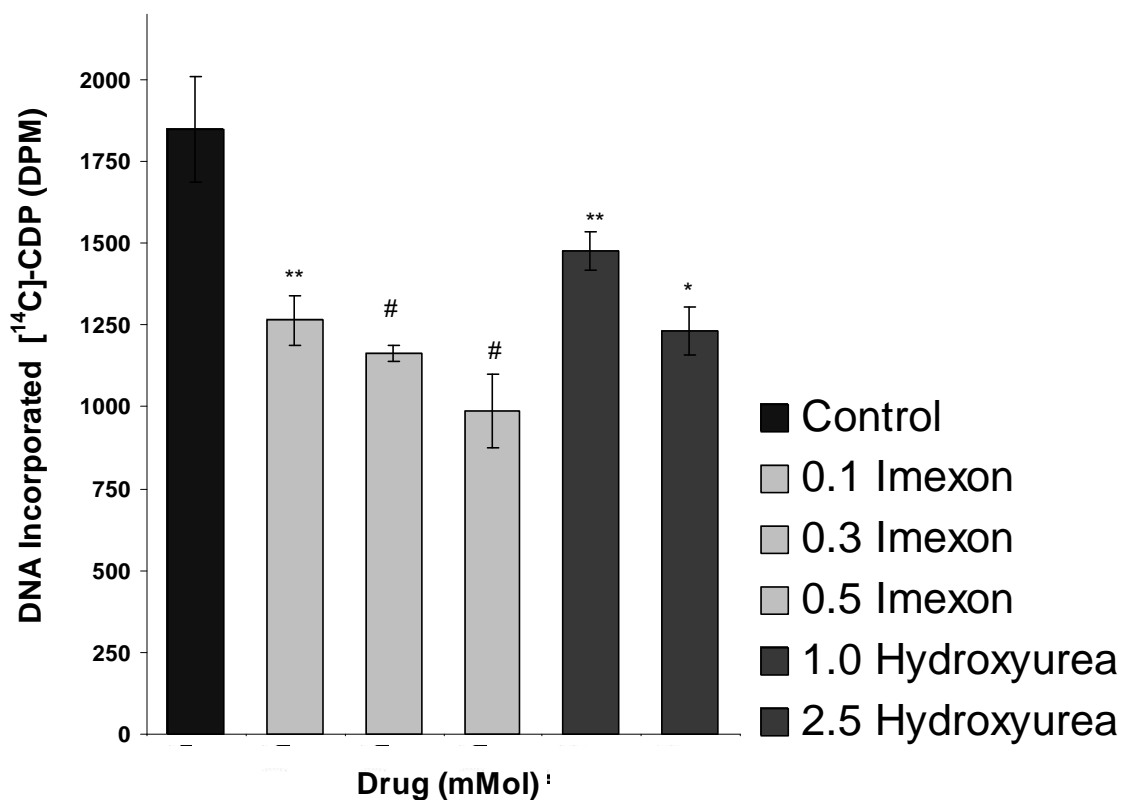


Figure 29 Ribonucleotide reductase (RNR) activity in PANC-1 cells. RNR inhibition was measured in PANC-1 cells by the enzymatic deoxygenation of radiolabeled cytidine diphosphate (CDP) to deoxycytidine diphosphate (dCDP). The data shows that concentrations ≥ 0.1 mMol imexon significantly inhibited RNR activity, similar to the known RNR inhibitor hydroxyurea. Significant RNR inhibition by imexon occurred at 100, 300 and 500 μ Mol concentrations (* $p < 0.05$, ** $p < 0.01$, # $p < 0.001$).

3.5. Ribonucleotide reductase (RNR) protein and mRNA

The upregulation of ribonucleotide reductase (RNR) M₁ and M₂ protein subunits in response to drug inhibition by hydroxyurea has been reported (Zhou et al., 1995). In addition, research has shown that the promoter regions of both RNR subunits are influenced by cellular redox status,, which can alter transcriptional regulation (Park and Levine, 2000; Parker et al., 1995). Further, mRNA message stability may be influenced by cellular oxidants (Amara et al., 1994; Parker et al., 1994). To determine if imexon exposure resulted in cellular alterations of RNR M₁ and M₂ protein subunits or their corresponding mRNA's, PANC-1 cells were treated with 100, 300 and 500 µMol imexon for 4, 8 and 24 hr. At 4 and 8 hr to ≥300 µMol of imexon, the expression of RNR M₁ and M₂ protein subunits increased compared to controls (Figure 30). In contrast, at 24 hr of imexon exposure, RNR protein expression decreased. RNR mRNA levels increased at 4 and 24 hr in response to ≥300 µMol imexon (Figure 31). The observations that cellular response to RNR inhibition results in the upregulation of RNR protein subunits and their corresponding mRNA's are consistent with research by Zhou et al. These data suggest that the PANC-1 cell line responds to imexon mediated RNR inhibition by the

upregulation of transcription and translation of RNR M_1 and M_2 subunits.

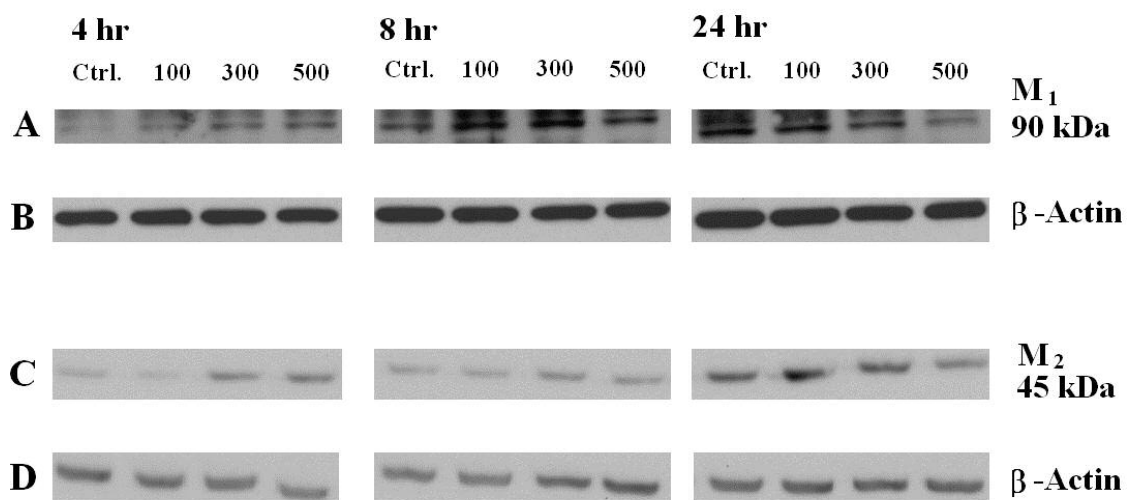


Figure 30 Ribonucleotide reductase (RNR) expression in PANC-1 human pancreatic cancer cells detected by western blot analysis. Immunoblot of M₁ subunit (Panel A) and M₂ subunit (Panel C) are shown in the control cells 4 hr, 8 hr and 24 hr. Cells treated with 100, 300 and 500 μ Mol for 4 hr; 8 hr; and 24 hr. Panel B and D demonstrate immunoblot for β -actin. The data represents RNR levels from PANC-1 cells as detected from whole cell lysates in 3 experiments.

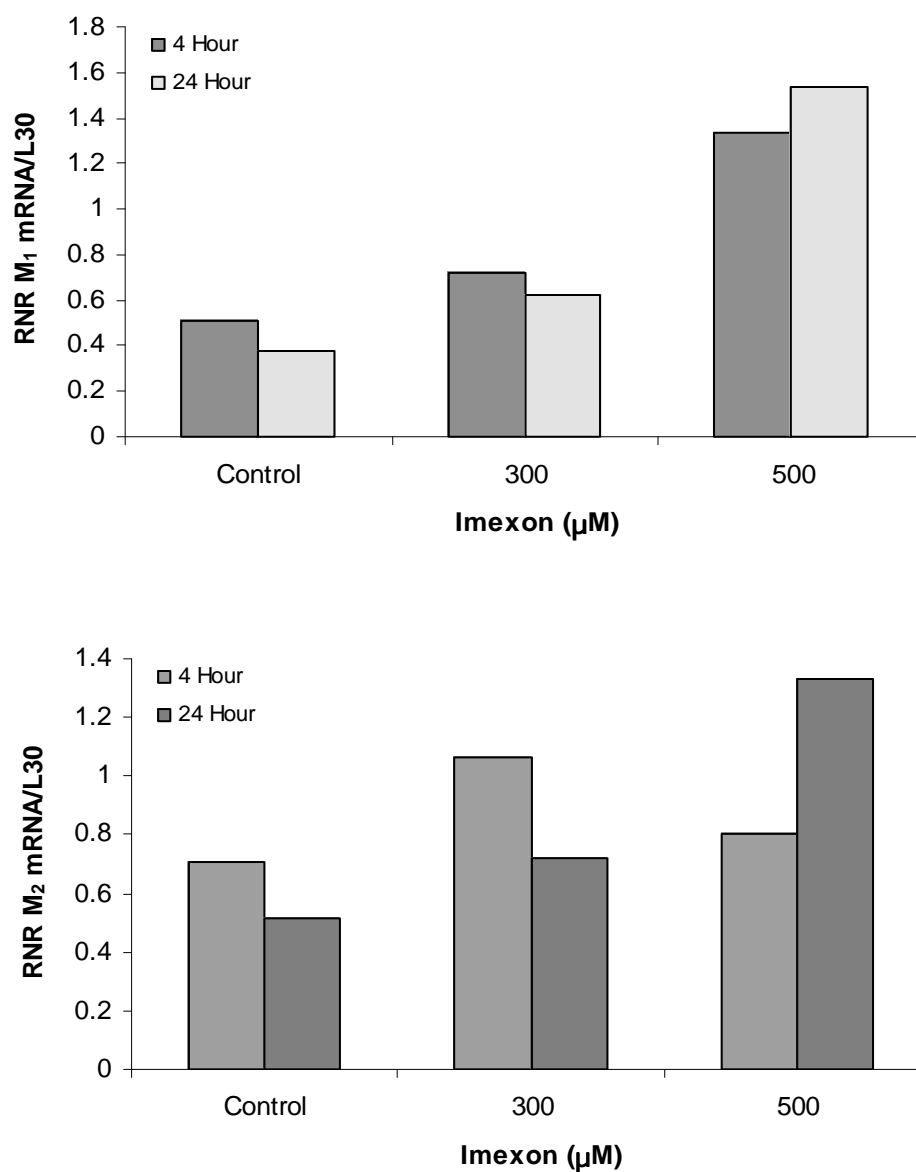


Figure 31 Ribonucleotide reductase (RNR) mRNA levels of subunits M₁ and M₂ detected by RT-PCR. The expression of M₁ and M₂ mRNA was normalized to the L30 housekeeping gene. Data shows that in the presence of ≥ 300 μMol imexon, mRNA levels for both RNR subunits increased at 4 and 24 hr. Data represents an n=2 experiments.

3.6. Cell-cycle analysis

3.6.1. Propidium iodide analysis of PANC-1 cells

Previously, it has been reported that agents, such as hydroxyurea, enhance gemcitabine DNA incorporation by inducing an S phase arrest (Zhou et al., 2002b). PANC-1 cells were exposed to 100, 300 and 500 μMol imexon for 4, 8 and 24 hr. At 24 hr, there was a significant decrease ($p < 0.001$) in the percent of cells appearing in the G_1 -phase and a significant increase ($p < 0.02$) in the percent of cells appearing in the S-phase of the cell-cycle compared to control (Table 5). These changes occurred only at concentrations ≥ 300 μMol imexon (Figure 32). No significant change occurred in the G_2 fraction of cells treated with imexon.

3.6.2. [^3H]-gemcitabine DNA incorporation

Previously, it has been reported that the MIA PaCa-2 cell line G2/M arrest at 24 hr with ≥ 300 μMol imexon treatment (Shoji F. et al., 2004). To determine if imexon mediated an S phase accumulation resulting in greater gemcitabine incorporation, PANC-1 cells were treated with 100, 300 and 500 μMol imexon for 24 hr. A 24 hr exposure to ≥ 100 μMol imexon resulted in a ≥ 2 -fold increase of gemcitabine incorporation into PANC-1 cellular DNA ($p > 0.05$).

The result is similar to that obtained with hydroxyurea (Figure 33). These data suggests that imexon mediates an S-phase accumulation which enhances gemcitabine incorporation into DNA.

Table 5 Propidium iodide cell cycle analysis of PANC-1 human pancreatic cancer cells.

	4 hr			8 hr			24 hr		
	G1	S	G2/M	G1	S	G2/M	G1	S	G2/M
Control	41.9±2.1	35.7±4.1	22.4±2.0	40.4±2.3	35.4±7.5	24.2±5.2	39.9±0.9	37.2±1.0	22.9±1.0
100	40.5±2.6	40.5±0.5	19.0±2.9	37.5±0.5	40.1±4.0	22.5±3.4	34.9±5.3	38.3±4.8	26.8±0.6
300	43.3±1.9	38.8±0.4	17.9±2.0	37.1±0.8	43.7±1.3	19.3±0.6	22.2±1.0	53.4±6.8	24.4±5.8
500	43.0±2.4	38.3±2.4	18.1±1.2	38.3±1.4	44.2±2.0	17.6±0.7	27.7±1.2	50.6±4.1	21.7±5.3

Table 5 Propidium iodide cell cycle analysis of PANC-1 human pancreatic cancer cells. The table shows that a significant increase of PANC-1 cells accumulate in S phase with $\geq 300 \mu\text{Mol}$ imexon treatment at 24 hr.

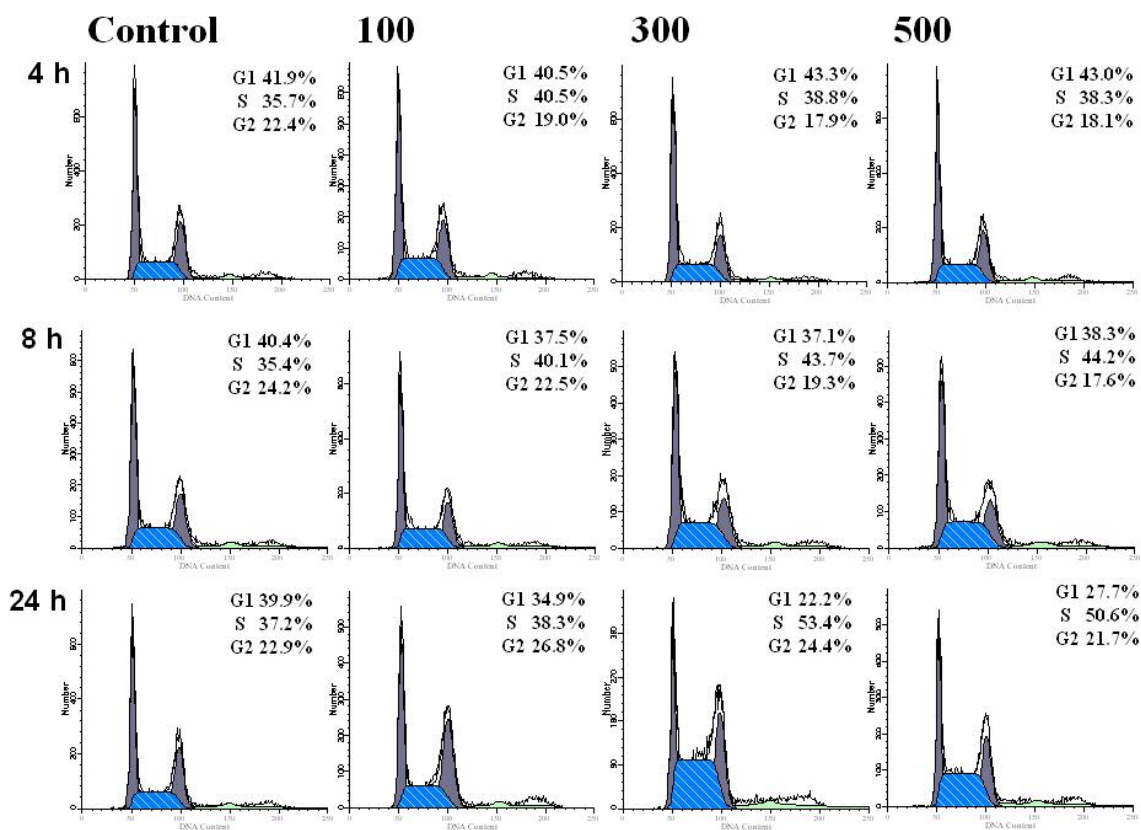


Figure 32 Cell cycle analysis of PANC-1 cells was assessed at 4, 8 and 24 hr. The graph shows PANC-1 cells treated with 100, 300 and 500 μ Mol imexon. At 24 hr there was a significant increase of cells accumulating in the S phase ($p < 0.05$) with 300 and 500 μ Mol imexon treatment. No significant change occurred in the G₂ fraction. The data represents mean \pm S.E. of three experiments.

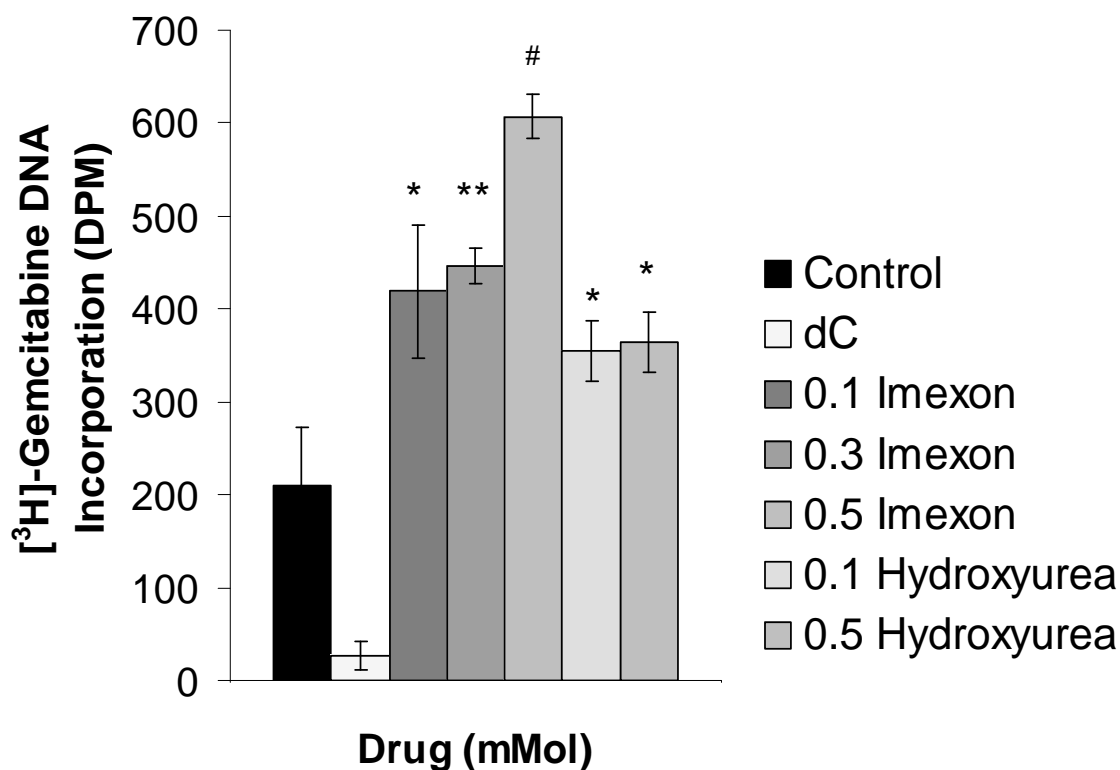


Figure 33 DNA incorporation of [³H]-gemcitabine in PANC-1 cells. Cell cycle analysis of PANC-1 cells was assessed at 4, 8 and 24 hr. Panel A, B, C and D show control, 100, 300 and 500 μ Mol imexon treated cells, respectively. The data show that at 24 hr there was a significant increase of cells accumulating in the S phase ($p < 0.05$) at 300 and 500 μ Mol imexon, with the G₁ fraction decreasing. No significant change occurred in the G₂ fraction. The data represents mean \pm S.E. of three experiments.

3.7. Effect of imexon on p38 kinase activation

The mitogen activated protein (MAP) kinase pathways relay extracellular stimuli into intracellular signaling, coordinating a variety of responses, including cell proliferation, differentiation, motility and survival (Roux and Blenis, 2004). Three MAP kinase signaling pathways in mammalian cells have been identified, including the extracellular signal-regulated kinase (ERK) pathway, the c-jun N-terminal kinase (JNK) pathway, and p38 MAP kinase pathway (Kyosseva, 2004). Research has shown that cellular redox changes and reactive oxygen species, (ROS), activate MAP kinase pathways, acting as stress signals, and resulting in cell death (Ueda et al., 2002a; Adler et al., 1999a). To determine whether imexon induced cellular stress would activate the p38 kinase pathway, PANC-1 cells were treated with 100, 300 and 500 μMol imexon for 4, 8 and 24 hr. The results show that at 24 hr ≥ 300 μMol imexon activated p38 kinase (Figure 34).

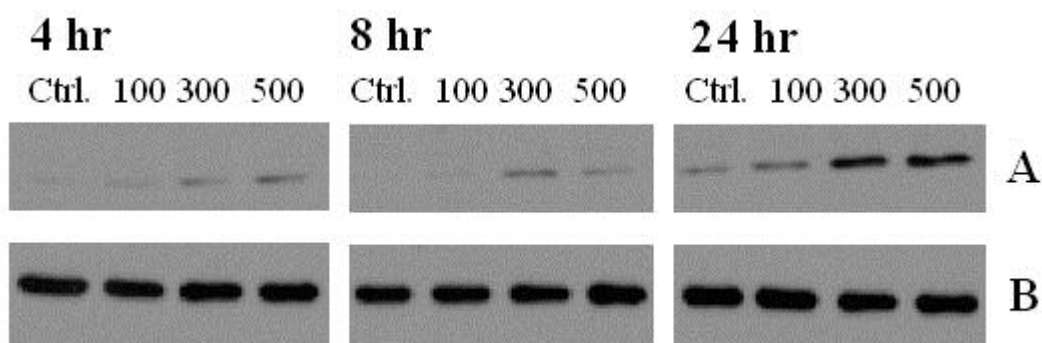
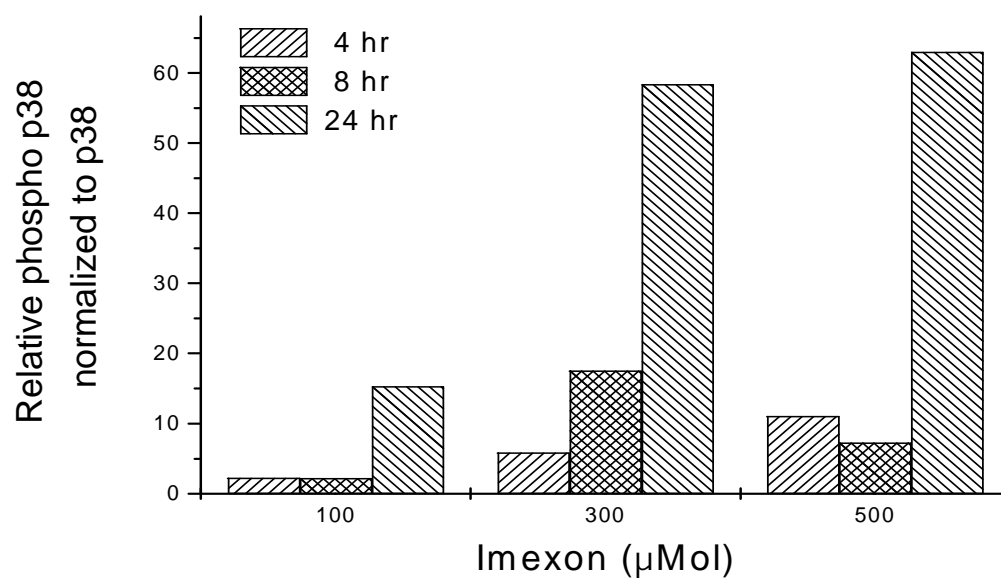


Figure 34 Phosphorylation of p38 in PANC-1 human pancreatic cancer cells as detected by western blot analysis. Immunoblot of phosphorylated p38 (Panel A) and total p38 (Panel B) are shown in the control cells 4 hr, 8 hr, and 24 hr.

3.8. ^{60}Co Irradiation of PANC-1, MIA PaCa-2, MutJ and BxPC-3 human pancreatic cancer cells

Ionizing radiation results in the formation of reactive oxygen specie (ROS), initiating the induction of redox-sensitive stress response cascades which can lead to cell death (Gius, 2004b). Because imexon induces oxidative stress resulting in ROS formation, these experiments were designed to test the hypothesis that imexon would enhance the effects of ionizing radiation. Human pancreatic cancer cells were plated in 96-well plates and exposed to imexon for 24 hr prior to ≤ 10 Gy ^{60}Co irradiation. Median effect analysis combination indices of drug plus radiation cytotoxicity were acquired after 96 hr incubation following ^{60}Co irradiation and imexon exposure. The data show that enhanced cell death was cell-line dependent. Imexon and ^{60}Co irradiation resulted in additivity in the PANC-1 cell line (Figure 35). Imexon and ^{60}Co irradiation resulted in synergy in the MIA PaCa-2 and MutJ cell lines (Figures 36-37). In contrast, the combination resulted in an antagonistic effect in the BxPC-3 cell line (Figure 38). The data suggest that synergy between imexon and ^{60}Co ionizing radiation in human pancreatic cancer cells is cell-

line dependent and further investigation of cell-line dependency is needed.

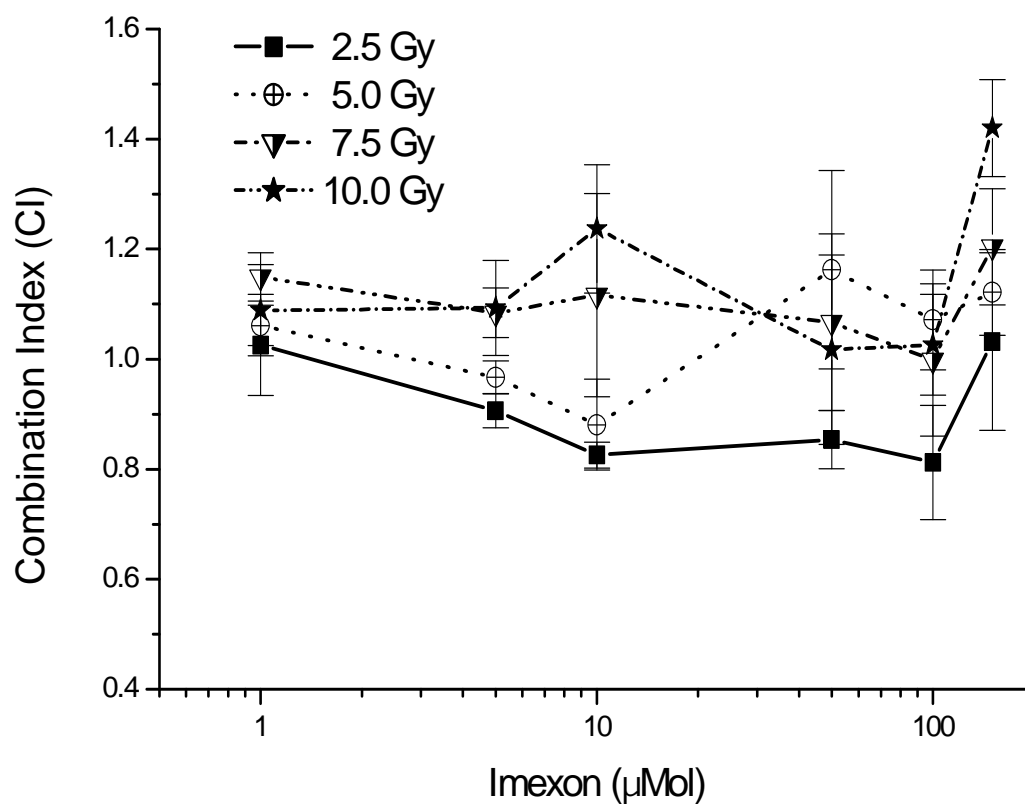


Figure 35 Combination index (CI) of PANC-1 human pancreatic cancer cells treated with imexon for 24 hr with subsequent ^{60}Co irradiation. The data shows that imexon plus ^{60}Co irradiation results in an additive effect in the PANC-1 cell line. The data represents mean \pm S.D. of three experiments.

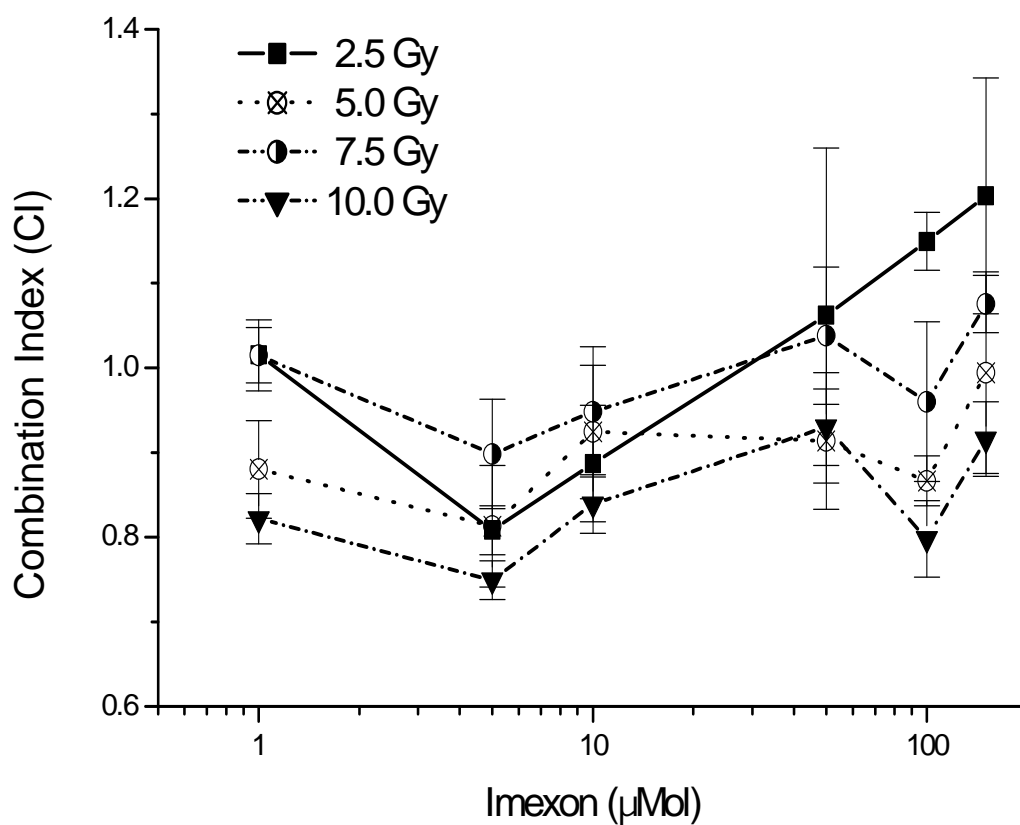


Figure 36 Combination index (CI) of MIA PaCa-2 human pancreatic cancer cells treated with imexon for 24 hr with subsequent ^{60}Co irradiation. The data shows that imexon plus ^{60}Co irradiation results in a synergistic effect in the MIA PaCa-2 cell line. The data represents mean \pm S.D. of three experiments.

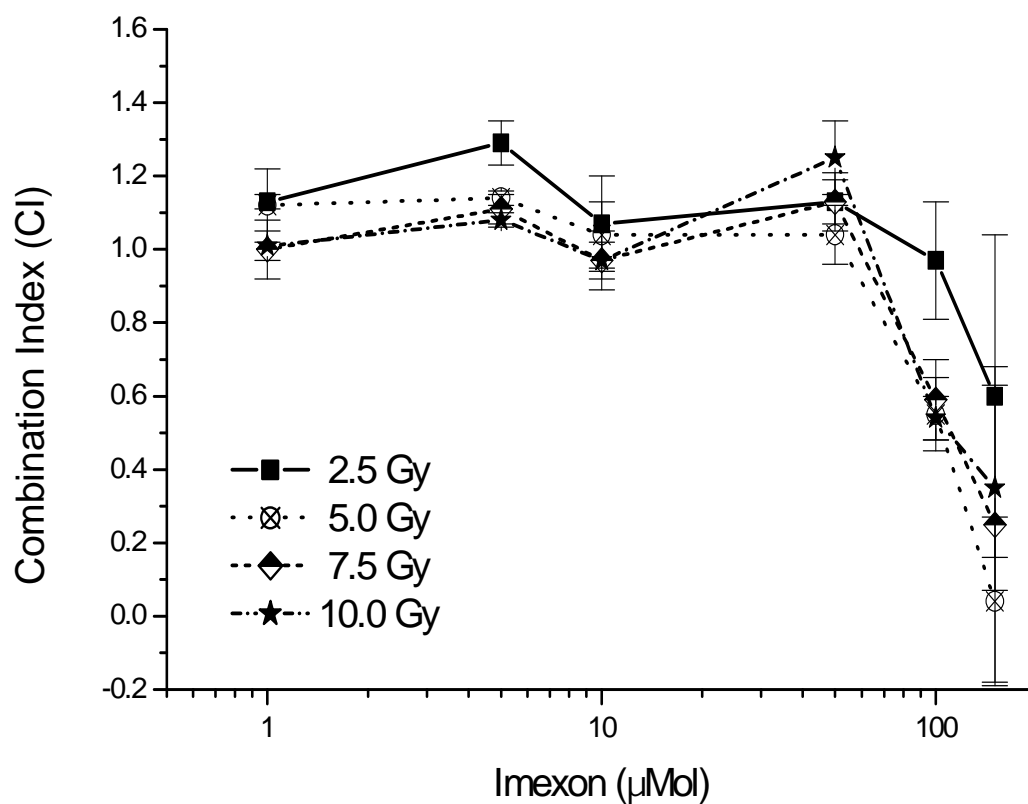


Figure 37 Combination index (CI) of MutJ human pancreatic cancer cells treated with imexon for 24 hr with subsequent ^{60}Co irradiation. The data shows that imexon plus ^{60}Co irradiation results in a synergistic effect in the MutJ cell line. The data represents mean \pm S.D. of three experiments.

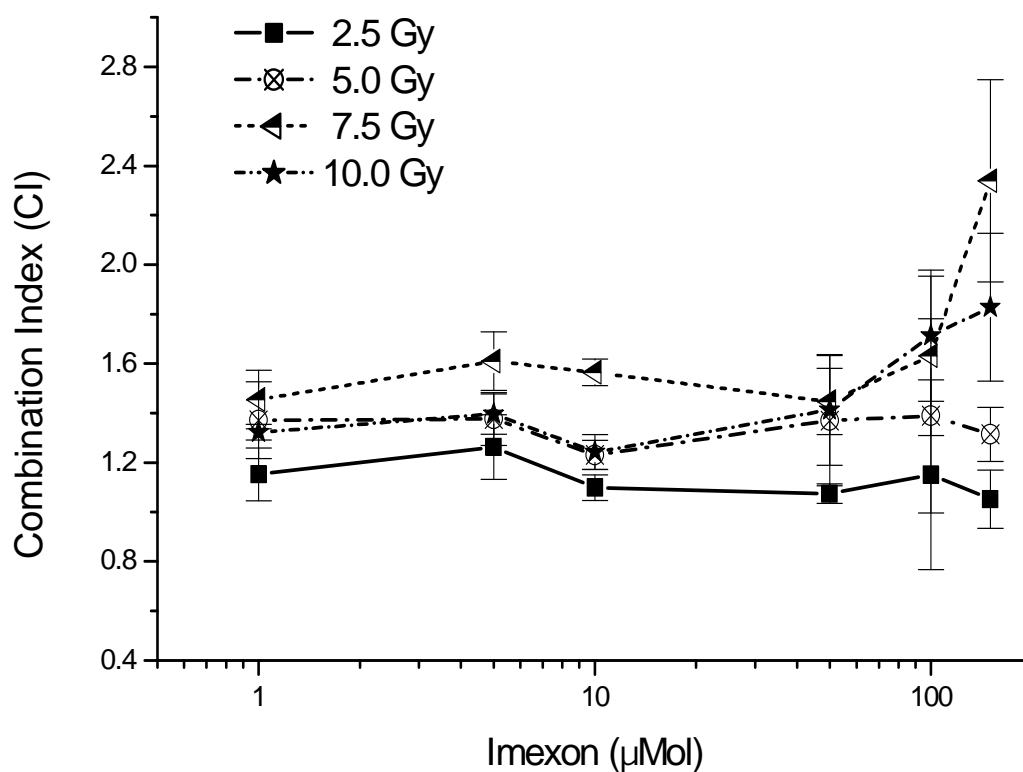


Figure 38 Combination index (CI) of BxPC-3 human pancreatic cancer cells treated with imexon for 24 hr with subsequent ^{60}Co irradiation. The data shows that imexon plus ^{60}Co irradiation results in a synergistic effect in the BxPC-3 cell line. The data represents mean \pm S.D. of three experiments.

4. CHAPTER

DISCUSSION

4.1. Mechanisms of Synergy

Adenocarcinoma of the pancreas thrives in a net-oxidative environment, characterized by a loss of antioxidant capacity and elevated ROS levels. Recent studies have shown that pancreatic cancer cells become sensitized to endogenous apoptotic machinery in response to ROS inducing agents (Lebedeva et al., 2004) and that changes in redox potential by ROS mediate cell death via stress response signaling (Matsuzawa and Ichijo, 2005b). Understanding that imexon binds cellular thiols and generates ROS, it was hypothesized that imexon may have considerable activity against pancreatic cancer, especially when combined with gemcitabine. The present study demonstrates that imexon is cytotoxic in four human pancreatic cell lines and exhibits schedule-dependent cytotoxicity in the PANC-1 cell line. This is consistent with observations previously reported in MIA PaCa-2 cells (submitted). In addition, when imexon and gemcitabine were simultaneously administered at a fixed ratio of 1:1 (imexon (μMol): gemcitabine (nMol)) *in vitro*, concentrations ≥ 50 μMol imexon resulted in synergy in the PANC-1, MutJ and

BxPC-3 cell lines, and concentrations ≥ 250 μMol imexon in the MIA PaCa-2 cell line. The evaluation of PANC-1 tumors inoculated in SCID mice showed that imexon or gemcitabine alone did not significantly affect tumor growth inhibition, while combination treated mice demonstrated marked tumor growth inhibition which extended median survival. The study of treating established tumors showed that combination treated mice experienced tumor regression, suggesting that imexon and gemcitabine would be an effective drug combination for patients with large, established pancreatic tumors.

To investigate the mechanism of synergy, an examination of the specific pathways of gemcitabine metabolism regulated by thiol-dependent enzymes or influenced by cellular changes in redox status was performed. It has been established that gemcitabine must gain cytosolic entry in order to exert cytotoxic effects and physiological uptake is mediated through nucleoside transport (NT) systems. Once within the cytosolic compartment, gemcitabine requires phosphorylation by deoxycytidine kinase (dCK) (Van Rompay et al., 2000a). Activity results from gemcitabine being incorporated into DNA. DNA incorporation of gemcitabine results in "masked" DNA chain termination, meaning, only one additional

nucleotide is added to the growing DNA strand before synthesis is halted (Ruiz, V et al., 1993a). Gemcitabine also inhibits prominent enzymes such as ribonucleotide reductase (RNR) and CTP synthase (Heinemann et al., 1995; Plunkett et al., 1996b; Plunkett et al., 1995a). The primary means of inactivation of the drug is mediated by enzymatic deamination by deoxycytidine deaminase (dCD), and to a lesser extent by 5'-nucleosidase and phosphorylase (PyNase) cleavage (Galmarini et al., 2001c).

In the present study results show that imexon does not affect cellular uptake of gemcitabine up to four hours after drug administration. The data also showed that imexon diffusion is unaffected by the presence of gemcitabine. These data suggest that imexon does not enhance gemcitabine uptake as a mechanism of synergy, and that simultaneous administration of both agents would not alter the cellular uptake of gemcitabine.

Phosphorylation of gemcitabine by deoxycytidine kinase (dCK) is the rate-limiting step in the activation of the drug and necessary for cytotoxicity (Heinemann V. et al., 1988). Research has demonstrated that dCK levels strongly correlate with gemcitabine sensitivity (Beausejour et al., 2002; Blackstock et al., 2001a; Kroep et al., 2002a).

Studies of purified dCK protein have demonstrated the need for reducing agents such as dithiothreitol, mercaptoethanol and thioredoxin (Bohman and Eriksson, 1990), moreover, studies have shown that cellular redox status contributes to the dCK activity (Liou et al., 2002a). Because imexon induces oxidative stress, we hypothesized that imexon would enhance phosphorylation of gemcitabine by dCK as a mechanism of synergy. These data suggest that concentrations of imexon up to 1 mMol do not enhance dCK activity. In contrast, research has shown that the dCK active site does not contain sulfhydryl residues (Sabini et al., 2003). These results suggest that imexon does not inhibit dCK mediated phosphorylation of gemcitabine.

Deoxycytidine deaminase (dCD) catalyzes the hydrolytic deamination of cytidine and deoxycytidine (dC) to their corresponding uridine derivatives. These are then recycled either for scavenging of pyrimidine nucleotide bases or generation of carbon and nitrogen sources (Somasekaram et al., 1999a). Major inactivation of cytosine nucleoside-based agents, including gemcitabine occurs by dCD (Plunkett et al., 1996c), and dCD levels have been shown to correlate with drug sensitivity *in vitro* and *in vivo* (Momparker and Laliberte, 1990; Neff and Blau, 1996a) The dCD enzyme is a

15 KDa homotetrameric enzyme composed of four identical subunits containing an essential zinc atom in the active site that is coordinated by three necessary cysteine residues, C65, C99, and C102 (Vincenzetti et al., 2003b). Previous studies have shown that dCD is sulfhydryl-dependent, and that pro-oxidants such as CMB inhibit enzymatic activity (Camiener, 1967b). The cysteine-rich active site could be inactivated by imexon, resulting in a longer half-life of gemcitabine as a mechanism of synergy. In the present study data suggest that concentrations of imexon up to 1.0 mMol do not inhibit dCD. It is known that the active site of dCD is completely sequestered from the cytosolic compartment and when ligand is bound, the ribose is completely buried within the complex (Carter, Jr., 1995). Research has shown that sulfhydryl-dependent active sites in proteins can be inaccessible to thiol-reactive compounds, depending on the compounds hydrophobic or hydrophilic properties (Hu and King, 1999; Jimenez-Vidal et al., 2004; Mueckler and Makepeace, 1997). Based upon these observations, consideration was made that a small, hydrophilic compound such as imexon may be excluded from the dCD hydrophobic active site, whereas, a more hydrophobic

compound, such as CMB has access to the active site and inhibits enzymatic deamination by dCD.

Research has shown that uridine phosphorylase (UPase) activity results in the reversible phosphorolysis (PyNase) of fluoropyrimidine nucleoside analogs resulting in activation or inactivation of the drug (Van Rompay et al., 2001a). Additional studies have shown that expression of UPase correlate with clinical disease progression in oral squamous cell and breast carcinoma (Miyashita et al., 2002; Kanzaki et al., 2002). Based upon these observations, the hypothesis that imexon would inhibit enzymatic activity of UPase by disrupting the binding pocket, resulting in a greater half-life of gemcitabine. In the present study data show that PyNase activity is unaffected by imexon concentrations up to 1.0 mMol, suggesting that imexon would not alter UPase mediated inactivation of gemcitabine.

The UPase crystal structure derived from *E. Coli* bacteria suggest that the active site is rich in glutamine and arginine residues and does not require reduced thiols for enzymatic activity (Caradoc-Davies et al., 2004). Hence, these data support the rationale that imexon would not inhibit the UPase active site due to a lack of sulfhydryl residues.

Gemcitabine is a suicide substrate inhibitor of ribonucleotide reductase (RNR), the rate-limiting enzyme required for the formation of deoxynucleotides (dNTPs) for DNA synthesis and repair (Pereira et al., 2004a). The RNR enzyme is composed of M_1 and M_2 subunits (Eklund et al., 2001a). The M_1 subunit contains critical cysteines at C225 and C462 that form an intermediate disulfide bridge. The disulfide is reduced by two other cysteines C754 and C759 located on the M_1 unit, and ultimately by thioredoxin or glutaredoxin to reactivate the enzyme (Eriksson et al., 1997). The M_2 active site consists of an active cysteine at C439 that is converted into a thiyl radical. This thiyl radical is responsible for abstraction of the hydrogen atom from the ribose ring of the substrate (Logan et al., 1996). Resistance to gemcitabine in pancreatic cancer has been associated with M_2 overexpression (Goan et al., 1999) and enhanced cytotoxicity with M_2 subunit inhibition (Duxbury et al., 2004b). Overexpression of the mRNA for the M_1 protein has been negatively associated with survival in gemcitabine-treated patients with non-small cell lung cancer (Davidson et al., 2004a). In the present study imexon inhibited RNR activity at concentrations $\geq 100 \mu\text{Mol}$ ($p < 0.02$), comparable to hydroxyurea, a known RNR inhibitor. It has been shown that

hydroxyurea exerts enzymatic inhibition of RNR by binding iron and quenching the tyrosyl radical in the M₂ subunit, which is responsible for thiyl radical formation (Yarbro, 1992). Currently, it is not known whether imexon interacts similarly with the M₂ subunit, or by depletion of cellular reducing equivalents necessary to regenerate enzymatic activity in the M₁ subunit.

Ribonucleotide reductase (RNR) M₁ and M₂ protein expression and their corresponding mRNA's have been shown to increase in response to RNR inhibition by hydroxyurea (Zhou et al., 2002c). Stability of M₁ mRNA has been correlated with oxidation/reduction agents (Burton et al., 2003). Research has also shown that RNR M₂ mRNA stability has been shown to be regulated, by a redox sensitive 3'-untranslated region (3'-UTR) (Amara et al., 1996). Furthermore, the inhibition of M₂ mRNA by siRNA resulted in enhanced sensitivity of pancreatic adenocarcinoma to gemcitabine (Duxbury et al., 2004a). These observations led to the hypothesis that imexon mediated inhibition of RNR and alterations in redox potential would cause an increase in RNR protein expression and mRNA levels. In the present study data suggest that PANC-1 cells responded to imexon treatment by increased RNR M₁ and M₂ protein expression and

mRNA with enzyme inhibition. Previously, it has been reported that gemcitabine suicide-inhibits the M₁ subunit by binding in the substrate-binding pocket and preventing thiyl radical transfer with a cellular response of resulting in increased protein and mRNA expression. Based upon these observations, a new hypothesis was formed: imexon mediated RNR inhibition may be due to thiol binding, resulting in the inactivation of necessary cysteine residues at position C225, C462 and C754. Interestingly, RNR protein levels of both subunits increased in the control samples over time and consistent with all three experiments. However, previous research has shown that increases in RNR protein expression have been correlated to normal cell-cycle changes (Chabes and Thelander, 2000).

It has been reported that pancreatic cancer cells deficient in wild-type p53 may undergo an S phase arrest instead of p53 mediated G₁ arrest (Chang et al., 2004). The PANC-1 cell line has only one mutated copy of p53, suggesting that this cell line would bypass normal G₁ blockade in response to oxidative stress (Butz et al., 2003). Interestingly, agents that enhance S phase arrest such as IFN- α have been shown to be synergistic with gemcitabine in

pancreatic cancer (Ziske et al., 2004). Prior studies have also demonstrated a G₂/M accumulation of MIA PaCa-2 cells at 24 hr in response to ≥ 300 μMol imexon. In the present study data suggest that imexon caused an increase in S phase accumulation of PANC-1 cells at 24 hr at concentration ≥ 300 μMol imexon. In human oropharyngeal carcinoma KB cells, RNR inhibition by hydroxyurea demonstrated enhanced gemcitabine mediated cell death by promoting S phase arrest depletion of dNTP pools (Zhou et al., 2002d). These observations led to the hypothesis that a similar mechanism could be mediated by imexon as an explanation of synergy. In the present study the data suggest that ≥ 100 μMol imexon enhanced >2 -fold the incorporation of gemcitabine into PANC-1 DNA at ($p < 0.05$), similar to hydroxyurea. These data suggest that S phase, cell cycle accumulation mediated by imexon treatment facilitates greater gemcitabine incorporation into pancreatic cancer cell DNA resulting in an enhanced gemcitabine cytotoxic effect. Because pancreatic cancer cells commonly have p53 mutations, these data support that the combination would have similar activity in patients (Sawabu et al., 2004).

The p38 MAP kinase pathway has been associated with stress response and programmed cell death, or apoptosis

(Kyriakis and Avruch, 2001). Recent research has shown that activation of the p38 MAP kinase pathway in the U937 and OCI-AML1a human leukemic cells results from an increased production of reactive oxygen species (ROS) by epigallocatechin-3-gallate (EGCG) (Saeki et al., 2002). Further, research has shown that alterations in redox potential by the generation of excess ROS modulates inter-molecular disulfide bonds between cysteine residues in proteins which regulate stress kinase pathways (Adler et al., 1999c). These observations led to the hypothesis that imexon induced cellular stress would activate the p38 MAP kinase pathway. In the present study data suggest that imexon activated p38 MAP kinase at 24 hr using concentrations ≥ 300 μMol imexon. Notably, this concentration is near the 24 hr IC_{50} value. Overall, these data suggest that imexon treatment results in activation of p38, potentially mediated the cell death cascade responsible for imexon induced apoptosis.

Ionizing radiation results in the formation of reactive oxygen species (ROS) leading to activation of stress pathways and apoptotic cell death (Ueda et al., 2002c; Gius, 2004a). Because imexon results in the generation of ROS species, these studies are based on the hypothesis that

imexon would sensitize pancreatic cancer cells to ionizing radiation, enhancing activation of stress response pathways and apoptotic cell death. The data showed that pre-treatment of pancreatic cancer cells with imexon before ^{60}Co irradiation resulted in synergy in the MIA PaCa-2 and MutJ cell line, additivity in the PANC-1 cell line, and antagonism in the BxPC-3 cell line. These data suggest that imexon-induced sensitization of pancreatic cancer cells to ionizing radiation is cell-line dependent and that the combination treatment of imexon plus radiation therapy may be of clinical benefit since gemcitabine has also been shown to be a potent sensitizer of pancreatic cancer cells to ionizing radiation (Pauwels et al., 2005; Lawrence et al., 2003).

4.2. Summary

In the present study data suggest that imexon is cytotoxic to human pancreatic cancer cells in a schedule-dependent manner. This supports the hypothesis that pancreatic cancer cells are susceptible to the pro-oxidant and -apoptotic effects of imexon. In addition, we found that combining imexon with gemcitabine *in vitro* and *in vivo* resulted in a synergistic interaction. The lack of nucleoside transporter and deoxycytidine kinase (dCK)

inhibition by imexon suggest that simultaneous administration of both agents would not affect cytosolic accumulation or activation of gemcitabine. The mechanisms of synergy do not appear to result from imexon mediated inhibition of enzymatic inactivation of gemcitabine by deoxycytidine deaminase (dCD) or uridine phosphorylase (UPase). In contrast, the data suggest that the mechanisms of synergy, in part, result from an imexon-mediated inhibition of ribonucleotide reductase (RNR) and modulation of cell cycle (Figures 39-40). Imexon mediated RNR inhibition would result in a decreased deoxynucleotide triphosphate (dNTP) pool for DNA synthesis and repair, facilitating preferred incorporation of gemcitabine, instead of deoxycytidine triphosphate (dCTP), into cellular DNA. This effect would be complemented by an imexon-induced S phase accumulation in pancreatic cells, resulting in greater DNA synthesis, hence, enhanced DNA incorporation of gemcitabine.

Activation of the p38 MAP kinase pathway by imexon suggests that apoptotic death signaling would be enhanced in combination with gemcitabine. Currently, imexon is in phase I/II clinical trials and the clinically tolerated dose of 750 mg/m² has produced plasma levels which exceed the

preliminary IC₅₀ values for pancreatic cancer cells *in vitro*. Importantly, there have been no grade 3 or greater toxicities observed to date and animal modeling suggest that gastrointestinal effects and not myelosuppression will ultimately be dose-limiting. The unique mechanisms of action and non-overlapping toxicities make imexon and gemcitabine an attractive drug combination for the treatment of pancreatic cancer. These data support the rationale for further evaluating this drug combination in patients.

4.3. Future studies

So far, the mechanisms of synergy between imexon and gemcitabine result from imexon mediated inhibition of RNR activity and modulation of cell-cycle, resulting in enhanced DNA incorporation and cytotoxicity of gemcitabine. Studies indicated for the future involve determining the mechanism of imexon mediated cell cycle arrest. In the present study, the MIA PaCa-2 cell line did not demonstrate synergy with combination treatment compared to the PANC-1 cell line. The MIA PaCa-2 cell line also G₂/M arrest with imexon treatment, whereas the PANC-1 cell line S phase arrest with imexon treatment. Interestingly, an S phase specific arrest has been correlated to cell lines lacking p53 and pancreatic cancer cells are known to have >60% p53 mutations. Thus,

understanding the mechanisms of imexon mediated S phase arrest would be beneficial in determining the populations of cancer cells that would respond to combination treatment. Future studies also involve determining how much synergy is due to RNR inhibition and cell cycle modulation. Research has shown that RNR inhibition by hydroxyurea leads to an enhanced cytotoxic effect of gemcitabine. This is due to decreased dNTP pools competing with gemcitabine. Therefore, determining if imexon depletes dNTP pools is considered as part of the mechanism of enhancing gemcitabine cytotoxicity. In addition, hydroxyurea has been shown to inhibit the M₂ subunit by quenching the tyrosyl radical involved in RNR mediated deoxygenation of the substrate-bound nucleoside diphosphate. So far, it is not known if imexon inhibits RNR activity by a similar mechanism, or by interacting with other cysteines in the substrate-binding site. Future studies also include determining if imexon mediated RNR inhibition results in S phase arrest, or is independent of enzyme inhibition. Finally, investigating the combination effect of imexon with other S-phase specific drugs for anti-cancer therapy is of future interest. The nucleoside analog 5-fluorouracil, 5-FU, is used for the treatment of colon cancer. Other analogs such as cladribine and fludarabine

are used for the treatment of chronic lymphocytic leukemia (CLL), and cytarabine is used to treat acute myeloid leukemia (AML). Based upon observations in the present study, combinations of imexon and other S phase specific drugs may have a potential clinical role in the treatment of other types of cancer.

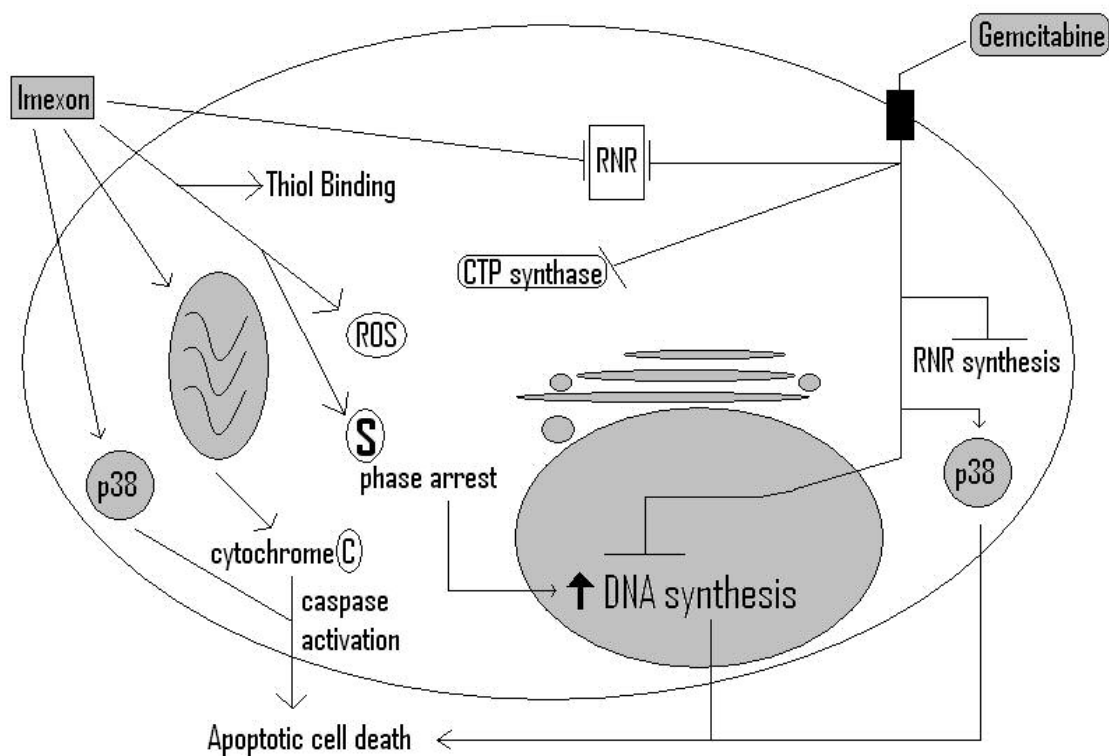


Figure 39 Mechanisms of action of imexon and gemcitabine. The illustration shows mechanisms of individual drugs and combined effects. Mechanisms include imexon thiol binding, resulting in generation of ROS, and induction of apoptosis. Imexon also inhibits ribonucleotide reductase (RNR) and results in S phase accumulation of pancreatic cancer cells. Mechanisms of gemcitabine include inhibition of RNR, CTP synthase, and DNA synthesis. Incorporation of gemcitabine into DNA leads to double strand breaks resulting in p38 mediated cell death.

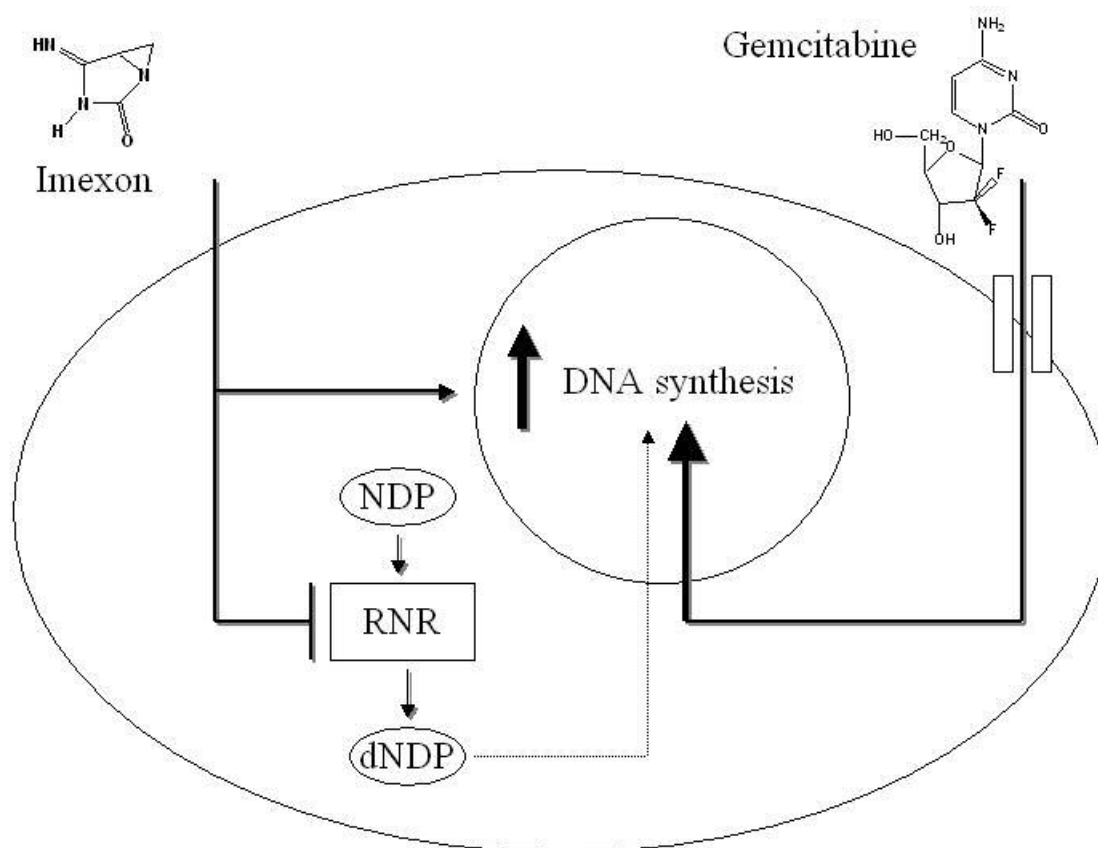


Figure 40 Proposed mechanisms of synergy of imexon and gemcitabine. Imexon enters a cancer cell and inhibits ribonucleotide reductase (RNR). Inhibition of RNR results in decreased deoxynucleotide diphosphates (dNDP) for DNA synthesis and repair. This facilitates greater gemcitabine incorporation into DNA enhancing the drug's cytotoxic effect. Imexon also induces an S phase accumulation of cells, resulting in greater DNA synthesis. This also results in enhanced accumulation of gemcitabine into DNA.

REFERENCE LIST

- Achiwa,H., Oguri,T., Sato,S., Maeda,H., Niimi,T., and Ueda,R. (2004). Determinants of sensitivity and resistance to gemcitabine: the roles of human equilibrative nucleoside transporter 1 and deoxycytidine kinase in non-small cell lung cancer. *Cancer Sci.* 95, 753-757.
- Adler,V., Yin,Z., Tew,K.D., and Ronai,Z. (1999a). Role of redox potential and reactive oxygen species in stress signaling. *Oncogene* 18, 6104-6111.
- Alberts,B., Johnson,A., Lewis,J., Raff,M., Roberts,K., and Walter,P. (2002). *Molecular Biology of the Cell*. Library of Congress Cataloging-in-Publication Data).
- Alberts,S.R., Schroeder,M., Erlichman,C., Steen,P.D., Foster,N.R., Moore,D.F., Jr., Rowland,K.M., Jr., Nair,S., Tschetter,L.K., and Fitch,T.R. (2004). Gemcitabine and ISIS-2503 for patients with locally advanced or metastatic pancreatic adenocarcinoma: a North Central Cancer Treatment Group phase II trial. *J. Clin. Oncol.* 22, 4944-4950.
- Alexakis,N., Halloran,C., Raraty,M., Ghaneh,P., Sutton,R., and Neoptolemos,J.P. (2004). Current standards of surgery for pancreatic cancer. *Br. J. Surg.* 91, 1410-1427.
- Amara,F.M., Chen,F.Y., and Wright,J.A. (1994). Phorbol ester modulation of a novel cytoplasmic protein binding activity at the 3'-untranslated region of mammalian ribonucleotide reductase R2 mRNA and role in message stability. *J. Biol. Chem.* 269, 6709-6715.
- Amara,F.M., Sun,J., and Wright,J.A. (1996). Defining a novel cis-element in the 3'-untranslated region of mammalian ribonucleotide reductase component R2 mRNA. cis-trans-interactions and message stability. *J. Biol. Chem.* 271, 20126-20131.
- Baldwin,S.A., Beal,P.R., Yao,S.Y., King,A.E., Cass,C.E., and Young,J.D. (2004). The equilibrative nucleoside transporter family, SLC29. *Pflugers Arch.* 447, 735-743.

Beausejour, C.M., Gagnon, J., Primeau, M., and Momparler, R.L. (2002). Cytotoxic activity of 2',2'-difluorodeoxycytidine, 5-aza-2'-deoxycytidine and cytosine arabinoside in cells transduced with deoxycytidine kinase gene. *Biochem. Biophys. Res. Commun.* 293, 1478-1484.

Beger, H.G., Rau, B., Gansauge, F., Poch, B., and Link, K.H. (2003). Treatment of pancreatic cancer: challenge of the facts. *World J. Surg.* 27, 1075-1084.

Bicker, U. (1975). N-(2-cyanethylene-)urea--an asparagine analogous cytostatic compound? *Exp. Pathol. (Jena)* 10, 106-108.

Bicker, U. and Fuhse, P. (1975). Carcinostatic action of 2-cyanaziridines against a sarcoma in rats. *Exp. Pathol. (Jena)* 10, 279-284.

Bicker, U., Kampe, W., and Steingross, W. U.S. Patent 4,083,987. 4-11-1978.
Ref Type: Patent

Bissery, M.C. and Chabot, G.G. (1991). [History and new development of screening and evaluation methods of anticancer drugs used in vivo and in vitro]. *Bull. Cancer* 78, 587-602.

Blackstock, A.W., Lightfoot, H., Case, L.D., Tepper, J.E., Mukherji, S.K., Mitchell, B.S., Swarts, S.G., and Hess, S.M. (2001a). Tumor uptake and elimination of 2',2'-difluoro-2'-deoxycytidine (gemcitabine) after deoxycytidine kinase gene transfer: correlation with in vivo tumor response. *Clin. Cancer Res.* 7, 3263-3268.

Bohman, C. and Eriksson, S. (1990). Mammalian deoxynucleoside kinases. *Biochem. (Life Sci. Adv.)* 9, 11-35.

Bouffard, D.Y., Laliberte, J., and Momparler, R.L. (1993). Kinetic studies on 2',2'-difluorodeoxycytidine () with purified human deoxycytidine kinase and cytidine deaminase. *Biochem. Pharmacol.* 45, 1857-1861.

Boven, E., Schipper H., Erkelens, C.A.M., Hatty S.A., and Pinedo, H.M. (1991). Preclinical in vivo activity of 2',2'-difluorodeoxycytidine (gemcitabine) against human head and neck cancer. *Cancer Res.* 51, 211-214.

- Bramhall, S.R., Rosemurgy, A., Brown, P.D., Bowry, C., and Buckels, J.A. (2001). Marimastat as first-line therapy for patients with unresectable pancreatic cancer: a randomized trial. *J. Clin. Oncol.* *19*, 3447-3455.
- Burkes, R.L. and Shepherd, F.A. (1995). Gemcitabine in the treatment of non-small-cell lung cancer. *Ann. Oncol.* *6 Suppl 3*, S57-S60.
- Burris, H.A., III, Moore, M.J., Andersen, J., Green, M.R., Rothenberg, M.L., Modiano, M.R., Cripps, M.C., Portenoy, R.K., Storniolo, A.M., Tarassoff, P., Nelson, R., Dorr, F.A., Stephens, C.D., and Von Hoff, D.D. (1997a). Improvements in survival and clinical benefit with gemcitabine as first-line therapy for patients with advanced pancreas cancer: a randomized trial. *J. Clin. Oncol.* *15*, 2403-2413.
- Burton, T.R., Kashour, T., Wright, J.A., and Amara, F.M. (2003). Cellular signaling pathways affect the function of ribonucleotide reductase mRNA binding proteins: mRNA stabilization, drug resistance, and malignancy (Review). *Int. J. Oncol.* *22*, 21-31.
- Butz, J., Wickstrom, E., and Edwards, J. (2003). Characterization of mutations and loss of heterozygosity of p53 and K-ras2 in pancreatic cancer cell lines by immobilized polymerase chain reaction. *BMC. Biotechnol.* *3*, 11.
- Camiener, G.W. (1967a). Studies of the enzymatic deamination of cytosine arabinoside. 3. Substrate requirements and inhibitors of the deaminase of human liver. *Biochem. Pharmacol.* *16*, 1691-1702.
- Camiener, G.W. (1967b). Studies of the enzymatic deamination of cytosine arabinoside. II. Properties of the deaminase of
- Caradoc-Davies, T.T., Cutfield, S.M., Lamont, I.L., and Cutfield, J.F. (2004). Crystal structures of *Escherichia coli* uridine phosphorylase in two native and three complexed forms reveal basis of substrate specificity, induced conformational changes and influence of potassium. *J. Mol. Biol.* *337*, 337-354.

Carlow,D.C., Carter,C.W., Jr., Mejlhede,N., Neuhard,J., and Wolfenden,R. (1999). Cytidine deaminases from *B. subtilis* and *E. coli*: compensating effects of changing zinc coordination and quaternary structure. *Biochemistry* 38, 12258-12265.

Carmichael,J., Fink,U., Russell,R.C., Spittle,M.F., Harris,A.L., Spiessi,G., and Blatter,J. (1996). Phase II study of gemcitabine in patients with advanced pancreatic cancer. *Br. J. Cancer* 73, 101-105.

Carter,C.W., Jr. (1995). The nucleoside deaminases for cytidine and adenosine: structure, transition state stabilization, mechanism, and evolution. *Biochimie* 77, 92-98.

Casper,E.S., Green,M.R., Kelsen,D.P., Heelan,R.T., Brown,T.D., Flombaum,C.D., Trochanowski,B., and Tarassoff,P.G. (1994). Phase II trial of gemcitabine (2,2'-difluorodeoxycytidine) in patients with adenocarcinoma of the pancreas. *Invest New Drugs* 12, 29-34.

Chabes,A. and Thelander,L. (2000). Controlled protein degradation regulates ribonucleotide reductase activity in proliferating mammalian cells during the normal cell cycle and in response to DNA damage and replication blocks. *J. Biol. Chem.* 275, 17747-17753.

Chang,G.C., Hsu,S.L., Tsai,J.R., Wu,W.J., Chen,C.Y., and Sheu,G.T. (2004). Extracellular signal-regulated kinase activation and Bcl-2 downregulation mediate apoptosis after gemcitabine treatment partly via a p53-independent pathway. *Eur. J. Pharmacol.* 502, 169-183.

Chirigos,M.A., Ussery,M.A., and Black,P.L. (1991). Imexon and biological response modifiers in murine models of AIDS. *Int. J. Immunopharmacol.* 13 *Suppl 1*, 33-41.

Chirigos,M.A., Ussery,M.A., Rankin,J.T., Jr., Herrmann,D., Bicker,U., and Black,P.L. (1990). Antiviral efficacy of Imexon in the Rauscher murine retrovirus AIDS model. *Immunopharmacol. Immunotoxicol.* 12, 1-21.

Chou, T.C. and Talalay, P. (1984). Quantitative analysis of dose-effect relationships: the combined effects of multiple drugs or enzyme inhibitors. *Adv. Enzyme Regul.* 22, 27-55.

Clarke, M.L., Mackey, J.R., Baldwin, S.A., Young, J.D., and Cass, C.E. (2002). The role of membrane transporters in cellular resistance to anticancer nucleoside drugs. *Cancer Treat. Res.* 112, 27-47.

Cohen, S.J., Ho, L., Ranganathan, S., Abbruzzese, J.L., Alpaugh, R.K., Beard, M., Lewis, N.L., McLaughlin, S., Rogatko, A., Perez-Ruixo, J.J., Thistle, A.M., Verhaeghe, T., Wang, H., Weiner, L.M., Wright, J.J., Hudes, G.R., and Meropol, N.J. (2003). Phase II and pharmacodynamic study of the farnesyltransferase inhibitor R115777 as initial therapy in patients with metastatic pancreatic adenocarcinoma. *J. Clin. Oncol.* 21, 1301-1306.

Costanzi, S., Vincenzetti, S., Vita, A., Lambertucci, C., Taffi, S., Volpini, R., Vittori, S., and Cristalli, G. (2003). Human cytidine deaminase: understanding the catalytic mechanism. *Nucleosides Nucleotides Nucleic Acids* 22, 1539-1543.

Culine, S. (2002). [Gemcitabine and urogenital tumors]. *Bull. Cancer* 89 *Spec No*, S102-S106.

Cullen, J.J., Hinkhouse, M.M., Grady, M., Gaut, A.W., Liu, J., Zhang, Y.P., Weydert, C.J., Domann, F.E., and Oberley, L.W. (2003a). Dicumarol inhibition of NADPH:quinone oxidoreductase induces growth inhibition of pancreatic cancer via a superoxide-mediated mechanism. *Cancer Res.* 63, 5513-5520.

Cullen, J.J., Mitros, F.A., and Oberley, L.W. (2003b). Expression of antioxidant enzymes in diseases of the human pancreas: another link between chronic pancreatitis and pancreatic cancer. *Pancreas* 26, 23-27.

Cullen, J.J., Weydert, C., Hinkhouse, M.M., Ritchie, J., Domann, F.E., Spitz, D., and Oberley, L.W. (2003c). The role of manganese superoxide dismutase in the growth of pancreatic adenocarcinoma. *Cancer Res.* 63, 1297-1303.

Damaraju,V.L., Damaraju,S., Young,J.D., Baldwin,S.A., Mackey,J., Sawyer,M.B., and Cass,C.E. (2003). Nucleoside anticancer drugs: the role of nucleoside transporters in resistance to cancer chemotherapy. *Oncogene* 22, 7524-7536.

Davidson,J.D., Ma,L., Flagella,M., Geeganage,S., Gelbert,L.M., and Slapak,C.A. (2004a). An increase in the expression of ribonucleotide reductase large subunit 1 is associated with gemcitabine resistance in non-small cell lung cancer cell lines. *Cancer Res.* 64, 3761-3766.

DeLong, D. C., Hertel, L., Tang, L. W., Kroin, J. S., Wilson, J. D., Terry, J., and Lavender, J. F. Antiviral activity of 2',2'-difluorodeoxycytidine. Abstracts of Meeting of American Society of Microbiology . 3-24-1986. Ref Type: Abstract

Ding,X.Z. and Adrian,T.E. (2001). MEK/ERK-mediated proliferation is negatively regulated by P38 map kinase in the human pancreatic cancer cell line, PANC-1. *Biochem. Biophys. Res. Commun.* 282, 447-453.

Dorr,R.T. and Von Hoff,D.D. (1994). *Cancer Chemotherapy Handbook*. (Norwalk, CT: Appleton and Lange), pp. 375-380.

Duxbury,M.S., Ito,H., Zinner,M.J., Ashley,S.W., and Whang,E.E. (2004a). RNA interference targeting the M2 subunit of ribonucleotide reductase enhances pancreatic adenocarcinoma chemosensitivity to gemcitabine. *Oncogene* 23, 1539-1548.

Dvorakova,K., Payne,C.M., Landowski,T.H., Tome,M.E., Halperin,D.S., and Dorr,R.T. (2002). Imexon activates an intrinsic apoptosis pathway in RPMI8226 myeloma cells. *Anticancer Drugs* 13, 1031-1042.

Dvorakova,K., Payne,C.M., Tome,M.E., Briehl,M.M., McClure,T., and Dorr,R.T. (2000). Induction of oxidative stress and apoptosis in myeloma cells by the aziridine-containing agent imexon. *Biochem. Pharmacol.* 60, 749-758.

Dvorakova,K., Waltmire,C.N., Payne,C.M., Tome,M.E., Briehl,M.M., and Dorr,R.T. (2001). Induction of mitochondrial changes in myeloma cells by imexon. *Blood* 97, 3544-3551.

- Eklund,H., Uhlin,U., Farnegardh,M., Logan,D.T., and Nordlund,P. (2001b). Structure and function of the radical enzyme ribonucleotide reductase. *Prog. Biophys. Mol. Biol.* 77, 177-268.
- Eriksson,M., Uhlin,U., Ramaswamy,S., Ekberg,M., Regnstrom,K., Sjoberg,B.M., and Eklund,H. (1997). Binding of allosteric effectors to ribonucleotide reductase protein R1: reduction of active-site cysteines promotes substrate binding. *Structure.* 5, 1077-1092.
- Eriksson,S., Munch-Petersen,B., Johansson,K., and Eklund,H. (2002). Structure and function of cellular deoxyribonucleoside kinases. *Cell Mol. Life Sci.* 59, 1327-1346.
- Evens,A.M., Prachand,S., Shi,B., Paniaqua,M., Gordon,L.I., and Gartenhaus,R.B. (2004). Imexon-induced apoptosis in multiple myeloma tumor cells is caspase-8 dependent. *Clin. Cancer Res.* 10, 1481-1491.
- Fahy,B.N., Schlieman,M.G., Virudachalam,S., and Bold,R.J. (2003). Schedule-dependent molecular effects of the proteasome inhibitor bortezomib and gemcitabine in pancreatic cancer. *J. Surg. Res.* 113, 88-95.
- Galmarini,C.M., Mackey,J.R., and Dumontet,C. (2001a). Nucleoside analogues: mechanisms of drug resistance and reversal strategies. *Leukemia* 15, 875-890.
- Galmarini,C.M., Mackey,J.R., and Dumontet,C. (2001c). Nucleoside analogues: mechanisms of drug resistance and reversal strategies. *Leukemia* 15, 875-890.
- Garcia-Manteiga,J., Molina-Arcas,M., Casado,F.J., Mazo,A., and Pastor-Anglada,M. (2003). Nucleoside transporter profiles in human pancreatic cancer cells: role of hCNT1 in 2',2'-difluorodeoxycytidine- induced cytotoxicity. *Clin. Cancer Res.* 9, 5000-5008.
- Gius,D. (2004a). Redox-sensitive signaling factors and antioxidants: how tumor cells respond to ionizing radiation. *J. Nutr.* 134, 3213S-3214S.

- Goan, Y.G., Zhou, B., Hu, E., Mi, S., and Yen, Y. (1999). Overexpression of ribonucleotide reductase as a mechanism of resistance to 2,2-difluorodeoxycytidine in the human KB cancer cell line. *Cancer Res.* 59, 4204-4207.
- Goldstein, D., Carroll, S., Apte, M., and Keogh, G. (2004). Modern management of pancreatic carcinoma. *Intern. Med. J.* 34, 475-481.
- Goodridge, T.H., HUNTRESS, W.T., and BRATZEL, R.P. (1963). Survey of aziridines. *Cancer Chemother. Rep.* 26, 341-443.
- Gray, J.H., Owen, R.P., and Giacomini, K.M. (2004). The concentrative nucleoside transporter family, SLC28. *Pflugers Arch.* 447, 728-734.
- Griffith, D.A. and Jarvis, S.M. (1996). Nucleoside and nucleobase transport systems of mammalian cells. *Biochim. Biophys. Acta* 1286, 153-181.
- Habiro, A., Tanno, S., Koizumi, K., Izawa, T., Nakano, Y., Osanai, M., Mizukami, Y., Okumura, T., and Kohgo, Y. (2004). Involvement of p38 mitogen-activated protein kinase in gemcitabine-induced apoptosis in human pancreatic cancer cells. *Biochem. Biophys. Res. Commun.* 316, 71-77.
- Hansen, H.H. and Sorensen, J.B. (1997). Efficacy of single-agent gemcitabine in advanced non-small cell lung cancer: a review. *Semin. Oncol.* 24, S7.
- Heinemann V., Hertel L.W., Grindey G.B., and Plunkett, W. (1988). Comparison of the cellular pharmacokinetics and toxicity of 2',2'-Difluorodeoxycytidine and 1- β -D-arabinofuranosylcytosine. *Cancer Res.* 48, 4024-4031.
- Heinemann V., Quietzsch D., and Gieseler F. (2003). A phase II trial comparing gemcitabine plus cisplatin versus gemcitabine alone in advanced pancreatic carcinoma. *Proc. Am. Soc. Clin. Oncol.* 22, 250.
- Heinemann, V., Schulz, L., Issels, R.D., and Plunkett, W. (1995). Gemcitabine: A Modulator of Intracellular Nucleotide and Deoxynucleotide Metabolism. *Seminars in Oncology* 4, 11-18.

- Hersh, E.M., Grogan, T.M., Funk, C.Y., and Taylor, C.W. (1993). Suppression of human lymphoma development in the severe combined immune-deficient mouse by imexon therapy. *J. Immunother.* 13, 77-83.
- Hertel, L.W., Boder, G.B., Kroin, J.S., Rinzel, S.M., Poore, G.A., Todd, G.C., and Grindey, G.B. (1990a). Evaluation of the antitumor activity of gemcitabine (2',2'-difluoro-2'-deoxycytidine). *Cancer Res.* 50, 4417-4422.
- Hertel, L.W., Kroin, J.S., Misner, J.W., and Tustin, J.M. (1987). Synthesis of 2-deoxy-2,2-difluoro-D-ribose and 2-Deoxy-2,2-difluoro-D-ribofuranosyl Nucleosides. *J. Org. Chem.* 53, 2406-2409.
- Hruban, R.H., Adsay, N.V., Albores-Saavedra, J., Compton, C., Garrett, E.S., Goodman, S.N., Kern, S.E., Klimstra, D.S., Kloppel, G., Longnecker, D.S., Luttges, J., and Offerhaus, G.J. (2001). Pancreatic intraepithelial neoplasia: a new nomenclature and classification system for pancreatic duct lesions. *Am. J. Surg. Pathol.* 25, 579-586.
- Hu, L.A. and King, S.C. (1999). Identification of the amine-polyamine-choline transporter superfamily 'consensus amphipathic region' as the target for inactivation of the *Escherichia coli* GABA transporter GabP by thiol modification reagents. Role of Cys-300 in restoring thiol sensitivity to Gabp lacking Cys. *Biochem. J.* 339 (Pt 3), 649-655.
- Huang, P. and Plunkett, W. (1995). Induction of apoptosis by gemcitabine. *Semin. Oncol.* 22, 19-25.
- Iigo, M., Nishikata, K., Nakajima, Y., Szinai, I., Veres, Z., Szabolcs, A., and De Clercq, E. (1990). Differential effects of 2,2'-anhydro-5-ethyluridine, a uridine phosphorylase inhibitor, on the antitumor activity of 5-fluorouridine and 5-fluoro-2'-deoxyuridine. *Biochem. Pharmacol.* 39, 1247-1253.
- Irani, K., Xia, Y., Zweier, J.L., Sollott, S.J., Der, C.J., Fearon, E.R., Sundaresan, M., Finkel, T., and Goldschmidt-Clermont, P.J. (1997). Mitogenic signaling mediated by oxidants in Ras-transformed fibroblasts. *Science* 275, 1649-1652.

- Iyengar, B.S., Dorr, R.T., and Remers, W.A. (2004b). Chemical basis for the biological activity of imexon and related cyanoaziridines. *J. Med. Chem.* 47, 218-223.
- Jagadis, B, Iyengar, B, Sólyom, A, Remers, W, Dorr, R, Yu, J, Gupta, S, and Mash, E. Synthesis of [¹⁴C]-imexon. *Journal of Labelled Compounds and Radiopharmaceuticals* 48, 165-170. 2005.
Ref Type: Abstract
- Jimenez-Vidal, M., Gasol, E., Zorzano, A., Nunes, V., Palacin, M., and Chillaron, J. (2004). Thiol modification of cysteine 327 in the eighth transmembrane domain of the light subunit xCT of the heteromeric cystine/glutamate antiporter suggests close proximity to the substrate binding site/permeation pathway. *J. Biol. Chem* 279, 11214-11221.
- Johansson, M. (2003a). Identification of a novel human uridine phosphorylase. *Biochem. Biophys. Res. Commun.* 307, 41-46.
- Kamata, H. and Hirata, H. (1999). Redox regulation of cellular signalling. *Cell Signal.* 11, 1-14.
- Kanzaki, A., Takebayashi, Y., Bando, H., Eliason, J.F., Watanabe, S.S., Miyashita, H., Fukumoto, M., Toi, M., and Uchida, T. (2002). Expression of uridine and thymidine phosphorylase genes in human breast carcinoma. *Int. J. Cancer* 97, 631-635.
- Kaye, S.B. (1994). Gemcitabine: current status of phase I and II trials. *J. Clin. Oncol.* 12, 1527-1531.
- Kolberg, M., Strand, K.R., Graff, P., and Andersson, K.K. (2004a). Structure, function, and mechanism of ribonucleotide reductases. *Biochim. Biophys. Acta* 1699, 1-
- Korc, M., Meltzer, P., and Trent, J. (1986a). Enhanced expression of epidermal growth factor receptor correlates with alterations of chromosome 7 in human pancreatic cancer. *Proc. Natl. Acad. Sci. U. S. A* 83, 5141-5144.
- Kroep, J.R., Loves, W.J., van der Wilt, C.L., Alvarez, E., Talianidis, L., Boven, E., Braakhuis, B.J., van Groeningen, C.J., Pinedo, H.M., and Peters, G.J. (2002a).

Pretreatment deoxycytidine kinase levels predict in vivo gemcitabine sensitivity. *Mol. Cancer Ther.* 1, 371-376.

Kyosseva, S.V. (2004). Mitogen-activated protein kinase signaling. *Int. Rev. Neurobiol.* 59, 201-220.

Kyriakis, J.M. and Avruch, J. (2001). Mammalian mitogen-activated protein kinase signal transduction pathways activated by stress and inflammation. *Physiol Rev.* 81, 807-869.

Lawrence, T.S., Blackstock, A.W., and McGinn, C. (2003). The mechanism of action of radiosensitization of conventional chemotherapeutic agents. *Semin. Radiat. Oncol.* 13, 13-21.

Lawrence, T.S., Chang, E.Y., Hahn, T.M., Hertel, L.W., and Shewach, D.S. (1996). Radiosensitization of pancreatic cancer cells by 2',2'-difluoro-2'-deoxycytidine. *Int. J. Radiat. Oncol. Biol. Phys.* 34, 867-872.

Lebedeva, I.V., Su, Z.Z., Sarkar, D., Gopalkrishnan, R.V., Waxman, S., Yacoub, A., Dent, P., and Fisher, P.B. (2004). Induction of reactive oxygen species renders mutant and wild-type K-ras pancreatic carcinoma cells susceptible to Ad.mda-7-induced apoptosis. *Oncogene.*

Lieber, M., Mazzetta, J., Nelson-Rees, W., Kaplan, M., and Todaro, G. (1975). Establishment of a continuous tumor-cell line (panc-1) from a human carcinoma of the exocrine pancreas. *Int. J. Cancer* 15, 741-747.

Liou, J.Y., Dutschman, G.E., Lam, W., Jiang, Z., and Cheng, Y.C. (2002c). Characterization of human UMP/CMP kinase and its phosphorylation of D- and L-form deoxycytidine analogue monophosphates. *Cancer Res.* 62, 1624-1631.

Logan, D.T., Su, X.D., Aberg, A., Regnstrom, K., Hajdu, J., Eklund, H., and Nordlund, P. (1996). Crystal structure of reduced protein R2 of ribonucleotide reductase: the structural basis for oxygen activation at a dinuclear iron site. *Structure.* 4, 1053-1064.

Loor, R., Nowak, N.J., Manzo, M.L., Douglass, H.O., and Chu, T.M. (1982). Use of pancreas-specific antigen in immunodiagnosis of pancreatic cancer. *Clin. Lab Med.* 2, 567-578.

Louvet C., Labianca P., Hammel G., Liedo G., De Braud F., Andre T., and et al. (2003). Gemcitabine versus GEMOX (gemcitabine + oxaliplatin) in non resectable pancreatic adenocarcinoma. *Proc. Am. Soc. Clin. Oncol.* 22, 250.

Lund, B., Kristjansen, P.E., and Hansen, H.H. (1993). Clinical and preclinical activity of 2',2'-difluorodeoxycytidine (gemcitabine). *Cancer Treat. Rev.* 19, 45-55.

Mackey, J.R., Yao, S.Y., Smith, K.M., Karpinski, E., Baldwin, S.A., Cass, C.E., and Young, J.D. (1999). Gemcitabine transport in xenopus oocytes expressing recombinant plasma membrane mammalian nucleoside transporters. *J. Natl. Cancer Inst.* 91, 1876-1881.

Matsuzawa, A. and Ichijo, H. (2005b). Stress-responsive protein kinases in redox-regulated apoptosis signaling. *Antioxid. Redox. Signal.* 7, 472-481.

Mayr, C.A., Sami, S.M., and Dorr, R.T. (1997a). In vitro cytotoxicity and DNA damage production in Chinese hamster ovary cells and topoisomerase II inhibition by 2-[2'-(dimethylamino)ethyl]-1, 2-dihydro-3H-dibenz[de,h]isoquinoline-1,3-diones with substitutions at the 6 and 7 positions (azonafides). *Anticancer Drugs* 8, 245-256.

Meister, A. (1994). Glutathione, ascorbate, and cellular protection. *Cancer Res.* 54, 1969s-1975s.

Micksche, M., Kokoschka, E.M., Kokron, O., Sagaster, P., and Bicker, U. (1977). Immunostimulation in cancer patients by a new synthetic compound: BM 06 002. *Osterr. Z. Onkol.* 4, 29-32.

Micksche, M., Kokoschka, E.M., Sagaster, P., and Bicker, U. (1978). Phase I study for a new immunomodulating drug, BM 06 002, in man. Immune modulation and control of neoplasia by adjuvant therapy 403-412.

Miyashita, H., Takebayashi, Y., Eliason, J.F., Fujimori, F., Nitta, Y., Sato, A., Morikawa, H., Ohashi, A., Motegi, K., Fukumoto, M., Mori, S., and Uchida, T. (2002). Uridine phosphorylase is a potential prognostic factor in patients with oral squamous cell carcinoma. *Cancer* 94, 2959-2966.

Momparler,R.L. and Laliberte,J. (1990). Induction of cytidine deaminase in HL-60 myeloid leukemic cells by 5-aza-2'-deoxycytidine. *Leuk. Res.* 14, 751-754.

Moore,M.J., Hamm,J., Dancey,J., Eisenberg,P.D., Dagenais,M., Fields,A., Hagan,K., Greenberg,B., Colwell,B., Zee,B., Tu,D., Ottaway,J., Humphrey,R., and Seymour,L. (2003). Comparison of gemcitabine versus the matrix metalloproteinase inhibitor BAY 12-9566 in patients with advanced or metastatic adenocarcinoma of the pancreas: a phase III trial of the National Cancer Institute of Canada Clinical Trials Group. *J. Clin. Oncol.* 21, 3296-3302.

Mosmann,T. (1983). Rapid colorimetric assay for cellular growth and survival: application to proliferation and cytotoxicity assays. *J. Immunol. Methods* 65, 55-63.

Mueckler,M. and Makepeace,C. (1997). Identification of an amino acid residue that lies between the exofacial vestibule and exofacial substrate-binding site of the Glut1 sugar permeation pathway. *J. Biol. Chem* 272, 30141-30146.

Murphy,L.O., Cluck,M.W., Lovas,S., Otvos,F., Murphy,R.F., Schally,A.V., Permert,J., Larsson,J., Knezetic,J.A., and Adrian,T.E. (2001). Pancreatic cancer cells require an EGF receptor-mediated autocrine pathway for proliferation in serum-free conditions. *Br. J. Cancer* 84, 926-935.

Nagata,T., Nakamori,M., Iwahashi,M., and Yamaue,H. (2002). Overexpression of pyrimidine nucleoside phosphorylase enhances the sensitivity to 5'-deoxy-5-fluorouridine in tumour cells in vitro and in vivo. *Eur. J. Cancer* 38, 712-717.

Nakamura,H., Bai,J., Nishinaka,Y., Ueda,S., Sasada,T., Ohshio,G., Imamura,M., Takabayashi,A., Yamaoka,Y., and Yodoi,J. (2000). Expression of thioredoxin and glutaredoxin, redox-regulating proteins, in pancreatic cancer. *Cancer Detect. Prev.* 24, 53-60.

Neff,T. and Blau,C.A. (1996b). Forced expression of cytidine deaminase confers resistance to cytosine arabinoside and gemcitabine. *Exp. Hematol.* 24, 1340-1346.

- Park, J.B. and Levine, M. (2000). Characterization of the promoter of the human ribonucleotide reductase R2 gene. *Biochem. Biophys. Res. Commun.* 267, 651-657.
- Parker, N.J., Begley, C.G., and Fox, R.M. (1994). Human R1 subunit of ribonucleotide reductase (RRM1): 5' flanking region of the gene. *Genomics* 19, 91-96.
- Parker, N.J., Begley, C.G., and Fox, R.M. (1995). Human gene for the large subunit of ribonucleotide reductase (RRM1): functional analysis of the promoter. *Genomics* 27, 280-285.
- Pauwels, B., Korst, A.E., Lardon, F., and Vermorcken, J.B. (2005). Combined modality therapy of gemcitabine and radiation. *Oncologist* 10, 34-51.
- Pereira, S., Fernandes, P.A., and Ramos, M.J. (2004a). Mechanism for ribonucleotide reductase inactivation by the anticancer drug gemcitabine. *J. Comput. Chem.* 25, 1286-1294.
- Pino, S.M., Xiong, H.Q., McConkey, D., and Abbruzzese, J.L. (2004). Novel therapies for pancreatic adenocarcinoma. *Curr. Gastroenterol. Rep.* 6, 119-125.
- Plunkett, W., Gandhi, V., Chubb, S., and et al. (1989). 2',2'-difluorodeoxycytidine metabolism and mechanism of action in human leukaemia cells. *Nucleosides Nucleotides Nucleic Acids* 8, 775-785.
- Plunkett, W., Huang, P., Searcy, C.E., and Gandhi, V. (1996a). Gemcitabine: preclinical pharmacology and mechanisms of action. *Semin. Oncol.* 23, 3-15.
- Plunkett, W., Huang, P., Xu, Y.Z., Heinemann, V., Grunewald, R., and Gandhi, V. (1995a). Gemcitabine: metabolism, mechanisms of action, and self-potential. *Semin. Oncol.* 22, 3-10.
- Reynolds, R.C. (1995). Aziridines. In *Cancer Chemotherapeutic Agents.*, W.O.Foye, ed. (Washington, D.C.: American Chemical Society), pp. 186-197.
- Ritzel, M.W., Ng, A.M., Yao, S.Y., Graham, K., Loewen, S.K., Smith, K.M., Ritzel, R.G., Mowles, D.A., Carpenter, P., Chen, X.Z., Karpinski, E., Hyde, R.J., Baldwin, S.A., Cass, C.E., and Young, J.D. (2001). Molecular identification and characterization of novel human and mouse concentrative Na⁺-

nucleoside cotransporter proteins (hCNT3 and mCNT3) broadly selective for purine and pyrimidine nucleosides (system cib). *J. Biol. Chem.* 276, 2914-2927.

Roux, P.P. and Blenis, J. (2004). ERK and p38 MAPK-activated protein kinases: a family of protein kinases with diverse biological functions. *Microbiol. Mol. Biol. Rev.* 68, 320-344.

Royal, Richard E. The Multimodality Treatment of Patients with Pancreatic Cancer. *Cancer: principles and practice of oncology* 18[1], 3-7. 2004.

Ref Type: Generic

Ruiz van Haperen V.W. (1994). Development and molecular characterization of a 2'-2'-difluorodeoxycytidine-resistant variant of the human ovarian carcinoma cell line A2780. *Cancer Res.* 54, 4138-4143.

Ruiz, v.H., V, Veerman, G., Vermorcken, J.B., and Peters, G.J. (1993a). 2',2'-Difluoro-deoxycytidine (gemcitabine) incorporation into RNA and DNA of tumour cell lines. *Biochem. Pharmacol.* 46, 762-766.

Ruiz, v.H., V, Veerman, G., Vermorcken, J.B., and Peters, G.J. (1993b). 2',2'-Difluoro-deoxycytidine (gemcitabine) incorporation into RNA and DNA of tumour cell lines. *Biochem. Pharmacol.* 46, 762-766.

Sabini, E., Ort, S., Monnerjahn, C., Konrad, M., and Lavie, A. (2003). Structure of human dCK suggests strategies to improve anticancer and antiviral therapy. *Nat. Struct. Biol.* 10, 513-519.

Saeki, K., Kobayashi, N., Inazawa, Y., Zhang, H., Nishitoh, H., Ichijo, H., Saeki, K., Isemura, M., and Yuo, A. (2002). Oxidation-triggered c-Jun N-terminal kinase (JNK) and p38 mitogen-activated protein (MAP) kinase pathways for apoptosis in human leukaemic cells stimulated by epigallocatechin-3-gallate (EGCG): a distinct pathway from those of chemically induced and receptor-mediated apoptosis. *Biochem. J.* 368, 705-720.

- Sagaster,P., Kokoschka,E.M., Kokron,O., and Micksche,M. (1995). Antitumor activity of imexon. *J. Natl. Cancer Inst.* 87, 935-936.
- Salmon,S.E. and Hersh,E.M. (1994). Sensitivity of multiple myeloma to imexon in the human tumor cloning assay. *J. Natl. Cancer Inst.* 86, 228-230.
- Sato,H., Siow,R.C., Bartlett,S., Taketani,S., Ishii,T., Bannai,S., and Mann,G.E. (1997). Expression of stress proteins heme oxygenase-1 and -2 in acute pancreatitis and pancreatic islet betaTC3 and acinar AR42J cells. *FEBS Lett.* 405, 219-223.
- Sawabu,N., Watanabe,H., Yamaguchi,Y., Ohtsubo,K., and Motoo,Y. (2004). Serum tumor markers and molecular biological diagnosis in pancreatic cancer. *Pancreas* 28, 263-267.
- Schnelldorfer,T., Gansauge,S., Gansauge,F., Schlosser,S., Beger,H.G., and Nussler,A.K. (2000). Glutathione depletion causes cell growth inhibition and enhanced apoptosis in pancreatic cancer cells. *Cancer* 89, 1440-1447.
- Shoji F., Landowski,T.H., Raymond M.A., Roman,N.O., and Dorr,R.T. (2004). Imexon Induces Cell Cycle Arrest and Apoptosis against Human Pancreatic Cancer Cell Lines (MIA PaCa-2) in Vitro. Abstract: AACR Cell Cycle and Cancer: Pathways and Therapies, No. 1509.
- Sintchak,M.D., Arjara,G., Kellogg,B.A., Stubbe,J., and Drennan,C.L. (2002). The crystal structure of class II ribonucleotide reductase reveals how an allosterically regulated monomer mimics a dimer. *Nat. Struct. Biol.* 9, 293-300.
- Somasekaram,A., Jarmuz,A., How,A., Scott,J., and Navaratnam,N. (1999a). Intracellular localization of human cytidine deaminase. Identification of a functional nuclear localization signal. *J. Biol. Chem.* 274, 28405-28412.

- Spigel,D.R. and Greco,F.A. (2003). Chemotherapy in metastatic and locally advanced non-small cell lung cancer. *Semin. Surg. Oncol.* 21, 98-110.
- Spratlin,J., Sangha,R., Glubrecht,D., Dabbagh,L., Young,J.D., Dumontet,C., Cass,C., Lai,R., and Mackey,J.R. (2004). The absence of human equilibrative nucleoside transporter 1 is associated with reduced survival in patients with gemcitabine-treated pancreas adenocarcinoma. *Clin. Cancer Res.* 10, 6956-6961.
- Ueda,S., Masutani,H., Nakamura,H., Tanaka,T., Ueno,M., and Yodoi,J. (2002a). Redox control of cell death. *Antioxid. Redox. Signal.* 4, 405-414.
- Van Rompay,A.R., Johansson,M., and Karlsson,A. (2000a). Phosphorylation of nucleosides and nucleoside analogs by mammalian nucleoside monophosphate kinases. *Pharmacol. Ther.* 87, 189-198.
- Van Rompay,A.R., Norda,A., Linden,K., Johansson,M., and Karlsson,A. (2001a). Phosphorylation of uridine and cytidine nucleoside analogs by two human uridine-cytidine kinases. *Mol. Pharmacol.* 59, 1181-1186.
- Vincenzetti,S., Costanzi,S., Cristalli,G., Mariani,P., Quadrini,B., Cammertoni,N., and Vita,A. (2003b). Intersubunit interactions in human cytidine deaminase. *Nucleosides Nucleotides Nucleic Acids* 22, 1535-1538.
- Weydert,C., Roling,B., Liu,J., Hinkhouse,M.M., Ritchie,J.M., Oberley,L.W., and Cullen,J.J. (2003). Suppression of the malignant phenotype in human pancreatic cancer cells by the overexpression of manganese superoxide dismutase. *Mol. Cancer Ther.* 2, 361-369.
- Weyrer,K., Feichtinger,H., Haun,M., Weiss,G., Ofner,D., Weger,A.R., Umlauf,F., and Grunewald,K. (1996). p53, Ki-ras, and DNA ploidy in human pancreatic ductal adenocarcinomas. *Lab Invest* 74, 279-289.
- Willetts,C.G. and Clark,J.W. (2003). Update on combined-modality treatment options for pancreatic cancer. *Oncology (Huntingt)* 17, 29-36.

Yang, J.Q., Li, S., Domann, F.E., Buettner, G.R., and Oberley, L.W. (1999). Superoxide generation in v-Ha-ras-transduced human keratinocyte HaCaT cells. *Mol. Carcinog.* 26, 180-188.

Yarbro, J.W. (1992). Mechanism of action of hydroxyurea. *Semin. Oncol.* 19, 1-10.

Yunis, A.A., Arimura, G.K., and Russin, D.J. (1977). Human pancreatic carcinoma (MIA PaCa-2) in continuous culture: sensitivity to asparaginase. *Int. J. Cancer* 19, 218-235.

Zhou, B., Mi, S., Mo, X., Shih, J., Tsai, J., Hu, E., Hsu, M., Kay, K., and Yen, Y. (2002a). Time and sequence dependence of hydroxyurea in combination with gemcitabine in human KB cells. *Anticancer Res.* 22, 1369-1377.

Zhou, B.S., Hsu, N.Y., Pan, B.C., Doroshow, J.H., and Yen, Y. (1995). Overexpression of ribonucleotide reductase in transfected human KB cells increases their resistance to hydroxyurea: M2 but not M1 is sufficient to increase resistance to hydroxyurea in transfected cells. *Cancer Res.* 55, 1328-1333.

Ziske, C., Nagaraj, S., Marten, A., Gorschluter, M., Strehl, J., Sauerbruch, T., Abraham, N.G., and Schmidt-Wolf, I.G. (2004). Retroviral IFN- α gene transfer combined with gemcitabine acts synergistically via cell cycle alteration in human pancreatic carcinoma cells implanted orthotopically in nude mice. *J. Interferon Cytokine Res.* 24, 490-496.